Order Number 8814247

Simulation of nuclear power plant pressurizers with application to an inherently safe reactor

Khamis, Ibrahim Ahmad, Ph.D.

The University of Arizona, 1988

U·M·I
300 N. Zeeb Rd.
Ann Arbor, MI 48106

SIMULATION OF NUCLEAR POWER PLANT PRESSURIZERS WITH APPLICATION TO AN INHERENTLY SAFE REACTOR

by

Ibrahim Ahmad Khamis

A Dissertation submitted to the Faculty of the

DEPARTMENT OF NUCLEAR AND ENERGY ENGINEERING

In Partial Fulfillment of the Requirements
For the Degree of

DOCTOR OF PHILOSOPHY
WITH A MAJOR IN NUCLEAR ENGINEERING

In the Graduate College

THE UNIVERSITY OF ARIZONA

1 9 8 8

THE UNIVERSITY OF ARIZONA
GRADUATE COLLEGE

As members of the Final Examination Committee, we certify that we have read the dissertation prepared by Ibrahim Ahmad Khamis

entitled SIMULATION OF NUCLEAR POWER PLANT PRESSURIZERS WITH APPLICATION TO AN INHERENTLY SAFE REACTOR.

and recommend that it be accepted as fulfilling the dissertation requirement for the Degree of Doctor of Philosophy.

David L Hetrick	4/8/88
David L. Hetrick	Date
Robert L Seale	4/8/88
Robert L. Seale	Date
G W Nelson	4/8/88
George W. Nelson	Date
	Date
	Date

Final approval and acceptance of this dissertation is contingent upon the candidate's submission of the final copy of the dissertation to the Graduate College.

I hereby certify that I have read this dissertation prepared under my direction and recommend that it be accepted as fulfilling the dissertation requirement.

David L. Hetrick	4/8/88
Dissertation Director	Date
David L. Hetrick	

STATEMENT BY AUTHOR

This dissertation has been submitted in partial fulfillment of requirements for an advanced degree at The University of Arizona and is deposited in the University Library to be made available to borrowers under rules of the Library.

Brief quotations from this dissertation are allowable without special permission, provided that accurate acknowledgment of source is made. Requests for permission for extended quotation from or reproduction of this manuscript in whole or in part may be granted by the head of the major department or the Dean of the Graduate College when in his or her judgment the proposed use of the material is in the interests of scholarship. In all other instances, however, permission must be obtained from the author.

SIGNED: 

ACKNOWLEDGMENTS

I would like to express very special thanks and my deep gratitude to Prof. David L. Hetrick for his encouragement and guidance throughout my Ph.D. program.

I am deeply grateful to Prof. Robert L. Seale, chairman of the department of Nuclear and Energy Engineering, and all the faculty and staff of the department for their support.

Also, I would like to acknowledge the continued and unlimited support of the Syrian Atomic Energy Commission. For this, I wish to thank Prof. Ibrahim Haddad, the general director.

DEDICATION

To my wife, with love.

TABLE OF CONTENTS

		Page
	LIST OF ILLUSTRATIONS	7
	LIST OF TABLES	8
	ABSTRACT	9
CHAPTER		
1.	INTRODUCTION	11
	1.1 History of Pressurizer Simulation	11
	1.2 Comparison of Methods Used in Pressurizer Simulation	12
	1.3 Scope and Objective	13
2.	PRINCIPLES AND DESIGN OF THE PIUS SYSTEM	15
	2.1 Introduction and Background	15
	2.2 The PIUS Concept and Design Principles	16
3.	CONSTRUCTION OF THE DYNAMIC MODEL	18
	3.1 Primary System	19
	3.2 Secondary System	23
	3.3 Natural Loop	24
	3.4 Reactor Dynamics	25
4.	PIUS PRESSURIZER SIMULATION MODEL	30
	4.1 Mass Balance	34
	4.2 Volume Balance	35
	4.3 Energy Balance	35
	4.4 Pressurizer Heat Loss Evaluation	38
5.	RESULTS AND DISCUSSION	40
6.	CONCLUSION AND RECOMMENDATIONS	116
	6.1 Conclusion	116
	6.2 Recommendations	116

TABLE OF CONTENTS - Continued

APPENDIX A: COMPARISON OF THE QUALITY MODEL WITH NAHAVANDI, BARON AND EPRI MODELS 121

APPENDIX B: COMPARISON BETWEEN SUBCOOLING AND SATURATION 126

APPENDIX C: LIST OF VARIABLES 130

LIST OF REFERENCES 132

LIST OF ILLUSTRATIONS

Figure		Page
3.1	Representation of the Primary and Secondary Loop for PIUS	21
4.1	Schematic Diagram of the PIUS Pressurizer	33
5.1	PIUS System Response to a Reduction of the Circulation Pump Pressure Head (Initial RHP = 60 psi)	43
5.2	PIUS System Response to a Reduction of the Circulation Pump Pressure Head during Fictitious Blockage on W_{NL} . . .	60
5.3	PIUS System Response to an Electrical Power Interruption	74
5.4	PIUS System Response to a Twenty-Five cent Reactivity Insertion	83
5.5	PIUS System Response to a Twenty-Five Percent Decrease in the Feedwater Flow Rate	96
5.6	PIUS System Response to a Twenty-Five Percent Increase in the Feedwater Flow Rate	106

LIST OF TABLES

Table		Page
3.1	Assumed Principal Data for the PIUS System	22
3.2	Reactivity Coefficients	27

ABSTRACT

Pressurizer modeling for predicting the dynamic pressure of the PIUS system is presented. The transient behavior of this model for the PIUS system was investigated. The validity of this model for the PIUS system is limited to transients that are neither too large nor too long in duration. For example, the model is not capable of describing events following a complete loss of liquid for the pressurizer. However, the model can be used for qualitative prediction of the PIUS system behavior for a wide variety of severe transients. A review of pressurizer modeling indicates that the neglecting of the change in the internal energy of the subcooled water during transients is an acceptable assumption. The inherently safe feature of the PIUS system was confirmed through the self-shutdown of the reactor or, in some cases, through reactor power reduction as a result of the ingress of the pool boric acid solution into the primary system.

This dynamic model was constructed of three major components:

- The primary loop,
- The secondary loop, and
- The natural convection loop through the pool.

A lumped parameter model, uniform heat transfer, and point kinetics have been the main approximations in this model. Other approximations are mentioned during the modeling of each component of the model.

The dynamic model was simulated using the DARE-P continuous system simulation language which was developed in the Electrical Engineering Department at the University of Arizona.

CHAPTER 1

INTRODUCTION

1.1 History of Pressurizer Simulation

Primitive development of nuclear power plant pressurizer simulation models was mostly started in the late 1950's and the early 1960's. Such models were used to predict the pressure and to study the performance of the pressurizer primarily during normal operation. Simplified computer codes were developed for that purpose. However, the necessity for simplifying such codes resulted in some cases in poor predictions of the actual pressure during transients.

It is useful before proceeding further to quote Kim (1984) who wrote: "there is no single, best model." Thus, there is a trade-off between simplicity and accuracy. For example, Brown (1962) assumed that the change in the internal energy in the subcooled water during a transient can be neglected. The confirmation of this assumption will follow later during the construction of the Process Inherent Ultimate Safety (PIUS) pressurizer model (see Appendix B). However, more advanced models like those of

Nahavandi and Makkenchery (1970) and Baron (1973) did not employ the above assumption in order to predict more accurate pressure values in their transients.

Recently, several sophisticated models have been developed (Baek, et al, 1986; Sami, 1986 and Kim, 1984) to predict the overall behavior of pressurizers taking into consideration many important phenomena like wall condensation, boiling, and interfacial heat and mass transfer between vapor and liquid phases.

1.2 Comparison of Methods Used in Pressurizer Simulation

Some of the previously mentioned models like that of Sami (1986), as well as other published models like Abdallah et al (1982) and Hetrick et al (1981) were primarily based on the milestone of Nahavandi and Makkenchery (1970). For example, one could make the transition from Abdallah's steam quality model into Nahavandi's fourth case i.e., (Top-Condensing, Bottom-Boiling) using the definition of static qualities for the case of condensing steam and the case of boiling water separately (see Appendix A).

It is apparent that pressure prediction in a nuclear plant pressurizer has reached its current state of the art at the price of complexity and difficulty in employing such complicated codes. One should

always keep in mind that the pressurizer is only one of several components that are linked together during the simulation of a nuclear power plant under any conceived accident. And the overall production and performance of such a plant requires the development of a rather very large simulation code.

Consequently, some of the less severe assumptions can be justified for the purpose of simplifying the overall power plant simulation code. In fact, one such justification has been undertaken to develop a model that simulates the pressurizer of the PIUS system during the course of this work.

1.3 Scope and Objective

The scope of this work is to verify the intrinsic safety features of the PIUS system, and to provide an initial scoping of the PIUS system performance throughout various transients. In addition, an insight as to the relative significance of the various system parameters as identified in this model is provided.

Within the current research context outlined above, the objective described herein was to develop a computer code that simulates the overall behavior of the PIUS system. The PIUS plant was originally suggested and developed by the ASEA-ATOM in Sweden, and

most of the published data about the PIUS system was furnished by Hannerz (Hannerz, 1983a; Hannerz, 1983b; Hannerz and Isperg, 1984) and Babala (Babala, 1984a; Babala, 1984b; Babala and Hannerz, 1984; Babala, 1985).

CHAPTER 2

PRINCIPLES AND DESIGN OF THE PIUS SYSTEM

2.1 Introduction and Background

The public awareness of the safety issue was heightened by TMI-2 and then given further eminence by the Chernobyl accident. Among other things, such accidents have proven that the vulnerability of safety to certain mistakes during operation of a nuclear power plant may result in a disastrous outcome. The message of recent years is that all accident sequences are not of equal significances. Moreover, the attempts to impress the public by improving the engineered safety features and by improving probabilistic risk assessments (PRA) have failed. The PRA method helps us identify the sequences that dominate risks.

On the contrary, one might argue that the complexity that resulted from the increasing number of add-on type safety systems has enhanced the potential of another Chernobyl-like accident. This might suggest that the more safety features that are added to the existing nuclear systems, the more hazardous the

nuclear technology is becoming. As a result, the public is becoming more and more suspicious of this rather new technology and more than ever convinced that the risk of a large-scale accident is a significant probability.

Additional concerns about the possibility of a large-scale accident should be kept in mind when nuclear technology is made available to developing countries. Economical considerations as well as the lack of alternative energy resources have persuaded many such countries to acquire nuclear technology.

Many promising possibilities for solving the above mentioned problems have been developed or are under serious consideration. Among these possibilities is the PIUS system which is being developed by the ASEA-ATOM in Sweden.

In this chapter, we will attempt to shed some light on the safety features and the safety principles of the PIUS design. Also, we will discuss the expected behavior of the PIUS system under some conceivable accidents as compared to conventional PWR's.

2.2 The PIUS Concept and Design Principles

The PIUS reactor is an intrinsically safe pressurized water reactor (PWR). The essential

advantage of the PIUS reactor over conventional PWR's is the passive nature of the safety design of the reactor itself (Hannerz, 1983a; and Khamis, 1986). In the PIUS design, both the reactor and the primary coolant loop are submerged in a large pool of highly borated water. The primary loop is open to the surrounding borated pool in two places, above and below the core. Any disturbance of the existing balance between gravity and thermohydraulic forces will result in an ingress of the highly concentrated borated water from the pool (about 2200 ppm) into the less borated water of the primary loop (about 560 ppm). Subsequently, a transition from forced convection into natural circulation of cooler and highly borated water will dominate. Eventually, the reactor will be shut down due to the egress of highly borated water into the core region. This is the essence of an intrinsically safe design.

CHAPTER 3

CONSTRUCTION OF THE DYNAMIC MODEL

An early version of the dynamic model which simulates the transient behavior of the PIUS system was constructed by the author in 1986. In that version, the PIUS system was divided into three major subsystems. A detailed description of the system as well as the derivation of the differential equations that were used in studying the behavior of these subsystems can be found in Khamis, 1986. Later modifications of the early version will be described in what follows.

Some of the major assumptions that were made are:

- One dimensional and single-phase flow is assumed throughout the primary loop,
- Heat transfer between the primary loop and the surrounding pool on one side and between the steam generator shell and the pool on the other side are neglected,
- Perfect mixing is assumed in each region that does not have heat addition or subtraction,

- Thermodynamic properties are functions of the local specific energy and global pressure of each control volume, and
- The reactor core can be represented by the point model, i.e., (lumped parameter model) using the prompt jump approximation with six groups of delayed neutrons.

Further descriptions of the previously mentioned three regions as well as the recent modifications will now be discussed.

3.1 Primary System

The PIUS primary system was nodalized into 11 control volumes. The primary coolant, leaving the core, flows upward through the riser, regions 9 and 10. The riser ends in a plenum, region 11, from which the main flow passes into a suction pipe, region 1, then into the steam generator, regions 2 and 3. The flow continues into the main circulation pump, region 4. Finally, it continues downward through the downcomer, regions 5 and 6, until it reaches the inlet plenum, region 7. In region 8, the reactor core, it carries the heat generated in the fuel and completes its loop. The primary loop, as mentioned earlier, is open to the pool through region 7, i.e., the lower

hot/cold interface (the lower density lock), and region 11, i.e., the upper hot/cold interface (the upper density lock). Figure 3.1 is a schematic representation of the PIUS system. Data that are used in the simulating code are presented in Table 3.1.

The primary flow is represented as a state variable by integrating the general momentum equation along the 11 regions mentioned above. Energy and mass balances on every region are applied, and the specific enthalpy is calculated as a state variable in every region.

To avoid any numerical stiffness, and to reduce the number of differential equations that are used in the code, the mass of the primary liquid in each region is held constant. This assumption was made because continuity equations typically have time constants much smaller than the time frame of desired transients. As a result, the eigenvalues that are associated with the continuity equations are much larger than those of the momentum, energy, and fluid mechanics equations (The Babcock and Wilcox Company, 1983). Hence, the dynamics of the continuity equations are much faster.

An additional assumption was made during the startup of the natural circulation loop. It was

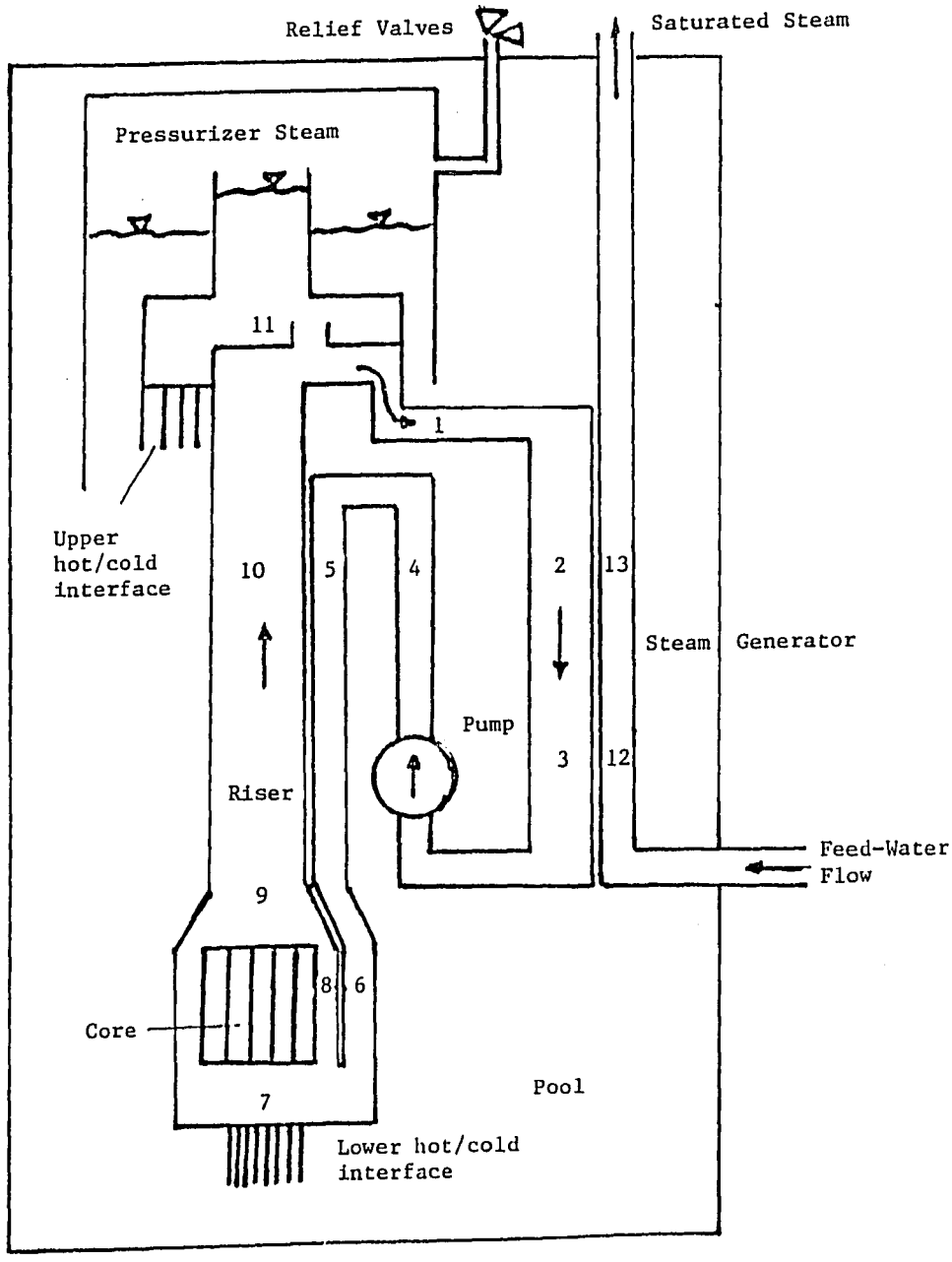

Figure 3.1 Representation of the Primary and Secondary Loop for PIUS

Table 3.1 Assumed Principal Data for the PIUS System (Hannerz, 1983a)

Primary Loop		
Thermal power	1,300	MW
Electrical power	400	MW
Total amount of uranium	55.6	metric tons
Equilibrium ingoing enrichment	2.82	%
Number of steam generators	2	
Core inlet temperature (full power)	500	F°
Core outlet temperature (full power)	550	F°
Pressure at core outlet	1,300	psi
Core pressure drop (dynamic)	4	psi
Number of fuel assemblies	157	
Fuel rod diameter	0.482	in
Active core height	6.46	ft
Equivalent core diameter	11.36	ft
Volumetric power density	63	kw/liter
Pressure head of primary circulating pump	60	psi
Operating pressure in the pressurizer	1,260	psi
Secondary Loop		
Feedwater temperature	410	F°
Secondary steam pressure	560	psi
Number of tubes in steam generator	4,000	
Feedwater flow rate	2.65×10^6	lbm/hr

assumed that the incoming flow from the pool into the primary loop will not affect the momentum balance equation applied to the primary loop. In fact, this incoming flow represents approximately less than ten percent of the primary flow rate. In addition, it is believed that this flow will leave the riser and enter the pool through the upper hot/cold interface. However, during the application of the energy and energy balances, the incoming flow was considered.

3.2 Secondary System

The once-through steam generator is simulated by two axial regions; the subcooled water region, region 12, and the saturated two-phase region, region 13. Mass, energy, and momentum balances were applied to each region. A uniformly distributed heat transfer in each region was assumed (El-Wakil, 1971). Furthermore, the heat transfer coefficients for both regions were held constant during various transients. Superheat was not allowed at the exit to the steam generator, i.e., only saturated steam is produced. The coolant heat transfer coefficients were obtained using the Colburn correlation, while the wall heat transfer coefficients, in each region, were obtained from Shinaishin, 1976, and are assumed equal. Linear thermodynamic approximations were used to build up

tables and relationships that are used to interpolate other coolant thermodynamic properties close to the operating points. These tables and relationships are used for the three subregions mentioned before.

3.3 Natural Loop

The natural loop consists of two parts connected through two openings as follows:

- The primary part which consists of the lower plenum, the core region, the upper plenum, and the riser,
- The pool part, and
- The lower and upper hot/cold interfaces.

As mentioned previously, the natural circulation loop startup or initiation is dependent on the violation of the thermal hydraulic balance which, in turn, is dependent on the difference in density between the cold pool water (about 120 F°) and the hot primary water (about 540 F°). Under normal operation, this pressure difference is designed to be equal to the dynamic pressure drop across the core. Once the circulation pump ceases to provide a heat that is sufficient to overcome that dynamic pressure drop, or equally, once the static density difference head is increased (due to the decrease in the primary density

compared to the pool density) a flow from the pool into the primary will take place.

The quasi-steady-state momentum equation which assumes the flow derivative to be always zero was applied to both the lower and upper hot/cold interface regions. Hence, the flow rates that interact with the primary loop may be calculated. For further details of the derivation of the equations that are used see either Shinaishin, 1976 or Khamis, 1986.

3.4 Reactor Dynamics

The kinetic behavior of the PIUS reactor is simulated by the point model (Hetrick, 1971). The prompt jump approximation with six groups of delayed neutrons was used to evaluate the changes in the neutron density during transients. Normalized power density and delayed neutron precursor density were used. Reactivity is expressed in this version of the simulator as a nonlinear function of mean values of fuel temperature, coolant temperature, and boron concentration. The boron concentration has two double effects on the reactivity (Asahi, 1986). First, the reactivity is affected instantaneously by the shift in boron concentration from the steady state. Second, it is affected indirectly by changes in the boron concentration as a result of the changes in the coolant

temperature from its steady state. Such changes in the coolant temperature will result in changes in the density of the coolant itself which, in turn, will affect the boron concentration. As a result, the reactivity equation becomes as follows:

$$\rho = \Gamma_f (\bar{T}_f - \bar{T}_{f0}) + \Gamma_{c1} (\bar{T}_c - \bar{T}_{c0}) + \Gamma_{c2} (\bar{T}_c - \bar{T}_{c0})^2 + \Gamma_B (C - C_0)$$

where

$\bar{T}_f$ and $\bar{T}_{f0}$ are mean fuel temperature at time t and at steady state,

$\bar{T}_c$ and $\bar{T}_{c0}$ are mean coolant temperature at time t and at steady state,

C and C_0 are the boron concentration at time t and at steady state,

Γ_f is fuel reactivity coefficient,

Γ_{c1} and Γ_{c2} coolant reactivity feedbacks, and

Γ_B is boron concentration reactivity feedback.

Reactivity feedbacks of the coolant and boron concentration that are used in the above reactivity equation are expressed as follows (Asahi, 1986):

$$\Gamma_{c1} = c_1 + c_2 C$$

$$\Gamma_{c2} = c_3 + c_4 C$$

$$\Gamma_B = c_5 + c_6 C_0$$

Values of the reactivity coefficients used in the reactor kinetics simulation are presented in Table 3.2 (Asahi, 1986).

Doppler coefficients for the above three feedback reactivities were held constant and limited to the neighborhood of the initial steady state values during transients.

The fuel element is simulated by utilizing the lumped model parameter (Lewis, 1977). The average fuel temperature as a state variable was found from applying an energy balance on a fuel element. Fuel specific heat, core thermal resistance, and fuel thermal conductivity were assumed constant and are not functions of fuel temperature during transients.

Table 3.2 Reactivity Coefficients

Γ_f	= - 3.45	x 10^{-5}	$\Delta k/k/F^\circ$
c_1	= 2.27	x 10^{-4}	$\Delta k/k/F^\circ$
c_2	= - 2.6133	x 10^{-7}	$\Delta k/k/F^\circ/ppm$
c_3	= - 1.0	x 10^{-6}	$\Delta k/k/F^{\circ 2}$
c_4	= 1.0833	x 10^{-9}	$\Delta k/k/F^{\circ 2}/ppm$
c_5	= - 2.015	x 10^{-4}	$\Delta k/k/ppm$
c_6	= - 2.5	x 10^{-7}	$\Delta k/k/ppm^2$

The boron concentration simulation in this version of the code is somewhat different from the early model. The difference is due to the time derivative of the boron content that is used here rather than the assumption of a complete mixing model that was used. The limitation of the complete mixing model is the nonphysical behavior of the boron concentration which would decrease following the decrease of the incoming pool flow. Typically, the boron concentration should increase with the increase of the incoming pool flow, and stay approximately constant as the incoming pool flow ceases. It is believed that even if this flow is reversed, i.e., the flow becomes outgoing to the pool, it should not have a great effect on the primary boron concentration.

Consequently, the boron concentration in the primary loop is modeled as follows (Mathieu and Distexhe, 1986):

$$M_p \frac{dC}{dt} = C_{pool} W_{NL}$$

where

M_p = primary coolant mass,

C = primary boron concentration,

C_{pool} = pool boron concentration, and

W_{NL} = mass flow that enters the primary loop through the lower hot/cold interface.

It should be mentioned that a check valve was assumed on the outgoing flow. The purpose of this valve is to eliminate the effects of reversed flow on the boron concentration and, hence, on the total reactivity of the PIUS system.

CHAPTER 4

PIUS PRESSURIZER SIMULATION MODEL

The pressurizer of the PIUS system is very unique compared to the conventional PWR pressurizers. The uniqueness lies in the following characteristics:

- There is no spray,
- Steam in the pressurizer dome is supplied from an external source specifically from an outside boiler,
- There is no non-condensible gas,
- The walls are thick concrete,
- The saturated steam presented in the dome is separated from the cold water of the pool and the hot subcooled water of the primary by layers of saturated water in the honeycombs,
- The concrete wall has double thermal insulation, and
- Hot primary liquid is circulated through the concrete pressurizer wall to save electric power for the pressurizer boiler.

Many physical phenomena that are relevant to PWR pressurizers and that play a very important role

in predicting the pressurizer pressure in conventional PWR systems are no longer important in the PIUS system. For example, the use of a thick concrete wall with double insulation will result in the absence of the following:

- Wall condensation due to the fact that concrete has a very poor conductivity coefficient (hence, the surface wall temperature can be assumed to be equal to the saturated steam in the dome), and
- Heat transfer by conduction through the wall or by natural convection on the wall surface.

Moreover, the absence of spray banks results in the absence of one of the most important phenomena in PWR's pressurizers, which is condensation on the spray banks. In addition, the presence of saturated steam which is being externally supplied to the dome, as well as the existence of the saturated layers in the honeycombs beneath the steam, will minimize heat transfer across the interfaces.

It is apparent from the preceeding discussion that the mathematical formulation for the PIUS pressurizer is somewhat simpler than that of the PWR's. In fact, this model consists only of two control

volumes separated by two interfaces across which mass transfer in the form of condensation or evaporation could occur. The upper control volume contains saturated steam only, while the lower control volume contains saturated water only. A schematic representation is shown in Figure 4.1.

The lower control volume consists of two different regions: the funnel region, which is the layer of saturated water that separates the primary coolant from the saturated steam in the pressurizer, and the upper part of the pool, which separates the cold water of the pool from the saturated steam of the pressurizer. During insurge, the level of the saturated layer at the top of the funnel moves up and compresses the saturated steam in the pressurizer. As a result, an increase in the pressurizer pressure may occur. Meanwhile, as the insurge occurs, the steam will condense and accomodate the insurge with minimum pressure rise. If the insurge rate were relatively large, a spill of the saturated water from the top of the funnel to the saturated water layer that is in the pool 1 region could take place. That spill will enhance the condensation rate of the saturated steam in the pressurizer. Hence, the pressure will drop further.

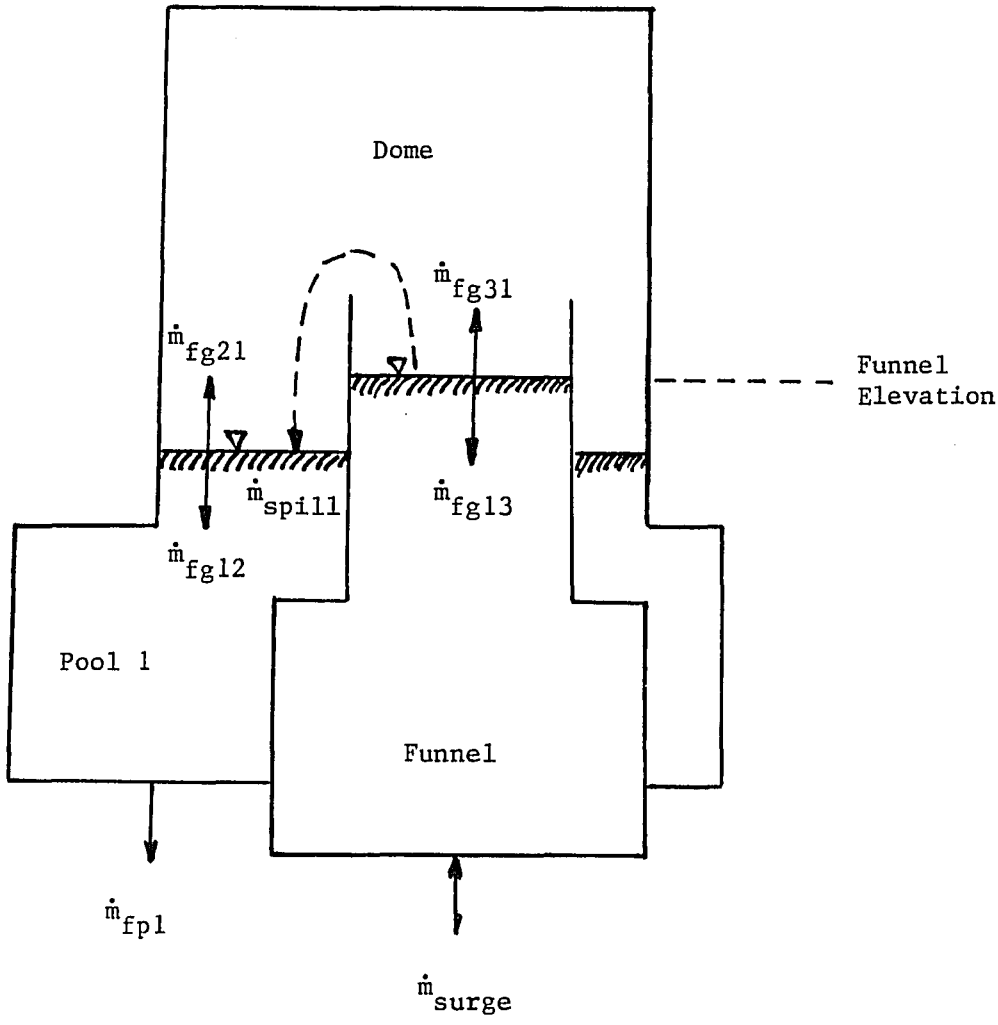

Figure 4.1 Schematic Diagram of the PIUS Pressurizer

Basic assumptions of the proposed pressurizer model are as follows:

- Pressure inside the pressurizer is uniform,
- Mass flow rates of the insurge or the outsurge are saturated liquid, and
- No superheated steam ever occurs in the pressurizer.

The differential equations that are used for as state variables during an insurge are derived as follows:

4.1 Mass Balance

The lumped parameter continuity equation is expressed as follows:

$$\frac{dM_i}{dt} = W_i \qquad 4.1.1$$

where

i = 1 represents the Dome region,

i = 2 represents the Pool 1 region, and

i = 3 represents the Funnel region.

and where

M_i = mass of the fluid in region i, and

W_i = fluid flow rate in region i.

Also

$$W_1 = - \dot{m}_{fg12} - \dot{m}_{fg13} - \dot{m}_{re} \qquad 4.1.3$$

$$W_2 = \dot{m}_{fg12} + \dot{m}_{spill} - \dot{m}_{FP1} \qquad 4.1.4$$

$$W_3 = \dot{m}_{fg13} + \dot{m}_{surge} - \dot{m}_{spill} \qquad 4.1.5$$

where

$$\dot{m}_{fg12} = \dot{m}_{fg}\, A_{12}/A_{tot} \qquad 4.1.6$$

and

$$\dot{m}_{fg13} = \dot{m}_{fg}\, A_{13}/A_{tot} \qquad 4.1.7$$

where

A_{12} and A_{13} are the pool 1 region area and the funnel area, respectively, and

A_{tot} is the pressurizer area.

4.2 Volume Balance

The volume equation is given as follows:

$$V_{tot} = \sum_{i=1}^{3} V_i \qquad 4.2.1$$

where

$$V_i = M_i\, v_i \qquad 4.2.2$$

For saturated regions, the equations of state are as follows:

$$v_i = v_i\,(P_{sat}) \qquad 4.2.3$$

4.3 Energy Balance

The energy equation was derived as follows:

$$H_i = U_i + PV_i \qquad 4.3.1$$

where

H_i = enthalpy of the fluid in region i,

U_i = internal energy of the fluid in region i,

P = pressure, and

V_i = fluid volume in region i.

Differentiating Eq. (4.3.1) with respect to time:

$$\frac{dU_i}{dt} = \frac{dH_i}{dt} - P\frac{dV_i}{dt} - V_i\frac{dP}{dt} \qquad 4.3.2$$

Since the enthalpy of the fluid is given by

$$H_i = M_i\, h_i \qquad 4.3.3$$

where

h_i = specific enthalpy in region i,

one can differentiate (4.3.3) to get:

$$\frac{dH_i}{dt} = M_i\frac{dh_i}{dt} + h_i\frac{dM_i}{dt} \qquad 4.3.4$$

Furthermore the change in the internal energy can be expressed by:

$$\frac{dU_i}{dt} = \sum(W\ h)_{in} - \sum(W\ h)_{out} + Q_i \qquad 4.3.5$$

where

Q_i = transferred heat rate into the i'th control volume.

Combining mass and volume balances will result in the following relationship between pressure change on one side and mass transfer rate at the interface; i.e., the condensation rate on the other side of the interface:

$$\dot{m}_{fg} = [M_v \, dp/dt - v_1 \, \dot{m}_{re} - v_2 \, \dot{m}_{FP1} + v_3 \, \dot{m}_{surge}] / A_v \qquad 4.3.6$$

where

$$M_v = \sum_{i=1}^{3} M_i \, \partial v_i / \partial P$$

and

$$A_v = - (v_1 - v_2 \, A_{12}/A_{tot} - v_3 \, A_{13}/A_{tot}).$$

Then, the mass transfer rate of the interface is determined as the result of applying an energy balance to each subregion of the pressurizer as well as to the system as a whole. The following equation is found:

$$\dot{m}_{fg} = - [(M_h - V_{tot}) \, dp/dt] / A_h \qquad 4.3.7$$

where

$$M_h = \sum_{i=1}^{3} M_i \, \partial h_i / \partial P$$

and

$$A_h = - (h_1 - h_2 \, A_{12}/A_{tot} - h_3 \, A_{13}/A_{tot}).$$

Solving equations (4.3.6) and (4.3.7) simultaneously, the rate of pressure change will be given by the following equation:

$$\frac{dp}{dt} = - [A_h [- v_1 \, \dot{m}_{re} + v_2 \, (\dot{m}_{spill} - \dot{m}_{FP1}) + v_3 \, (\dot{m}_{surge} - \dot{m}_{spill})]] / [A_h \, M_v - A_v \, (M_h - V_{tot})]. \qquad 4.3.8$$

During outsurge, the above equations for pressure change and mass rate will be modifed by reversing the insurge flow, hence the interface flow rate becomes an evaporation rate. In this case, no spilling will take place. The resulting equations are:

$$\dot{m}_{fg} = - [v_1 \dot{m}_{re} + v_2 (\dot{m}_{FP1} + \dot{m}_{surge}) - M_v \, dp/dt] / A_v \qquad 4.3.9$$

and

$$\frac{dp}{dt} = - [A_h [v_1 \dot{m}_{re} + v_2 (\dot{m}_{FP1} + \dot{m}_{surge})]] / [A_v (M_h - V_{tot}) - A_h M_v] \qquad 4.3.10$$

4.4 Pressurizer Heat Loss Evaluation

Heat loss from the pressurizer to the pool was calculated by solving the following one-dimensional time dependent heat diffusion equation:

$$\frac{\partial T}{\partial t} = \alpha \frac{\partial^2 T}{\partial x^2} \qquad 4.4.1$$

where

α = thermal diffusivity = $k/\rho c_p$,

k = thermal conductivity, and

c_p = specific heat.

The boundary conditions that are used to solve the above diffusion equation are:

$$T\ (t,\ x = 0) = T_{sat}\ (P) \qquad 4.4.2$$

$$T\ (t,\ x = L) = T_{pool} \qquad 4.4.3$$

with an initial condition as follows:

$$T\ (t = 0,\ x) = T\ (x = 0) + [\ T\ (x = L) - T\ (x = 0)]\ x/L \qquad 4.4.4$$

The total heat flux from the pressurizer into the pool is then evaluated using the simple Fourier Law of conduction as follows:

$$Q = - A\ k \frac{dT}{dx} \qquad 4.4.5$$

CHAPTER 5

RESULTS AND DISCUSSION

In this chapter, several simulated transients that are able to demonstrate the operating behavior of the PIUS system will be presented. Normally, such transients may have serious consequences in a conventional pressurized water reactor power plant. However, it can be concluded from the results that are presented later in this chapter that the PIUS system is indeed inherently safe to operate. That is to say, it can survive some potentially dangerous transients by virtue of its own passive safety characteristics without any active outside safety interferences.

The validity and accuracy of the results, however, are limited to the initial scoping studies of the PIUS system and cannot be expected to simulate accurately and extensively the real behavior of the PIUS system. Qualitatively, however, the presented results can illustrate theoretically the expected self-shutdown mechanism of the PIUS system throughout the insurge of the boron concentrated solution from the pool into the primary loop during almost all different kinds of transients.

Five major transients were selected to demonstrate the overall performance of the PIUS system. Then, for comparison the same five transients were repeated but with a fictitious blockage on the incoming highly borated flow from the pool into the primary. In the first two transients, the primary main circulation pump pressure head is reduced in steps by approximately 8, 17, or 25 percent. The third transients is a temporary electrical power loss for five seconds during which the main circulation pump head is reduced by approximately 17 percent. The fourth transient is a twenty-five cent reactivity step insertion. The fifth transient is a twenty-five percent decrease in the feedwater mass flow rate. Finally, the sixth transient is a twenty-five percent increase in the feedwater flow rate.

The first transient is intended to show the relationship between the recirculation pump pressure head reduction on one side, and the changes that occur in the system variables on the other side. When the recirculation pump pressure head is reduced, the hydrostatic pressure at the lower side of the lower density lock; i.e., the pool side, becomes greater than that on the upper side of the same lock; i.e., the primary side under the core. As a result, highly

borated pool water starts flowing into the primary loop through the lower density lock, as shown in Fig. 5.1. Practically, this flow marks the initiation of the natural circulation loop, especially in the cases of severe transients. In such cases, flow that enters the primary loop through the lower density lock will leave through the upper density lock and return to the pool. It is obvious from Fig. 5.1 that the incoming pool flow rate increases proportionally to the size of the reduction step in the circulation pump pressure head. The small inflections in the plots of the flow through the lower density lock, the flow through the upper density lock, and the evaporation rate in Fig. 5.1 are due to the use of a density vs. temperature function which is piecewise continuous with slight discontinuities in $d\rho/dt$ at the transitions in the segments of the fit.

The evolution of the natural circulation leads to an increase in the primary boron concentration, which, eventually will lead to reactor shutdown. It can also be seen from Fig. 5.1 that the more the pump pressure head is reduced, the more boron is added to the primary loop. Consequently, rapid reductions in reactor power, fuel temperature, coolant temperature, and reactivity take place.

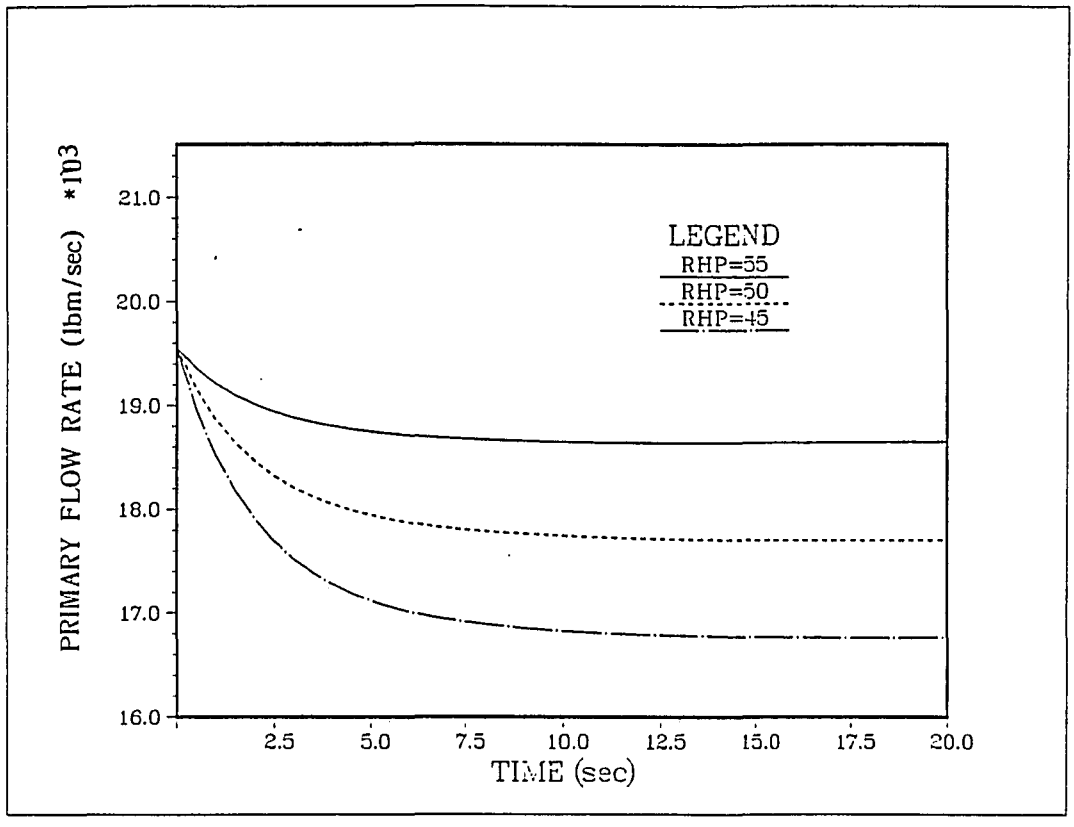

Figure 5.1 PIUS System Response to a Reduction of the Circulation Pump Pressure Head. -- (Initial RHP = 60 psi)

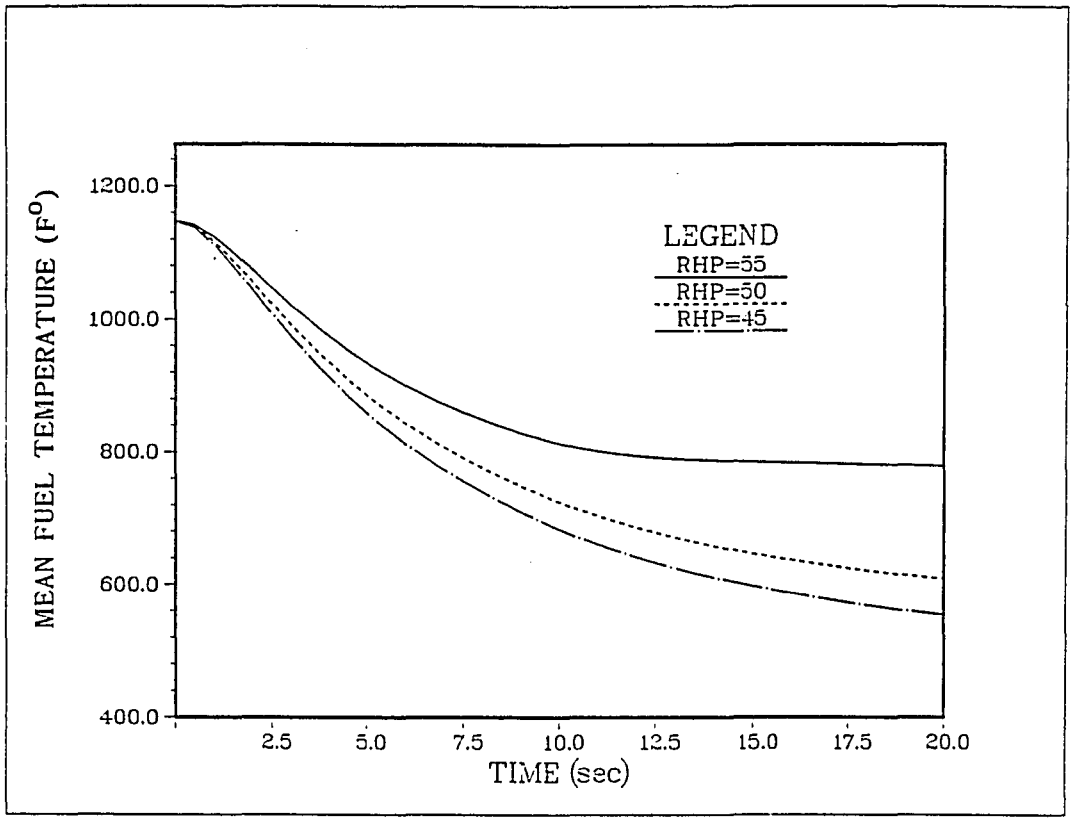

Figure 5.1--Continued

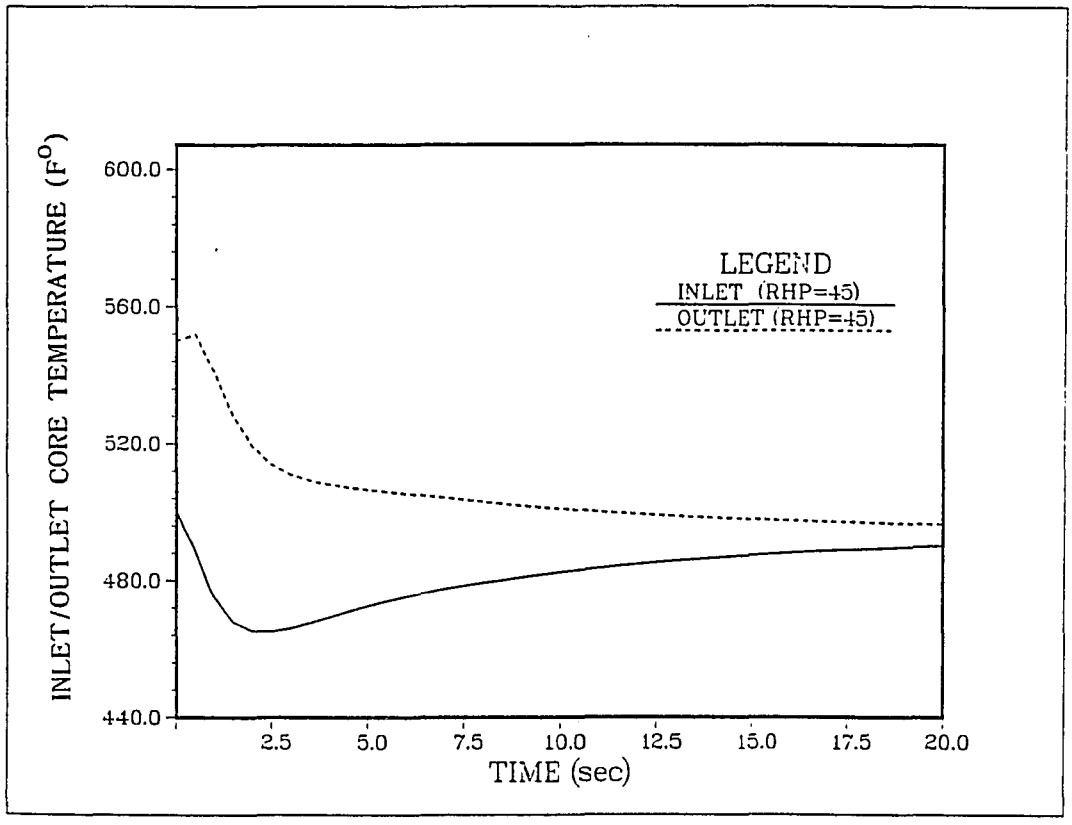

Figure 5.1--Continued

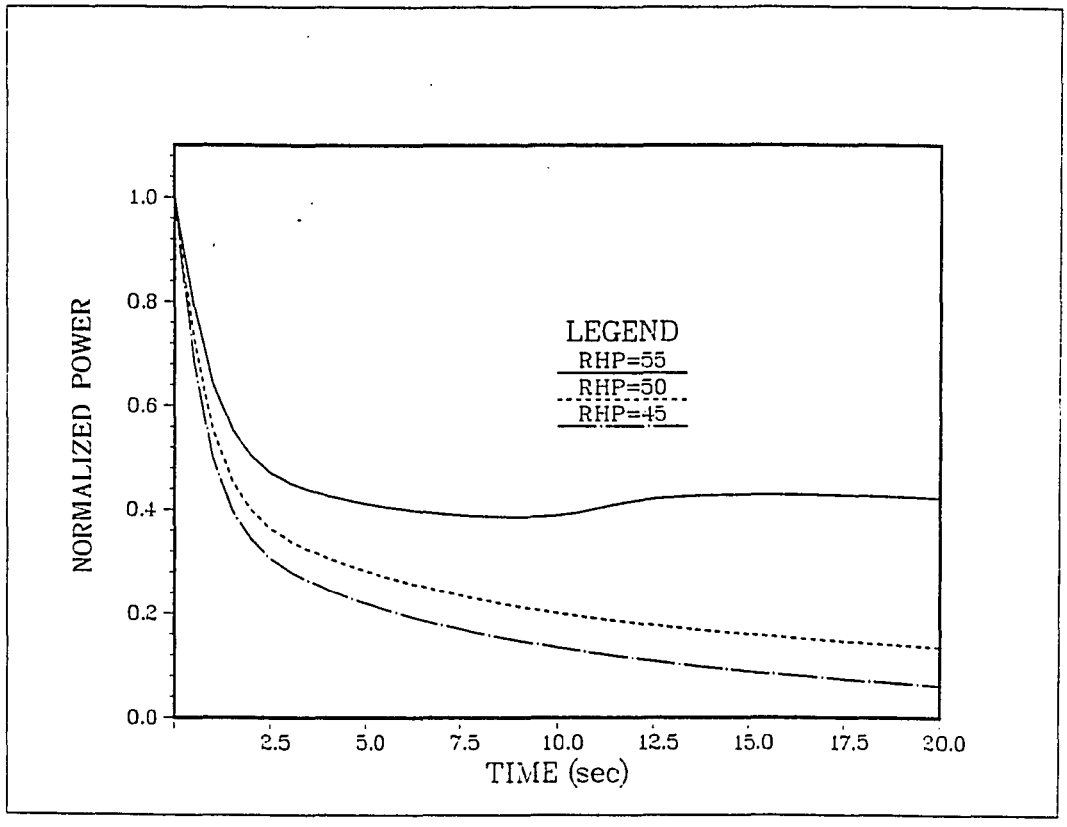

Figure 5.1 PIUS System Response to a Reduction of the Circulation Pump Pressure Head.--Continued

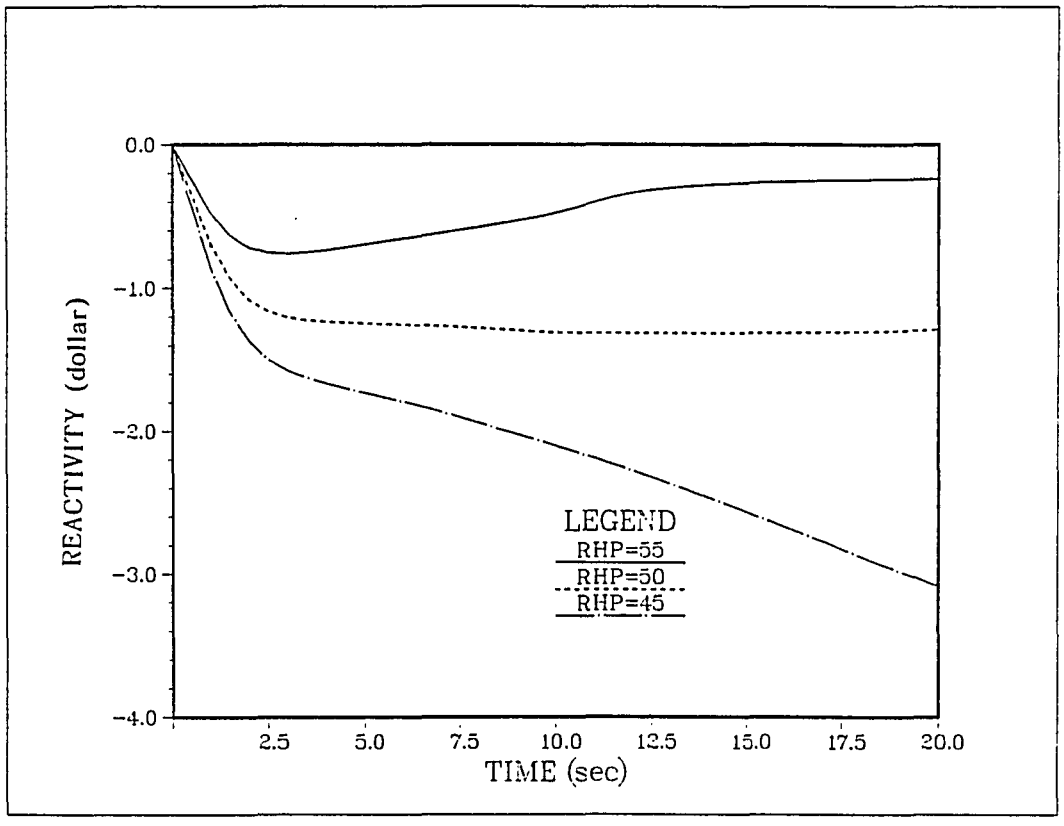

Figure 5.1--Continued

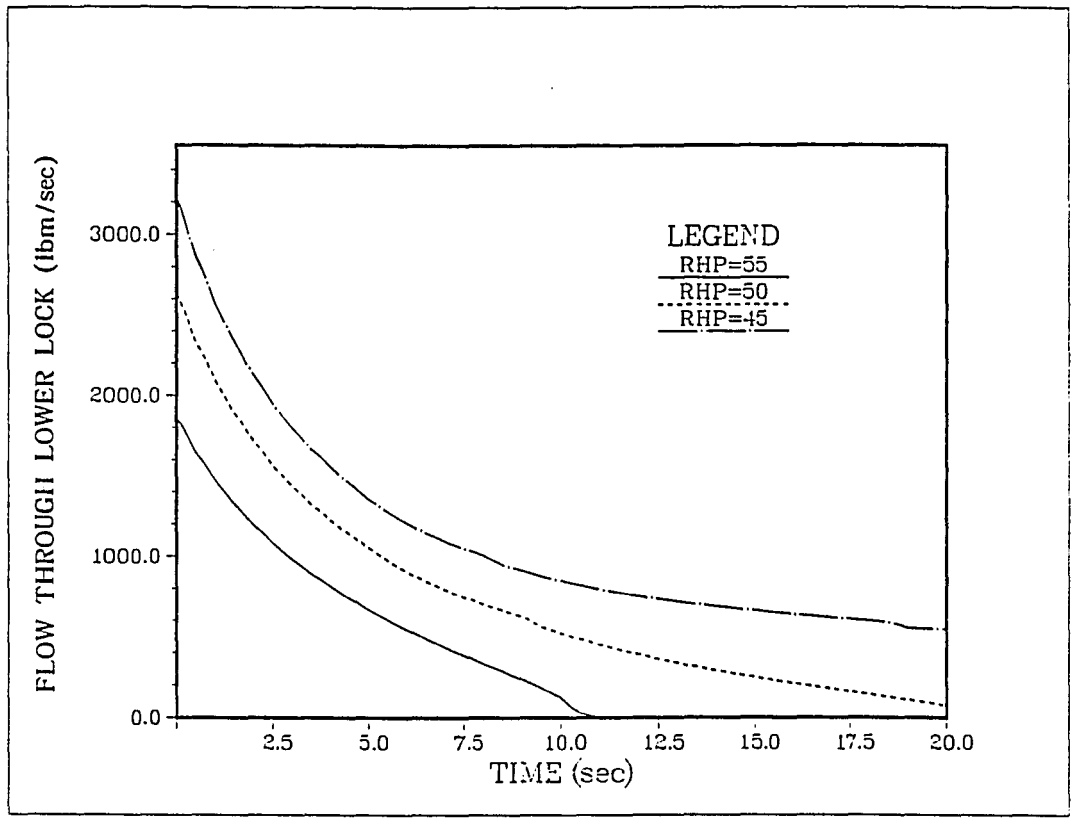

Figure 5.1--Continued

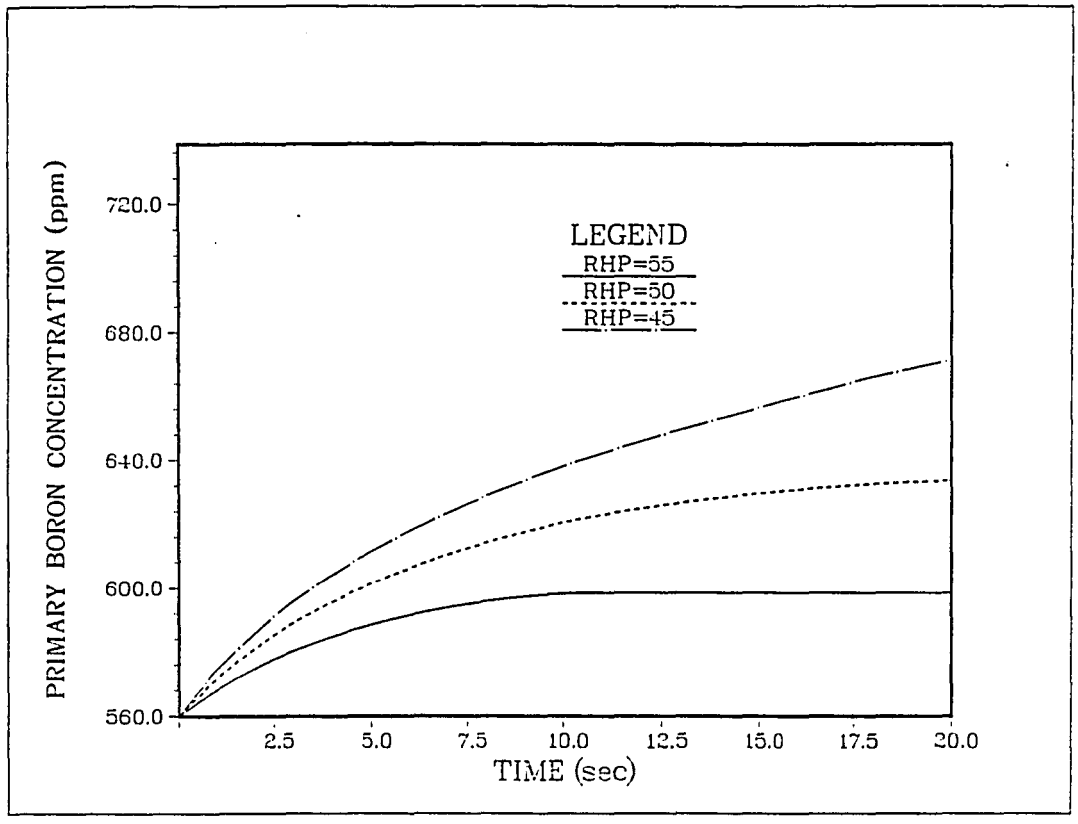

Figure 5.1 PIUS System Response to a Reduction of the Circulation Pump Pressure Head.--Continued

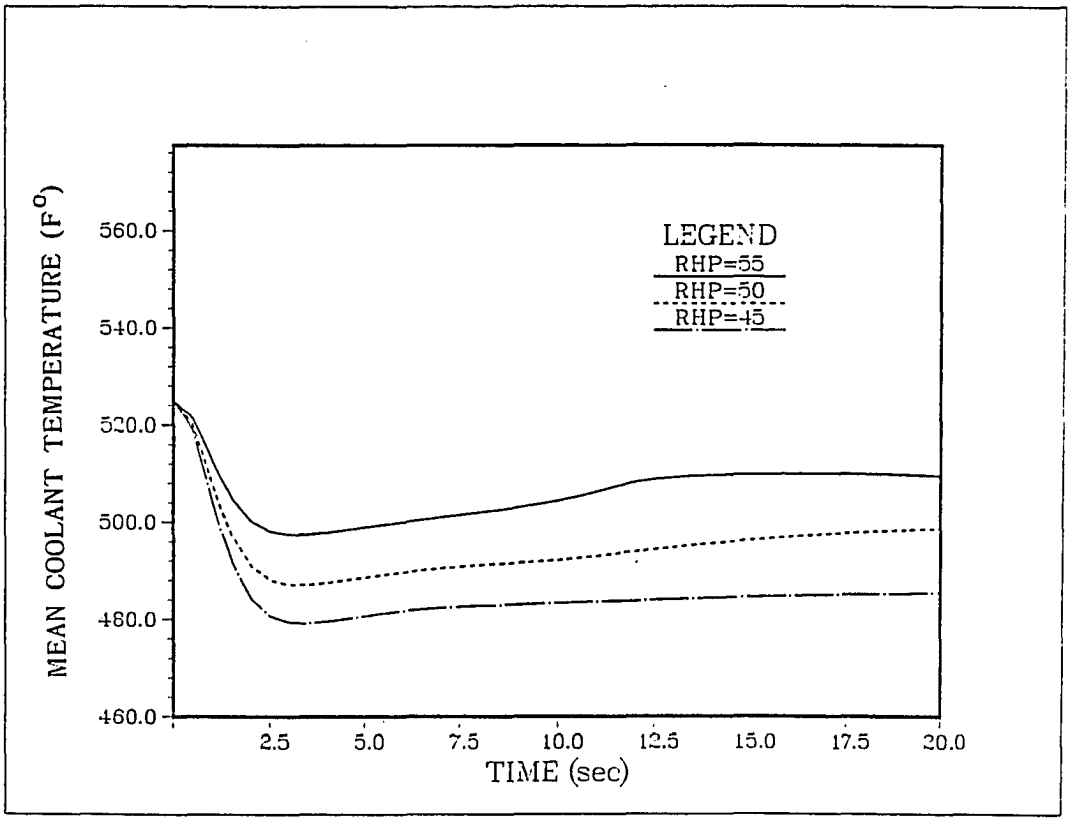

Figure 5.1--Continued

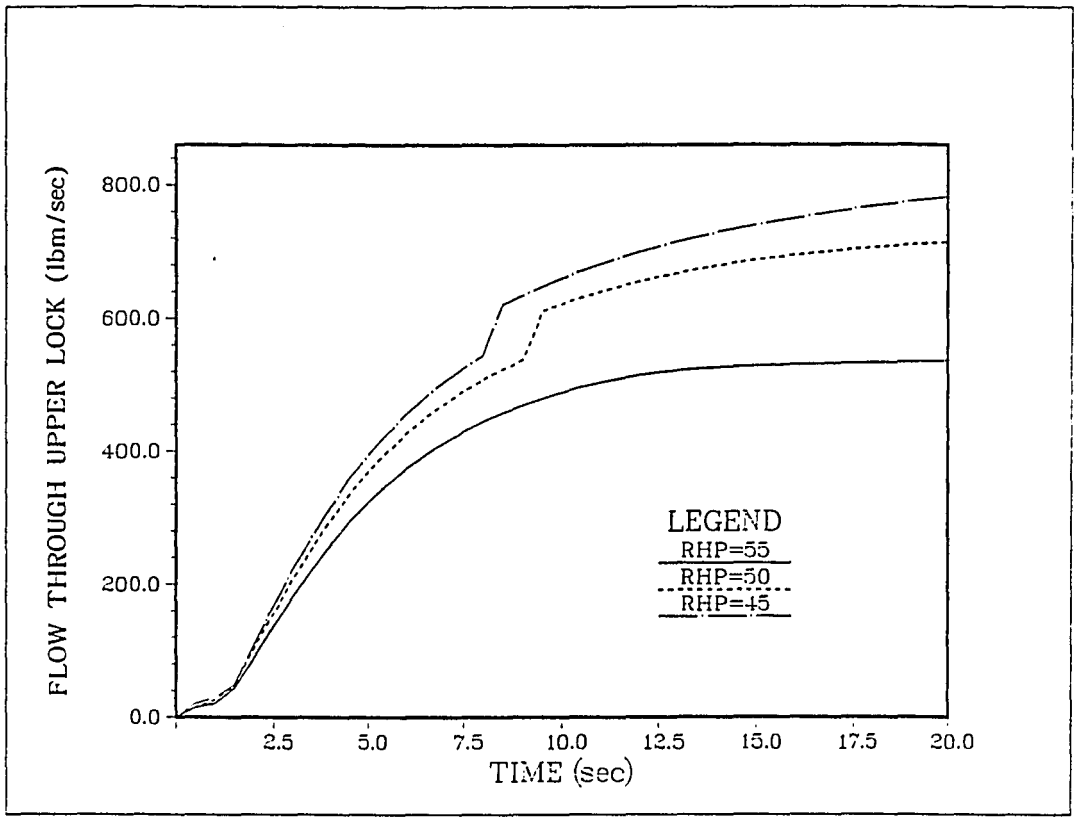

Figure 5.1--Continued

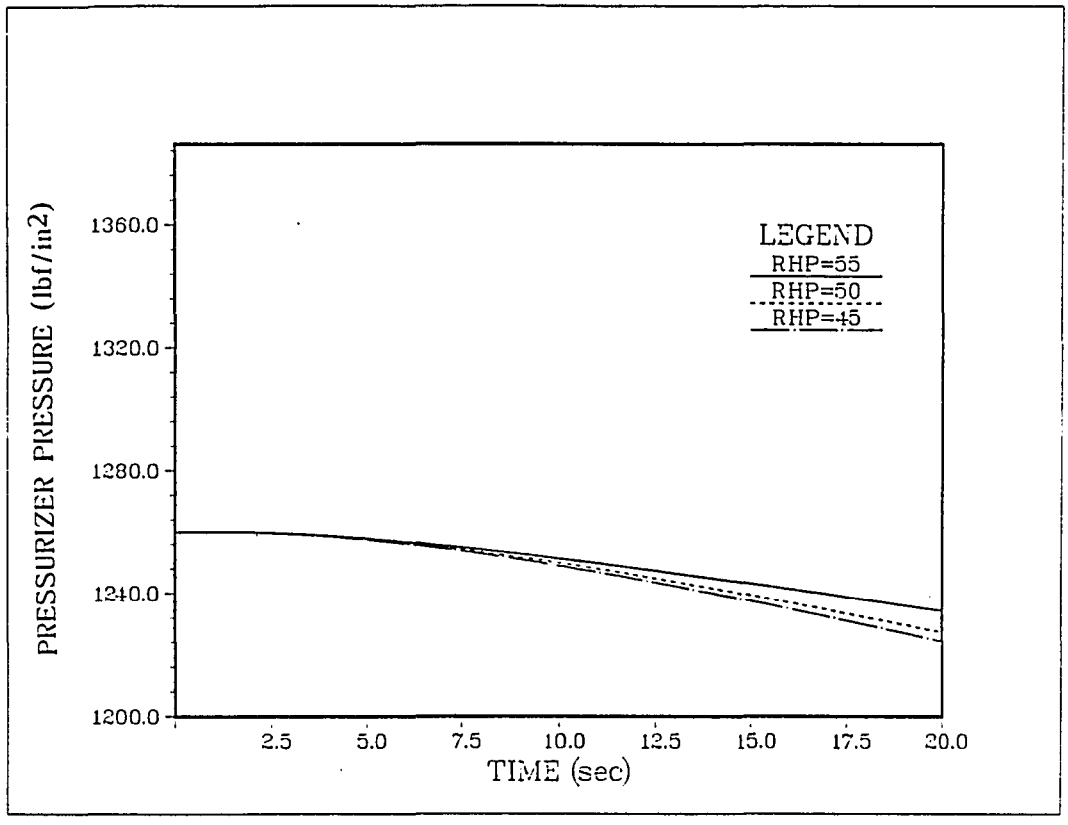

Figure 5.1 PIUS System Response to a Reduction of the Circulation Pump Pressure Head.--Continued

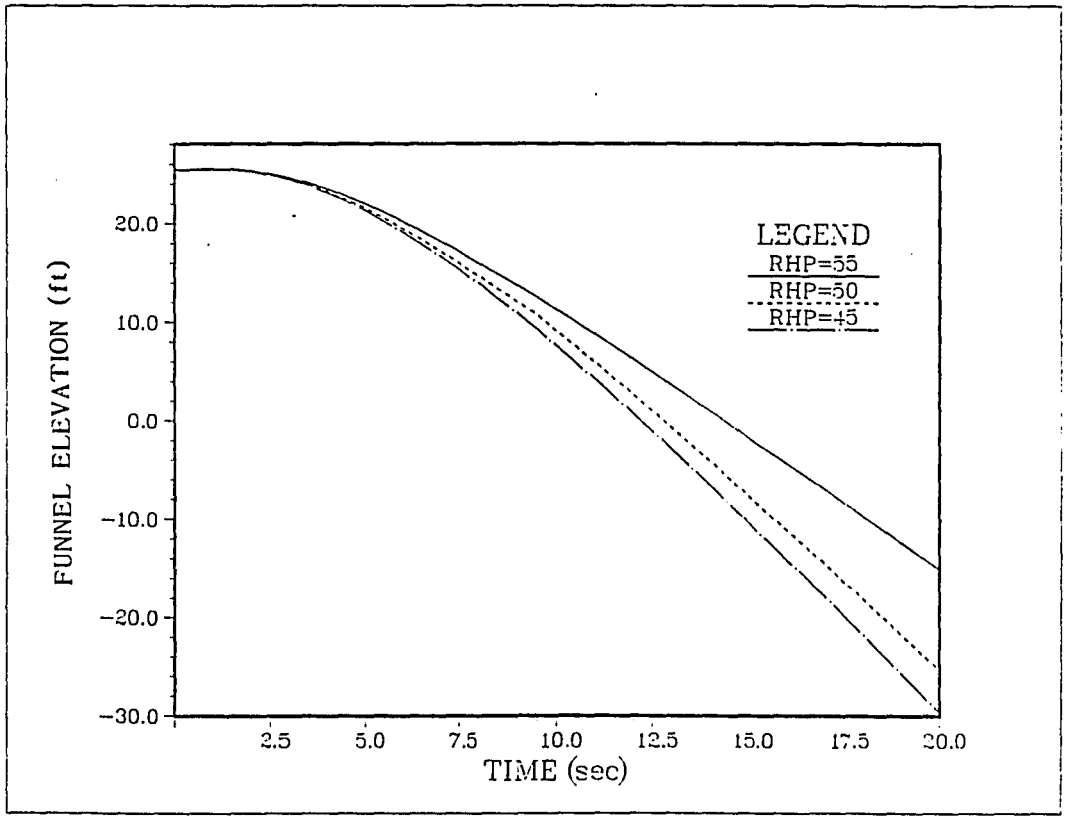

Figure 5.1--Continued

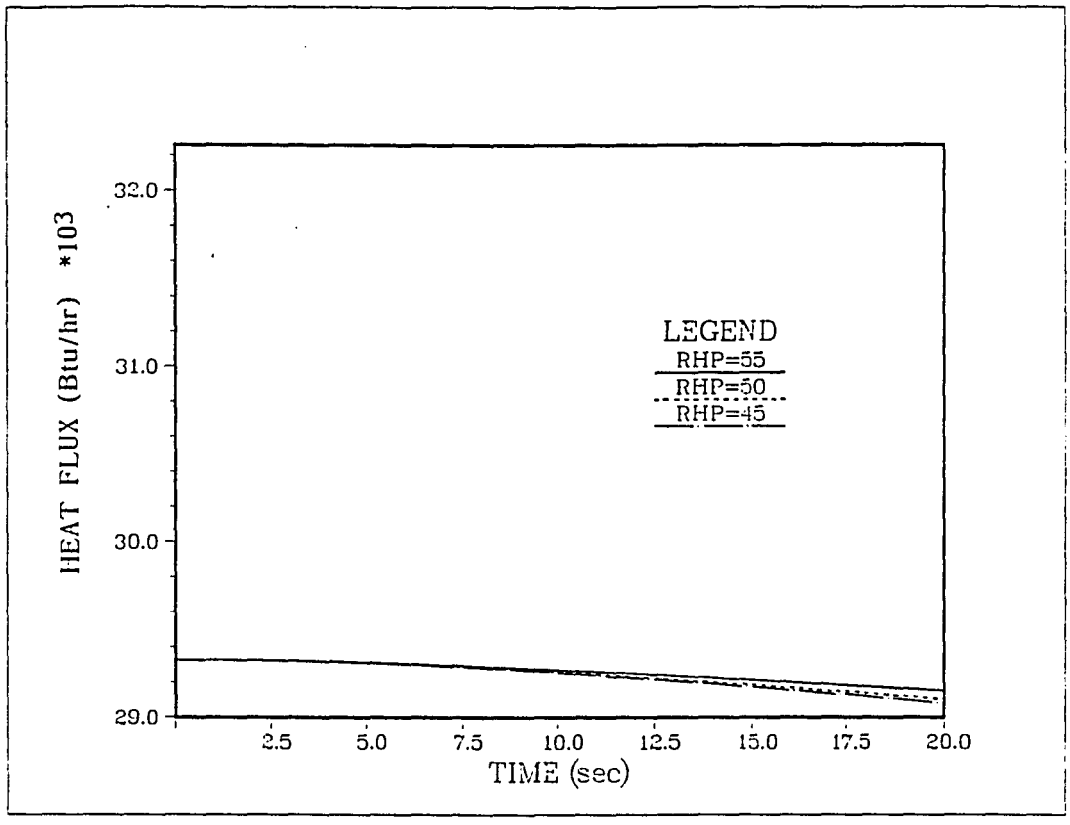

Figure 5.1--Continued

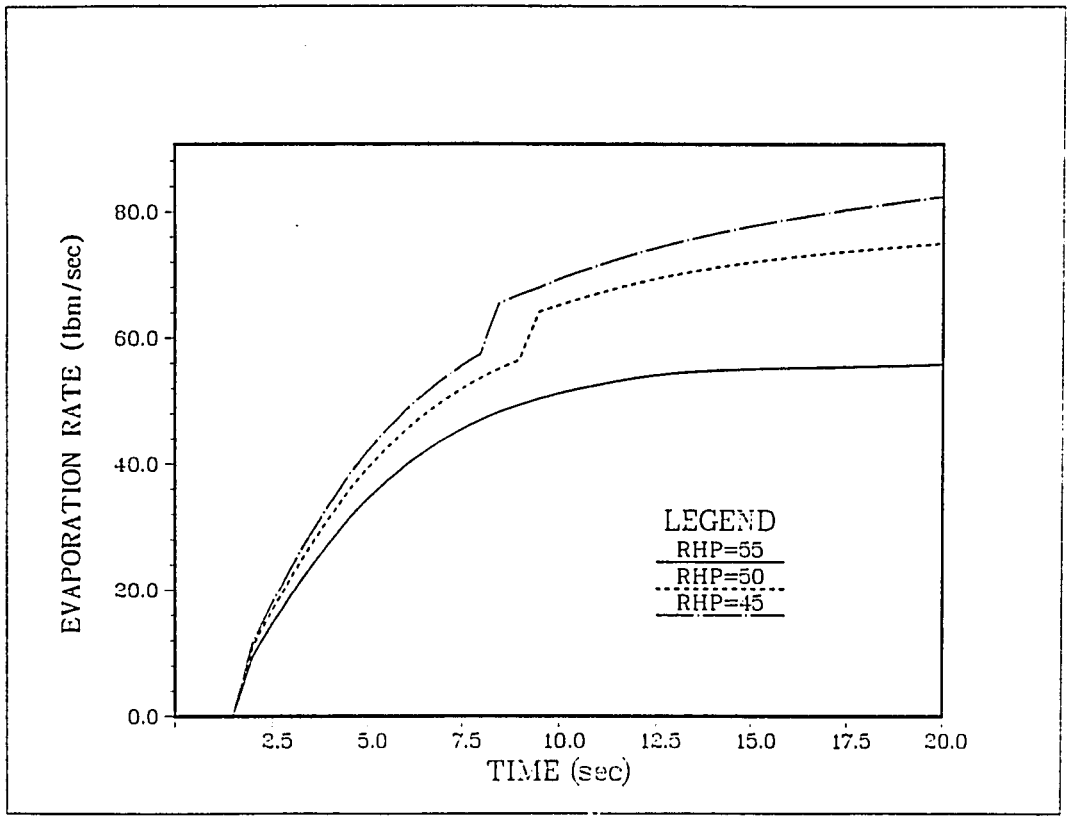

Figure 5.1 PIUS System Response to a Reduction of the Circulation Pump Pressure Head.--Continued

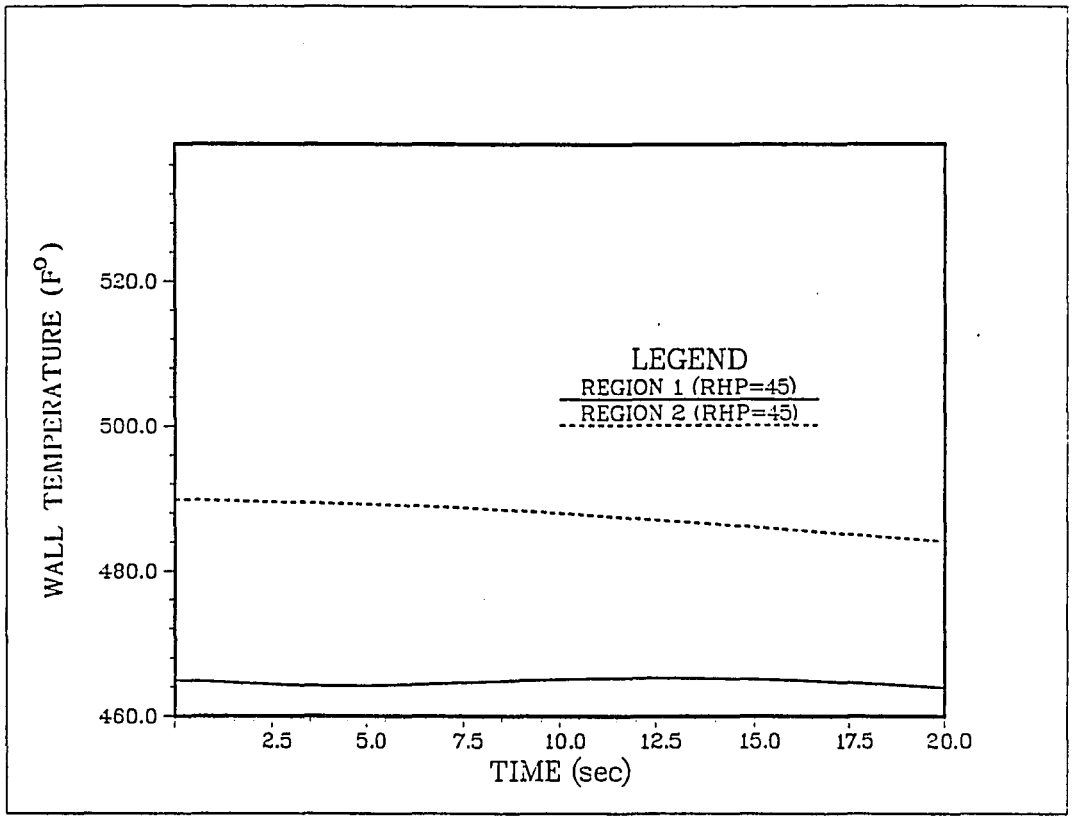

Figure 5.1--Continued

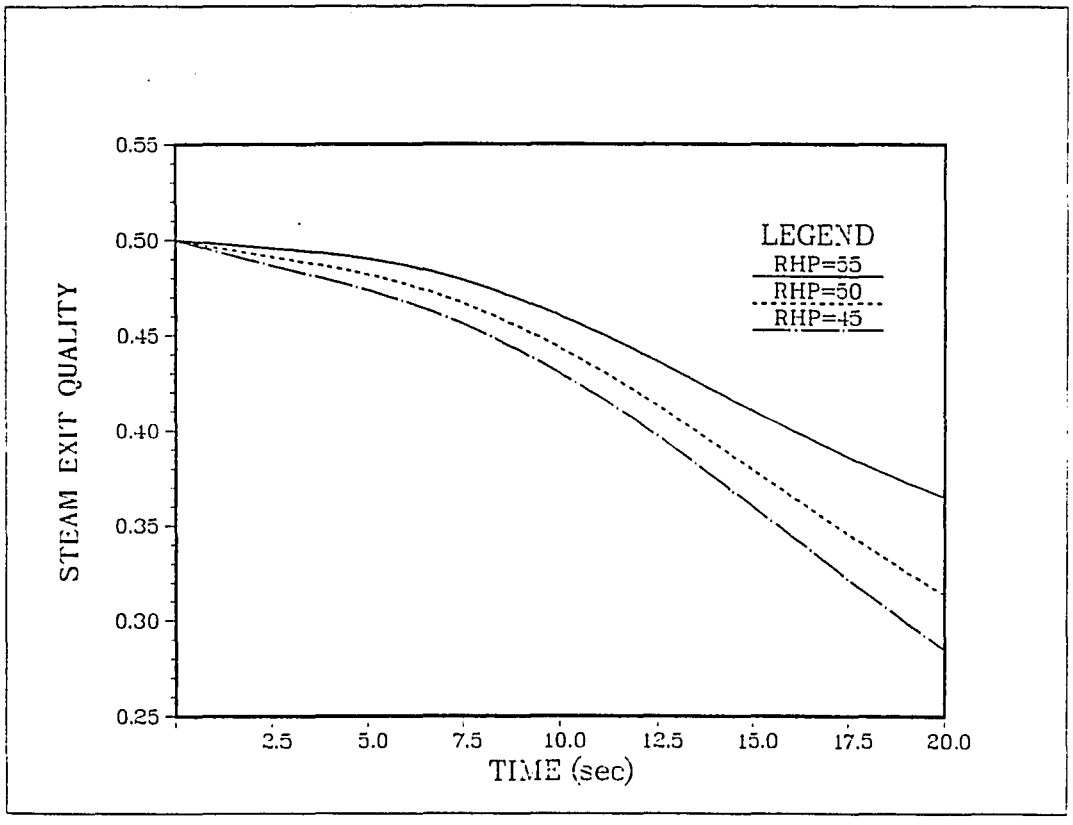

Figure 5.1--Continued

As anticipated theoretically, Fig. 5.1 shows a sharp decrease in the mean coolant temperature as well as in the inlet core temperature. This happens due to the ingress of the cold pool water that mixes with the lower plenum water before entering the core. Therefore, thermal shock might result at the lower part of the core.

It is also apparent from Fig. 5.1 that the system pressure decreases during this transient. The decrease in the primary flow rate due to the reduction in the pump pressure head leads to an outsurge in the pressurizer. Such outsurge is the main force behind the reduction in the system pressure. As the outsurge continues to flow, the saturated liquid in the bottom of the pressurizer, i.e., at the top of the funnel, evaporates into saturated steam and the liquid level continues to decrease. It should be noted that the pressurizer model becomes invalid once this level becomes equal to or less than zero.

It seems from results of this transient that tripping of the main circulation pump is a fast way of shutting down the reactor. However, such a procedure is not practically envisioned because of the temperature transient involved.

Fig. 5.2 illustrates the PIUS behavior during a recirculation pump pressure head reduction, as was done during the first transient, but with a fictitious blockage on the incoming highly borated pool water flow. In contrast to the rapid drop in reactor power and the negative reactivity that resulted during the first transient due to the ingress of pool water into the primary loop, reactor power and reactivity increase as the pump pressure head is reduced.

Compared with Fig. 5.1, the model predicts that the elimination of the peculiar inherently safe feature of the PIUS system will result, as is the case of the Light Water Reactor design (LWR), in a potentially dangerous accident. Clearly, the PIUS system will be unstable in the case of real blockage of the lower density lock. However, the ingress of highly borated pool water through the upper density lock is expected to protect the core integrity and minimize the failure of the system during such an accident by introducing a negative step of reactivity. It should be mentioned that the effect of such a step is not included in this model.

The third transient is an electrical power interruption of three seconds duration followed by a

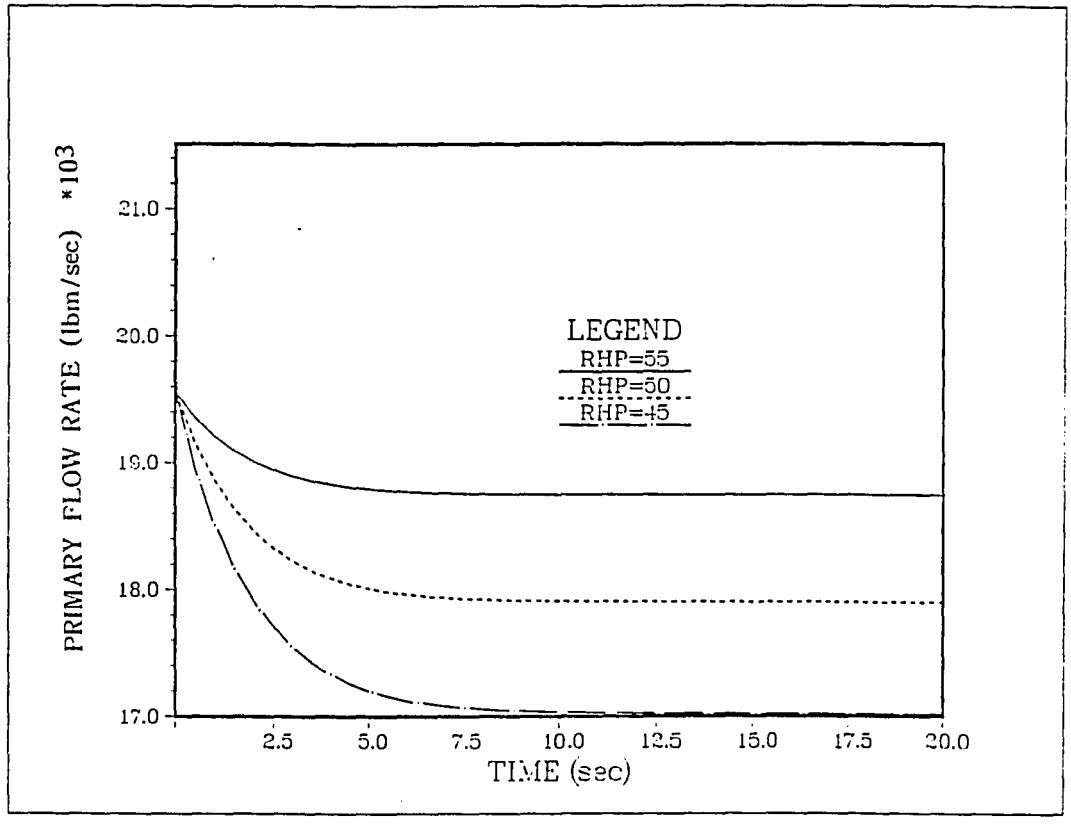

Figure 5.2 PIUS System Response to a Reduction of the Circulation Pump Pressure Head during Fictitious Blockage on WNL

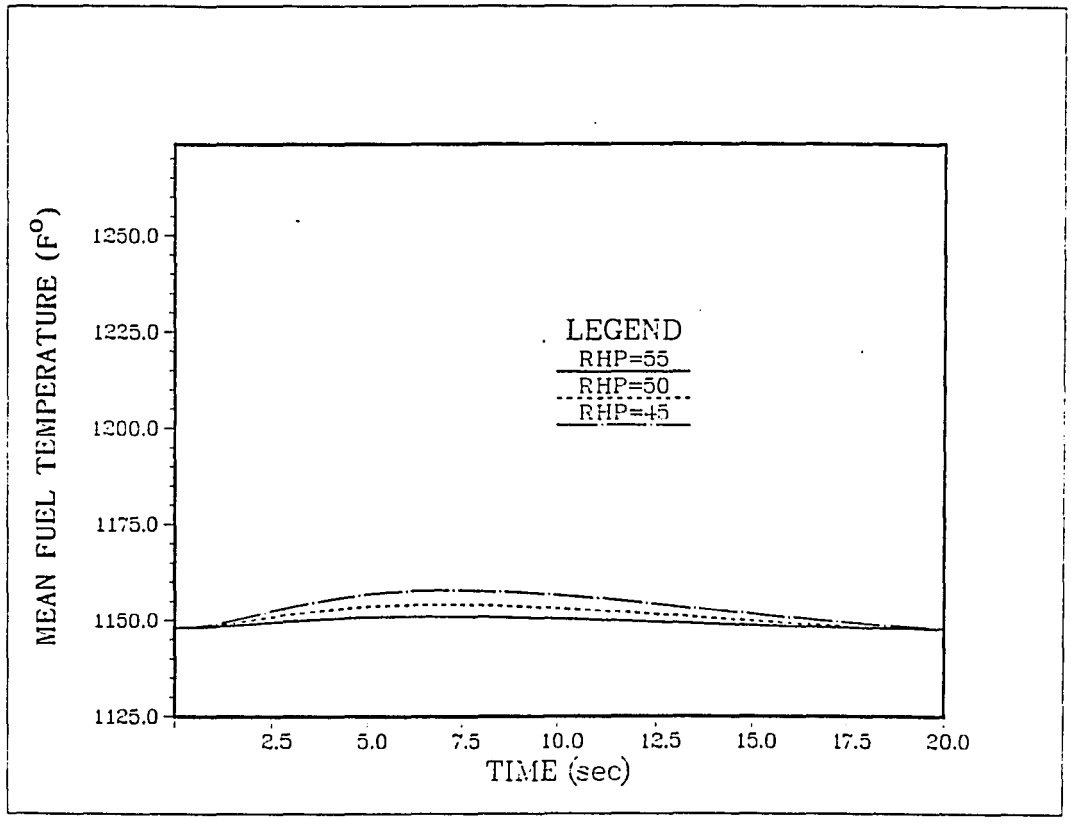

Figure 5.2--Continued

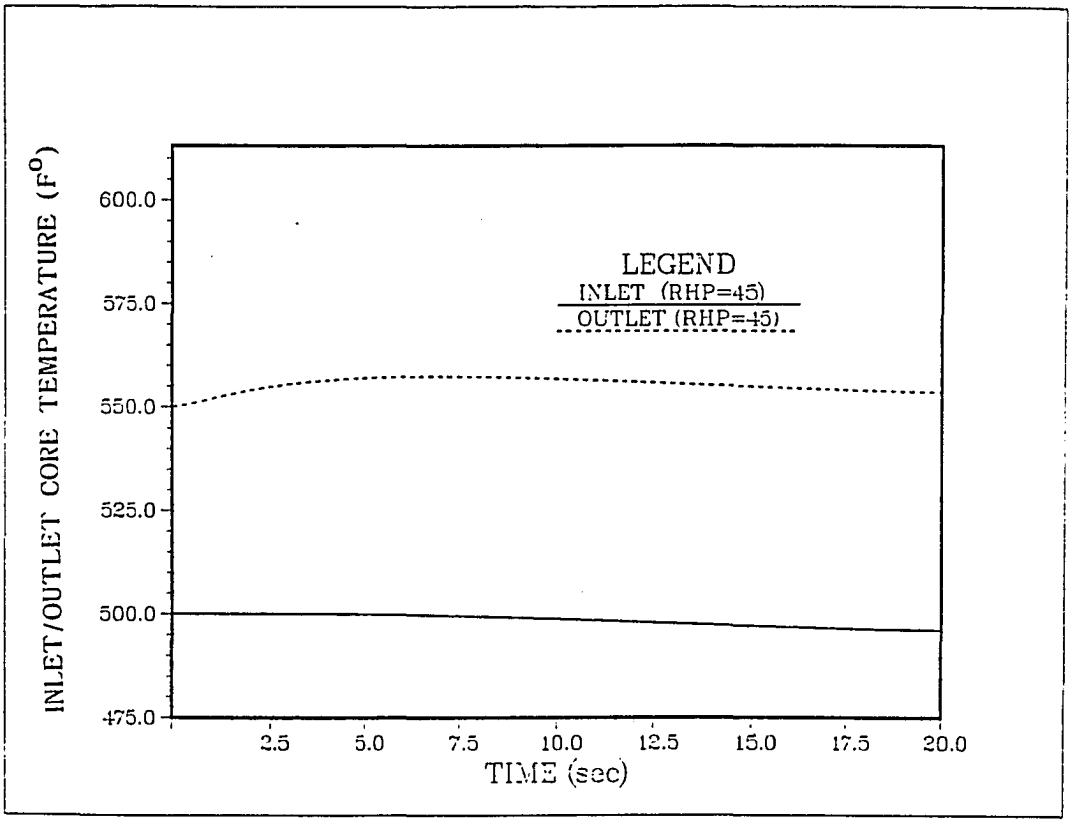

Figure 5.2--Continued

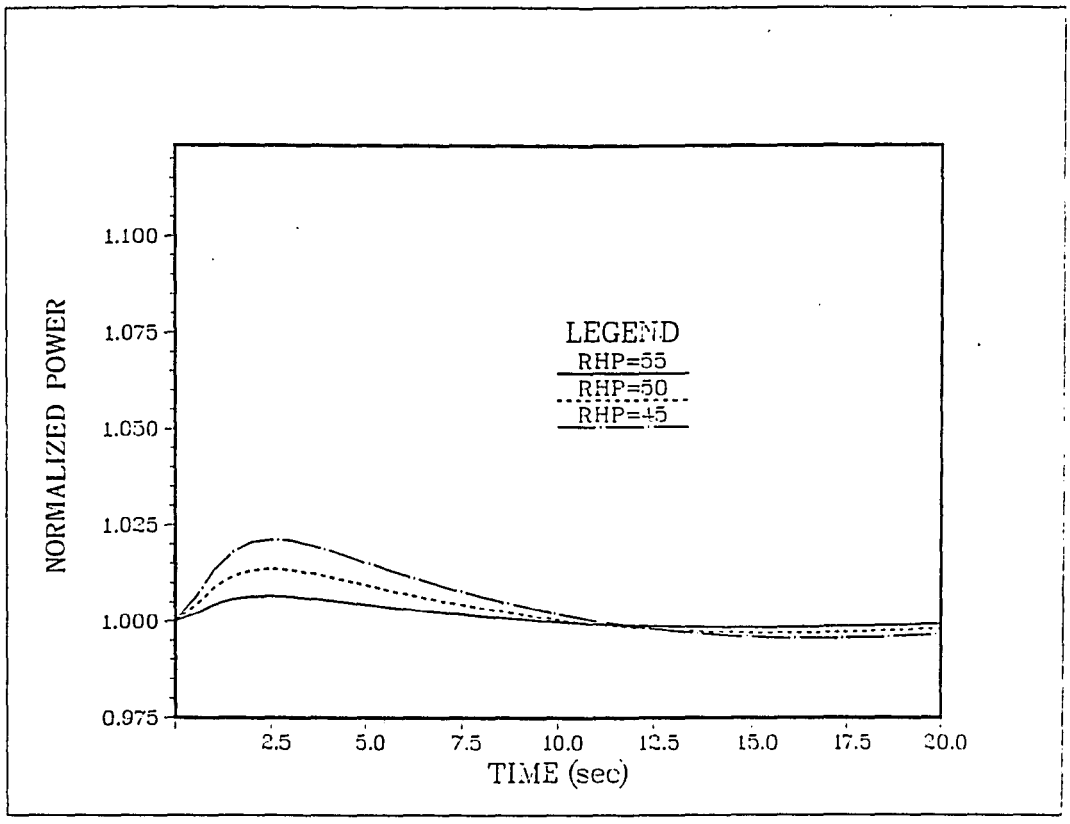

Figure 5.2 PIUS System Response to a Reduction of the Circulation Pump Pressure Head during Fictitious Blockage on WNL.--Continued

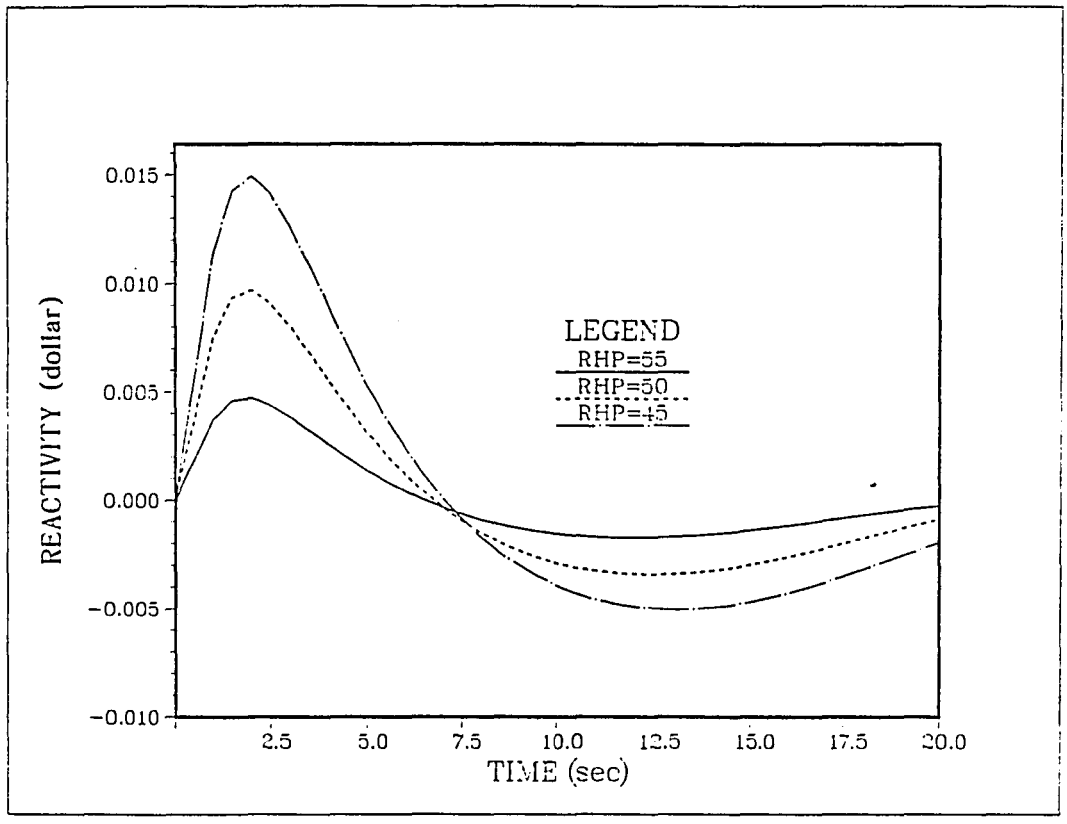

Figure 5.2--Continued

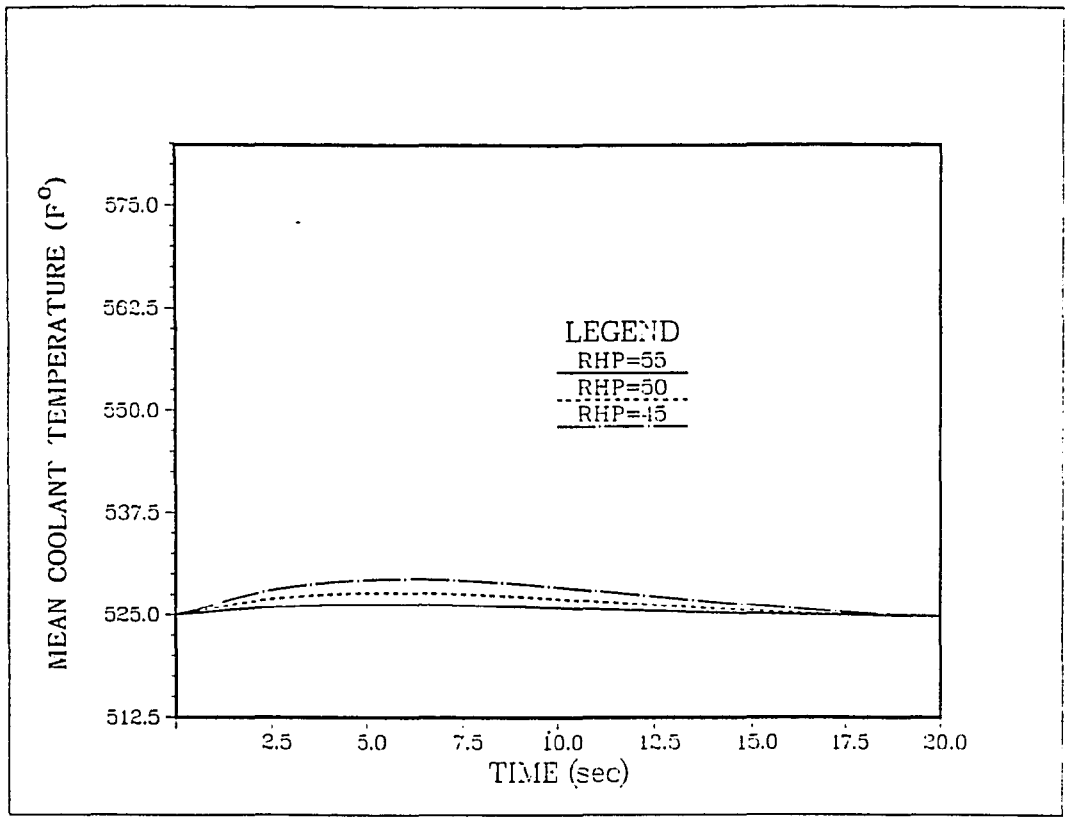

Figure 5.2--Continued

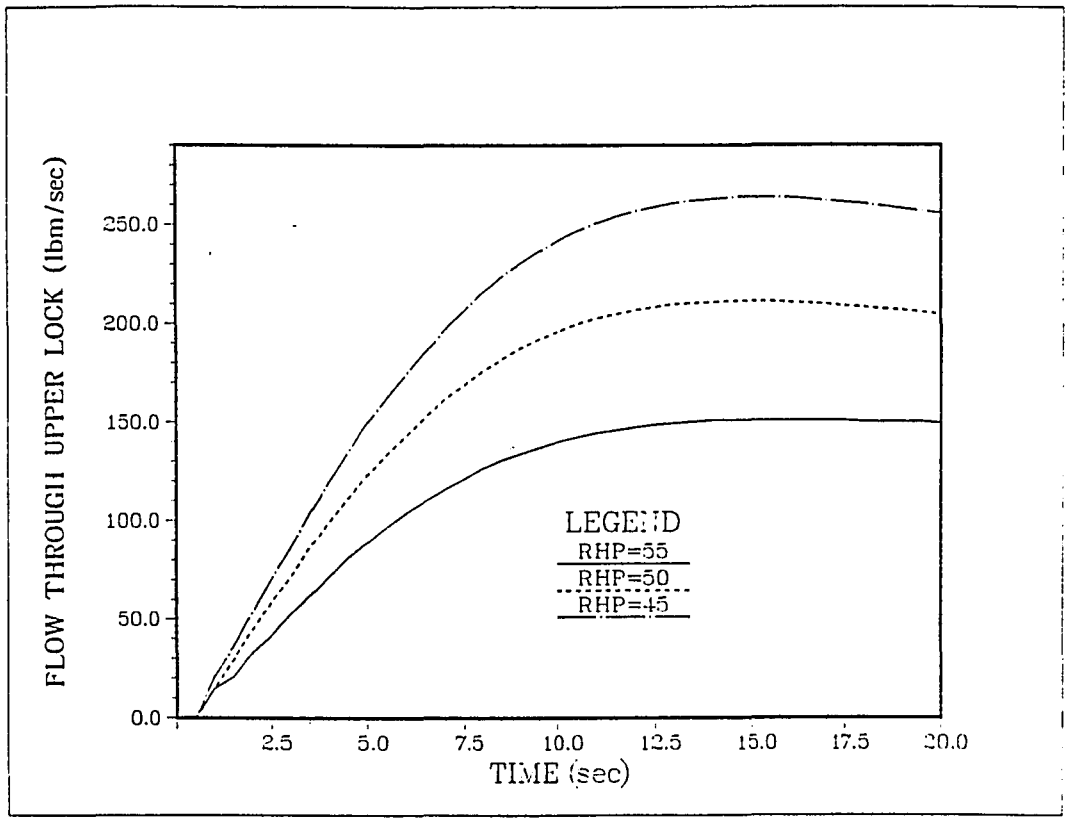

Figure 5.2 PIUS System Response to a Reduction of the Circulation Pump Pressure Head during Fictitious Blockage on WNL.--Continued

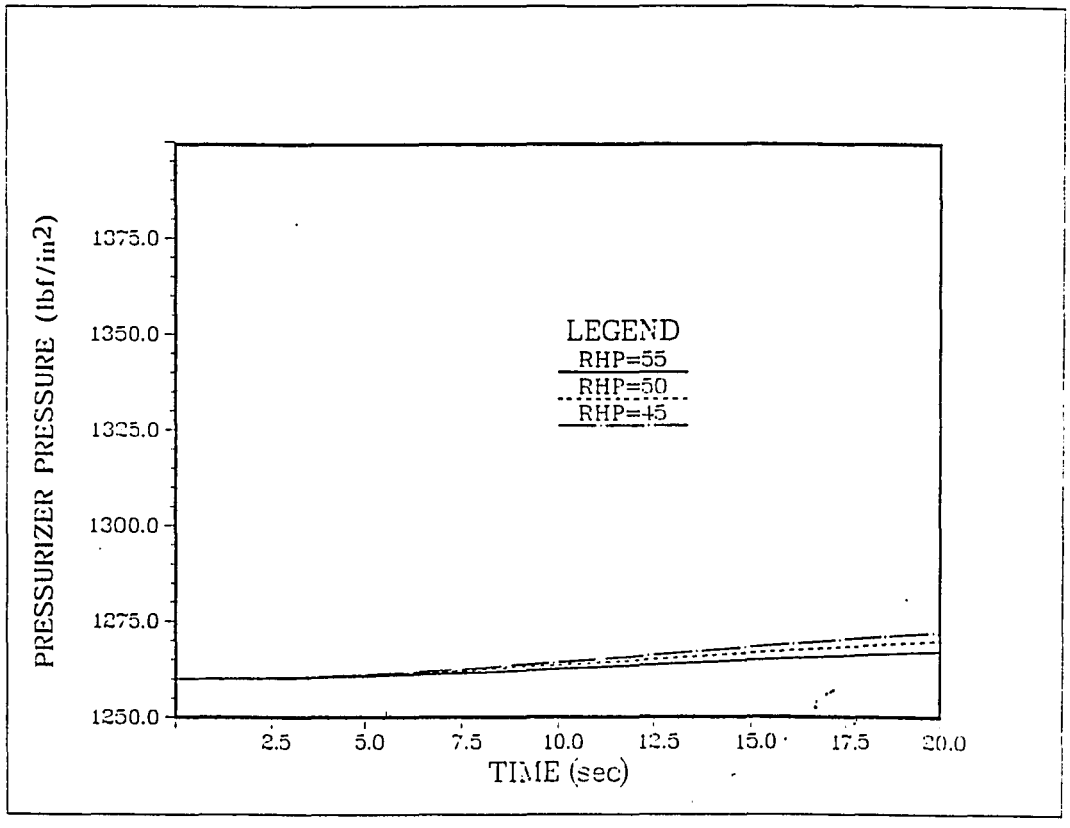

Figure 5.2--Continued

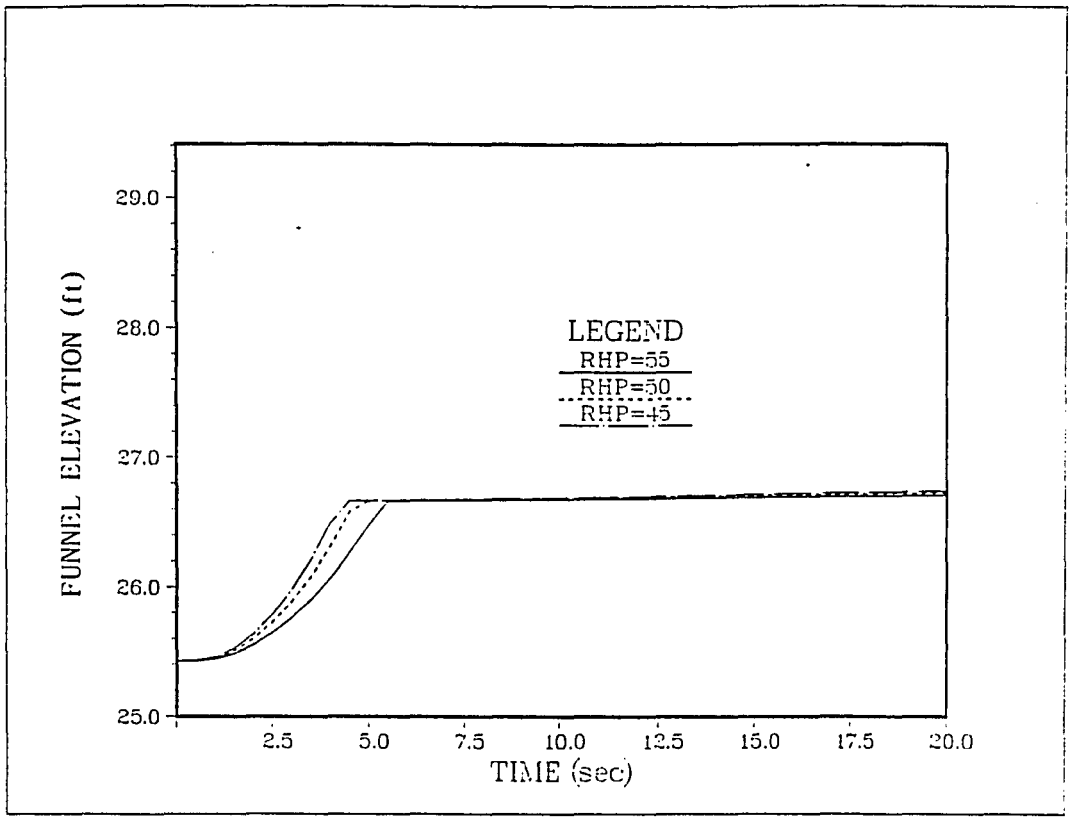

Figure 5.2--Continued

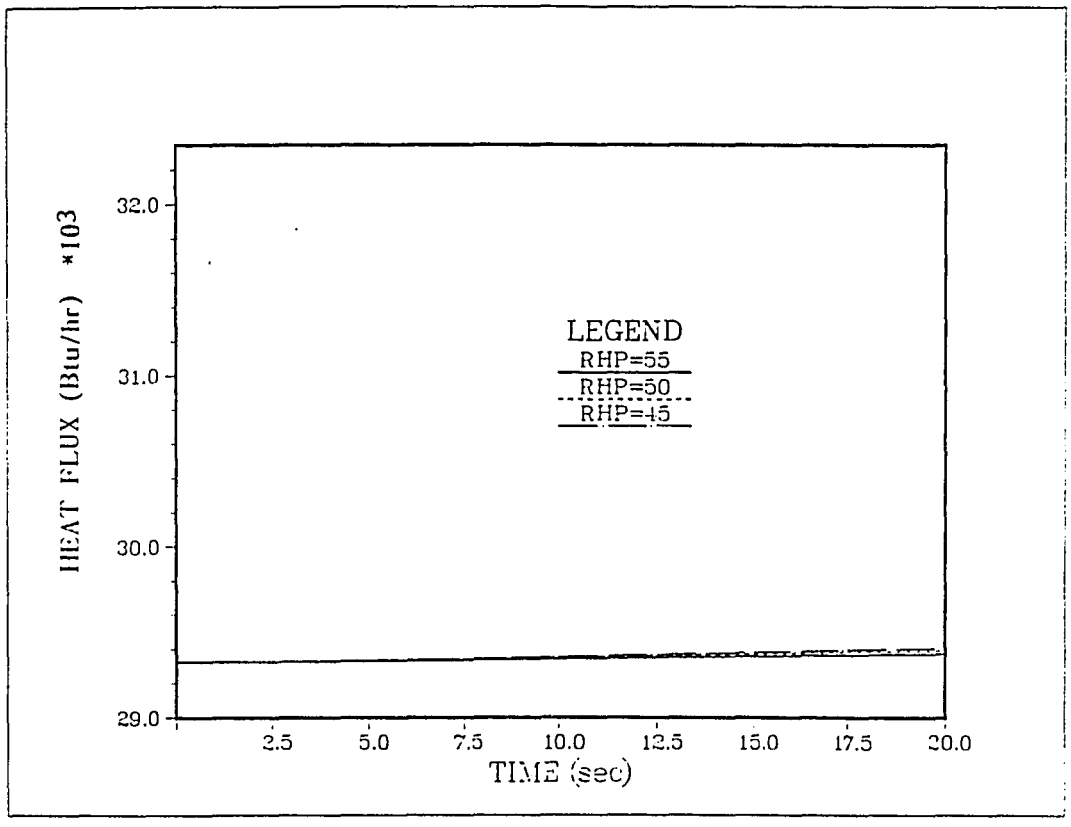

Figure 5.2 PIUS System Response to a Reduction of the Circulation Pump Pressure Head during Fictitious Blockage on WNL.--Continued

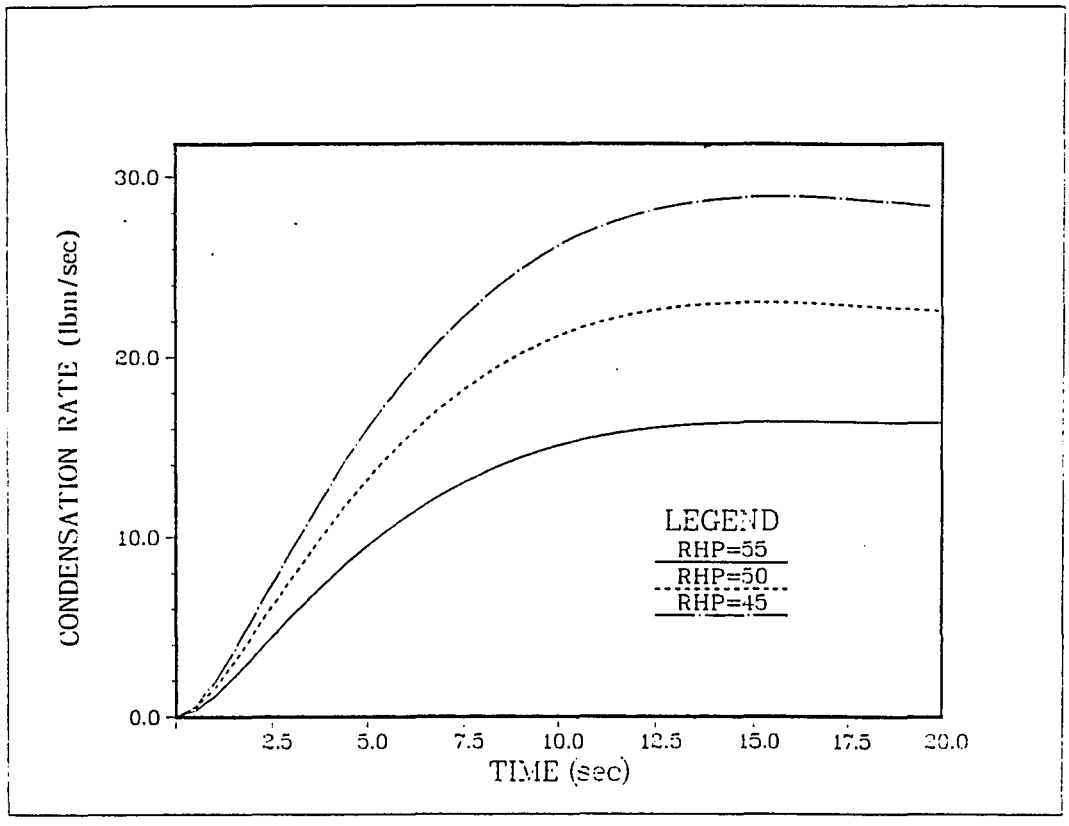

Figure 5.2--Continued

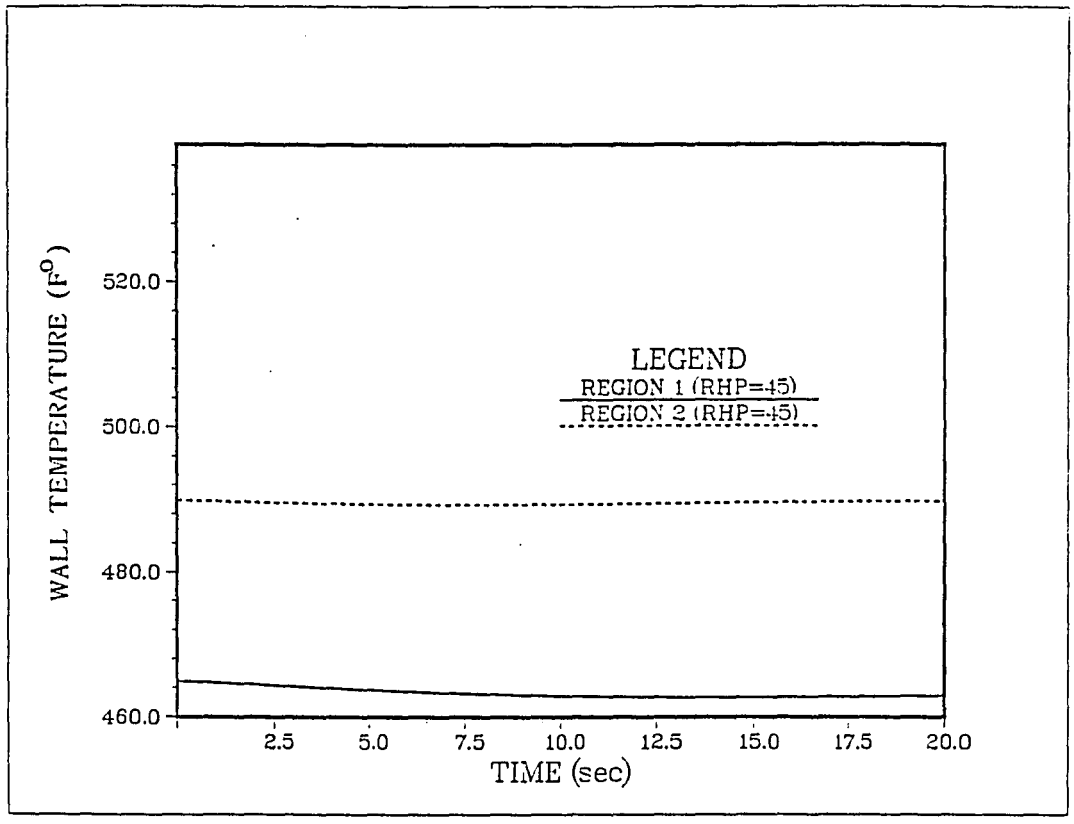

Figure 5.2--Continued

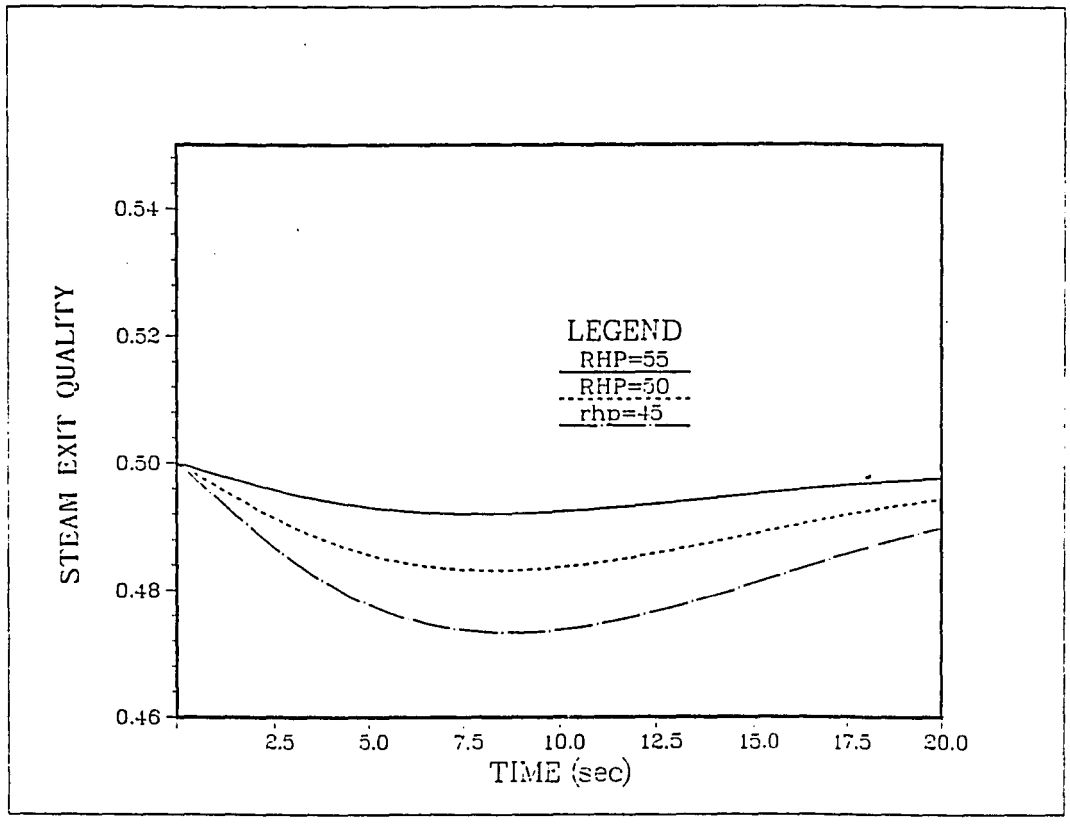

Figure 5.2 PIUS System Response to a Reduction of the Circulation Pump Pressure Head during Fictitious Blockage on WNL.--Continued

rapid recovery to normal value. Fig. 5.3 illustrates the response of the PIUS system for this transient.

This transient also consists of two cases in which the system is allowed first to respond normally to the transient, and then a fictitious blockage on the lower density lock is assumed. It is apparent that the PIUS system can withstand this transient by establishing a new steady state without being shutdown for the first case. However, in the second case, the system seems to become first critical and then unstable as the transient progresses.

As expected the system is more safe in the first case. It should be noticed that the flow through the upper lock in the second case is entering the primary loop. Also, Fig. 5.3 shows how the fuel temperature decreases in the first case. Consequently, reactor power drops to a lower and safe level where the PIUS system becomes slightly subcritical as can be seen from the reactivity response.

The fourth transient was introduced as a twentyfive cent reactivity step insertion. Fig. 5.4 illustrates the PIUS system response during such a transient. A comparison was also made between the behavior of the system for the two cases (with and without borated water inflow).

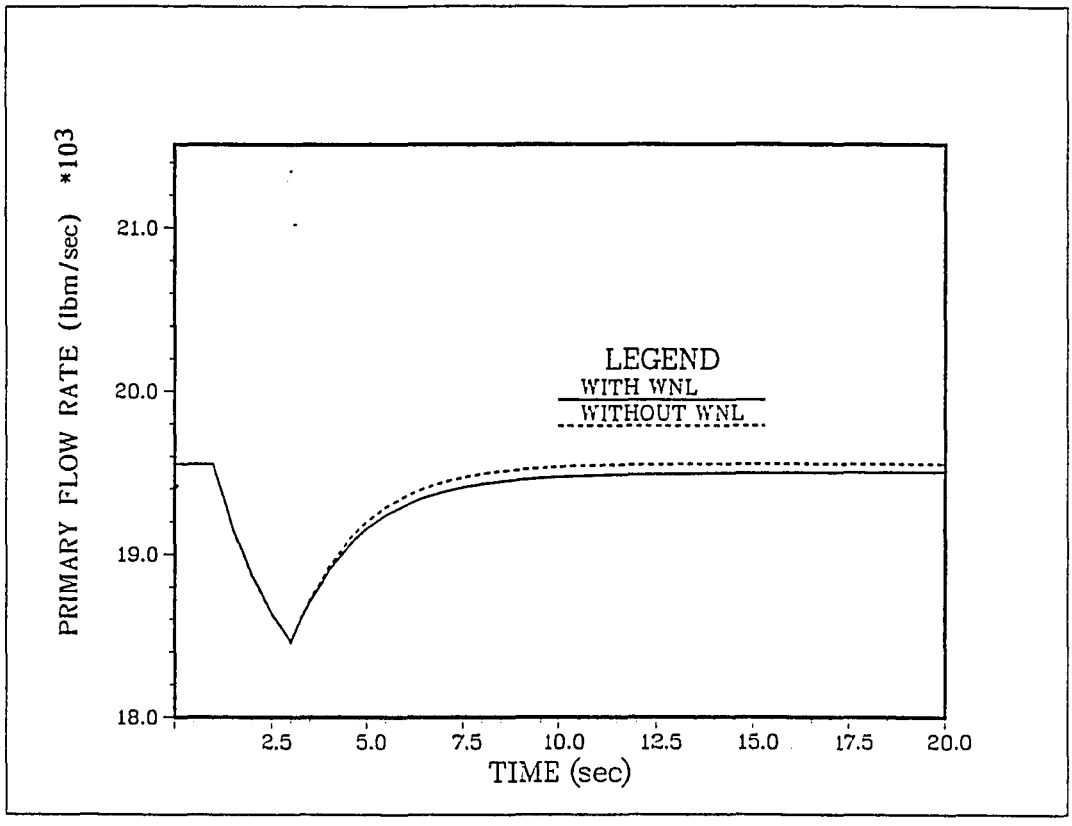

Figure 5.3 PIUS System Response to an Electrical Power Interruption

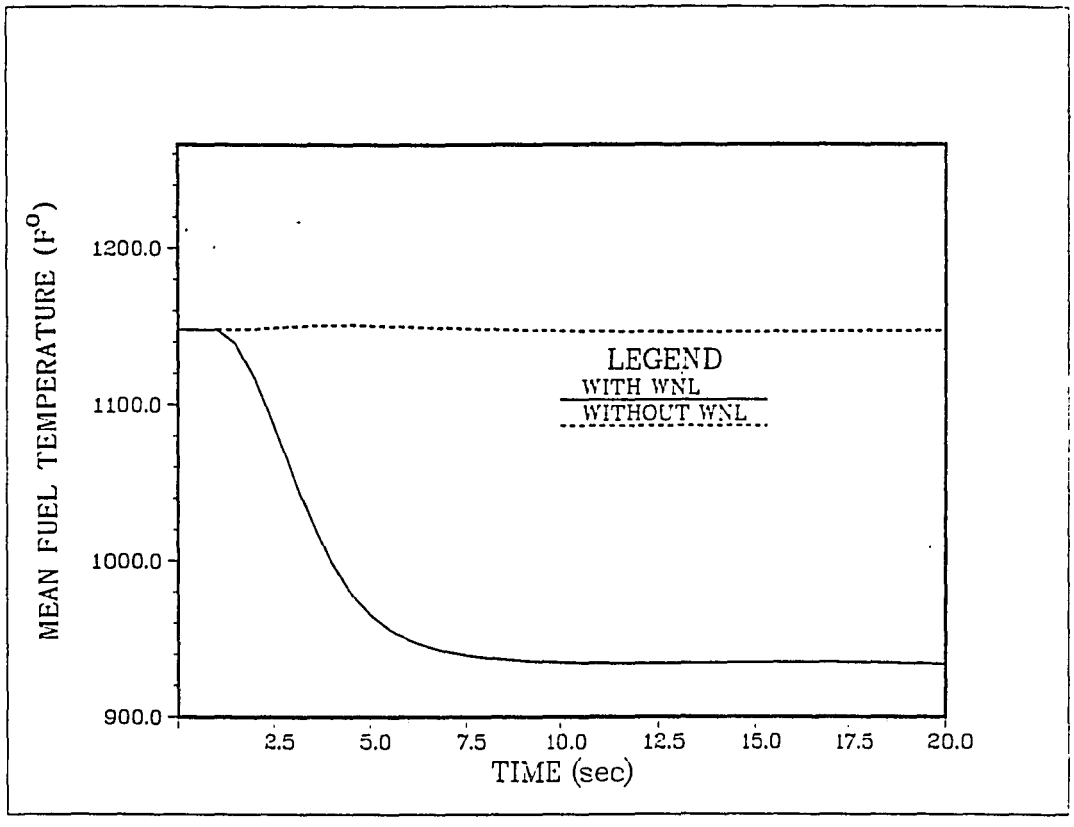

Figure 5.3--Continued

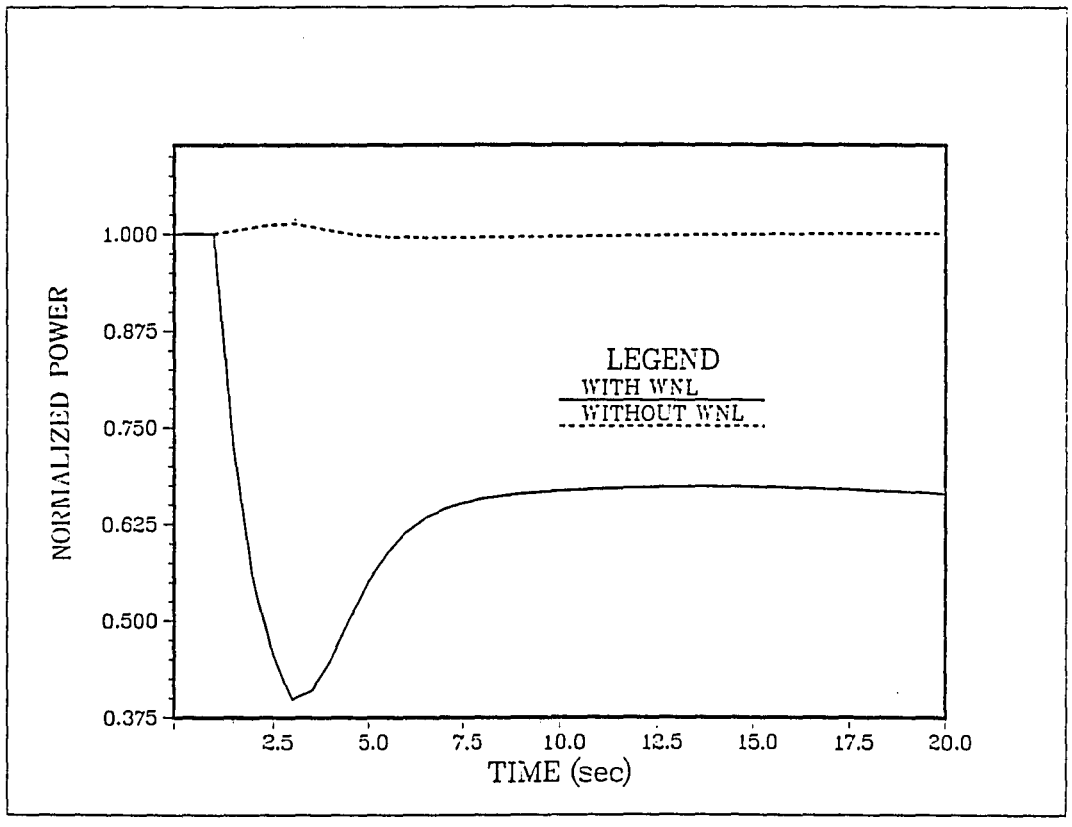

Figure 5.3--Continued

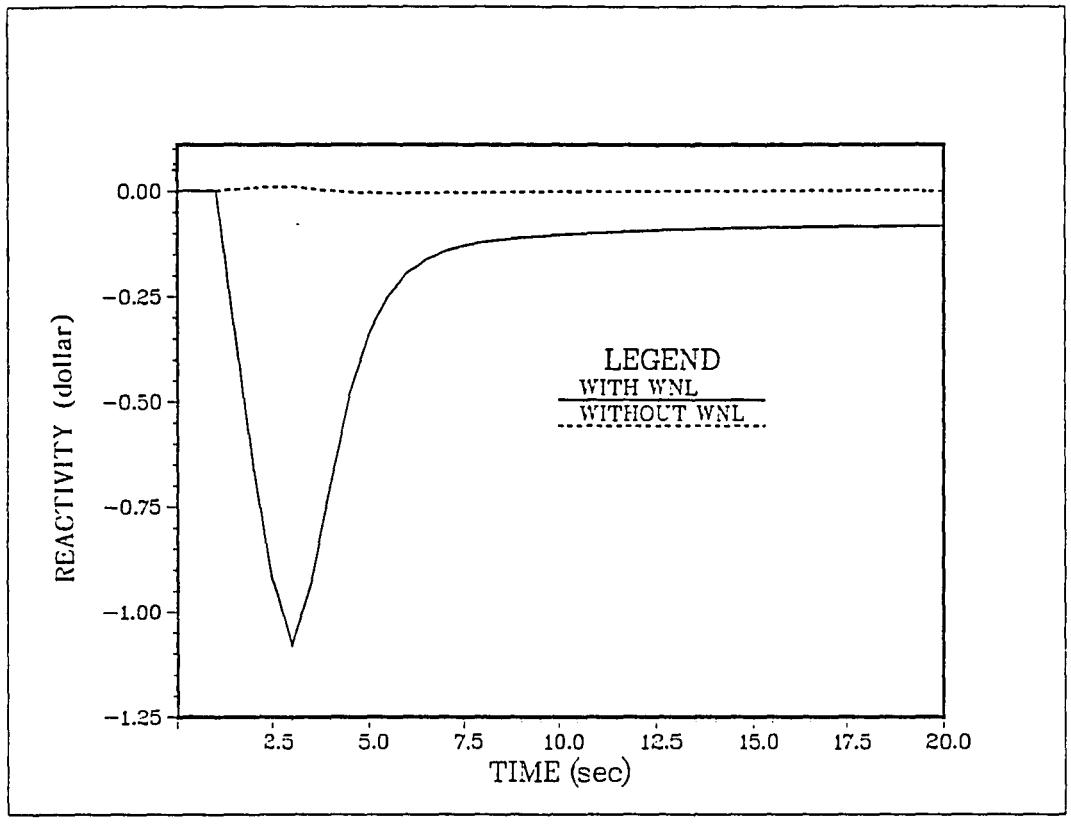

Figure 5.3 PIUS System Response to an Electrical Power Interruption.--Continued

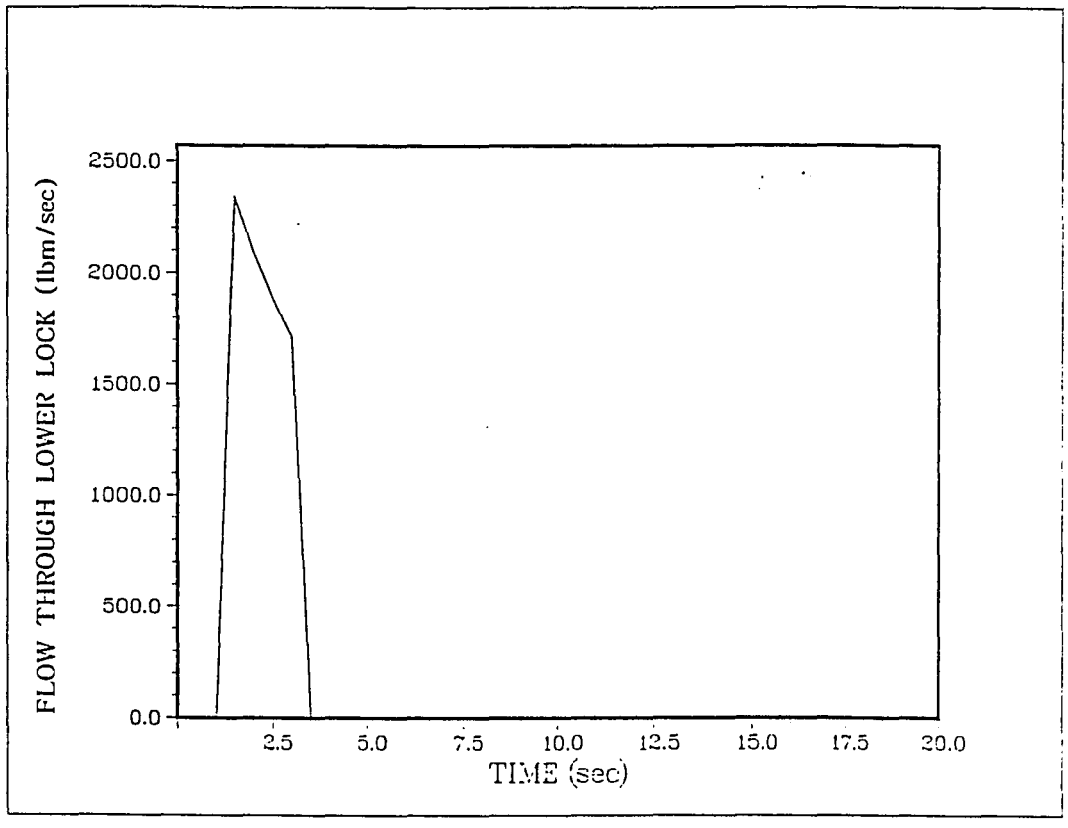

Figure 5.3--Continued

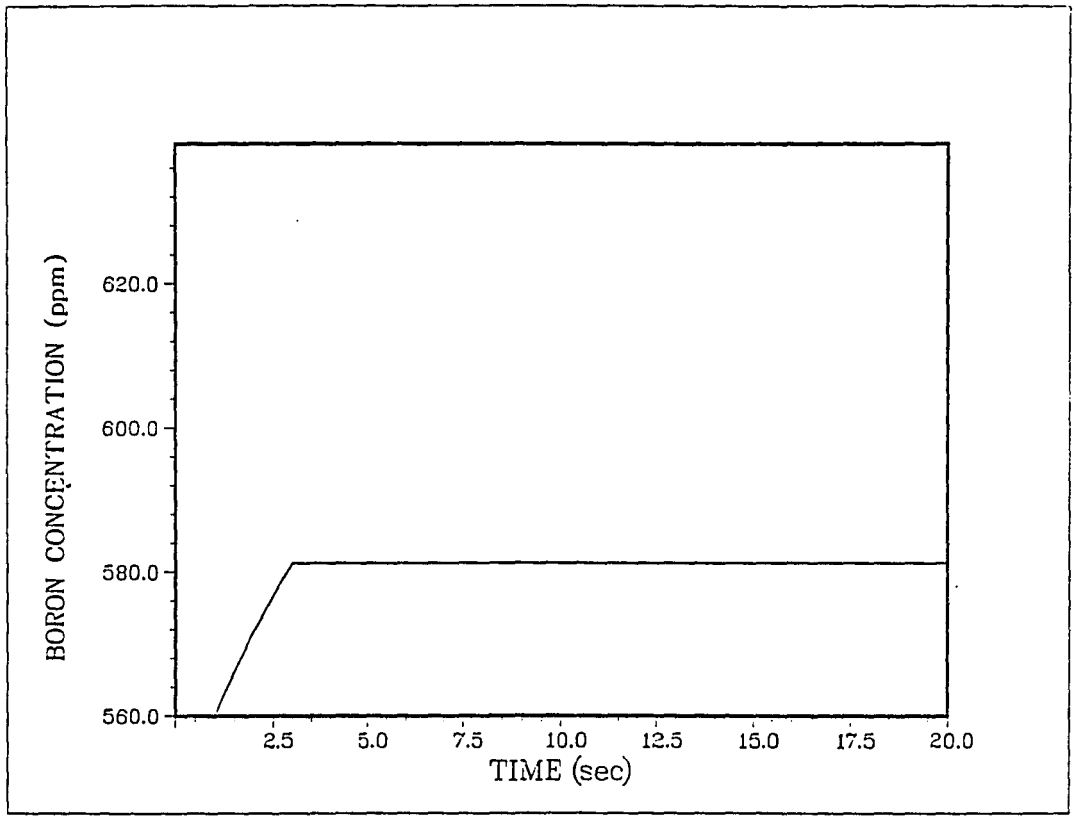

Figure 5.3--Continued

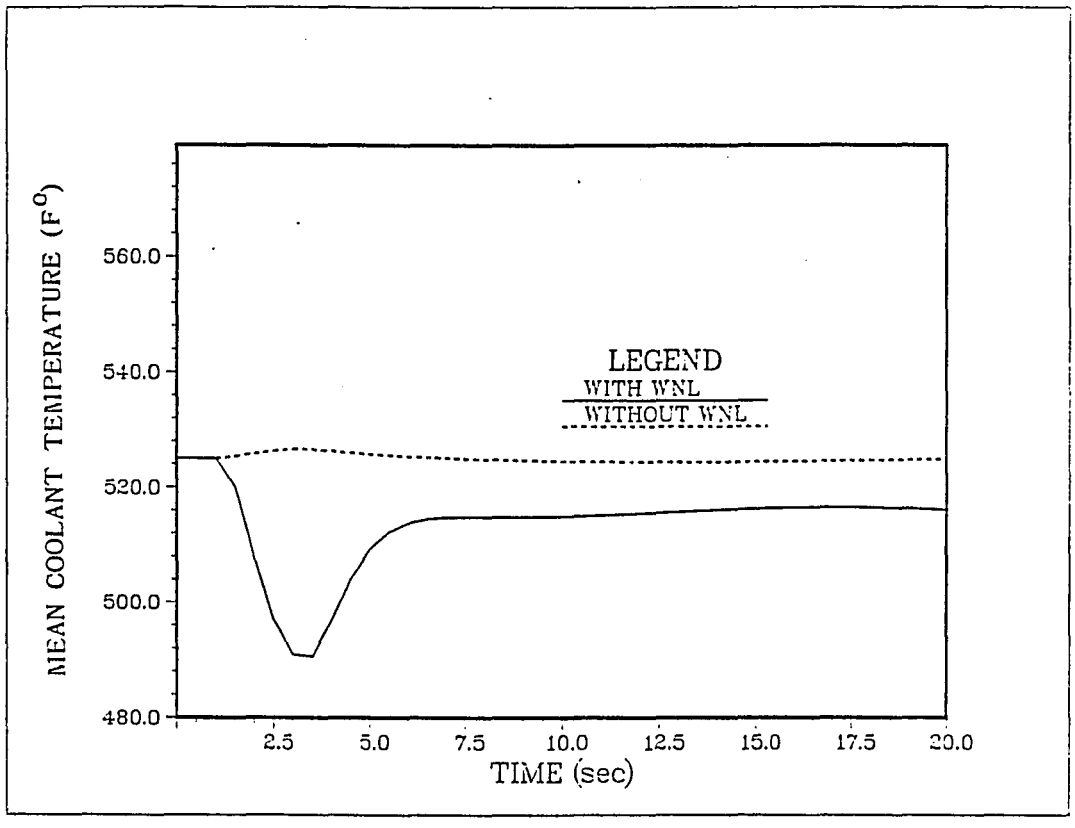

Figure 5.3 PIUS System Response to an Electrical Power Interruption.--Continued

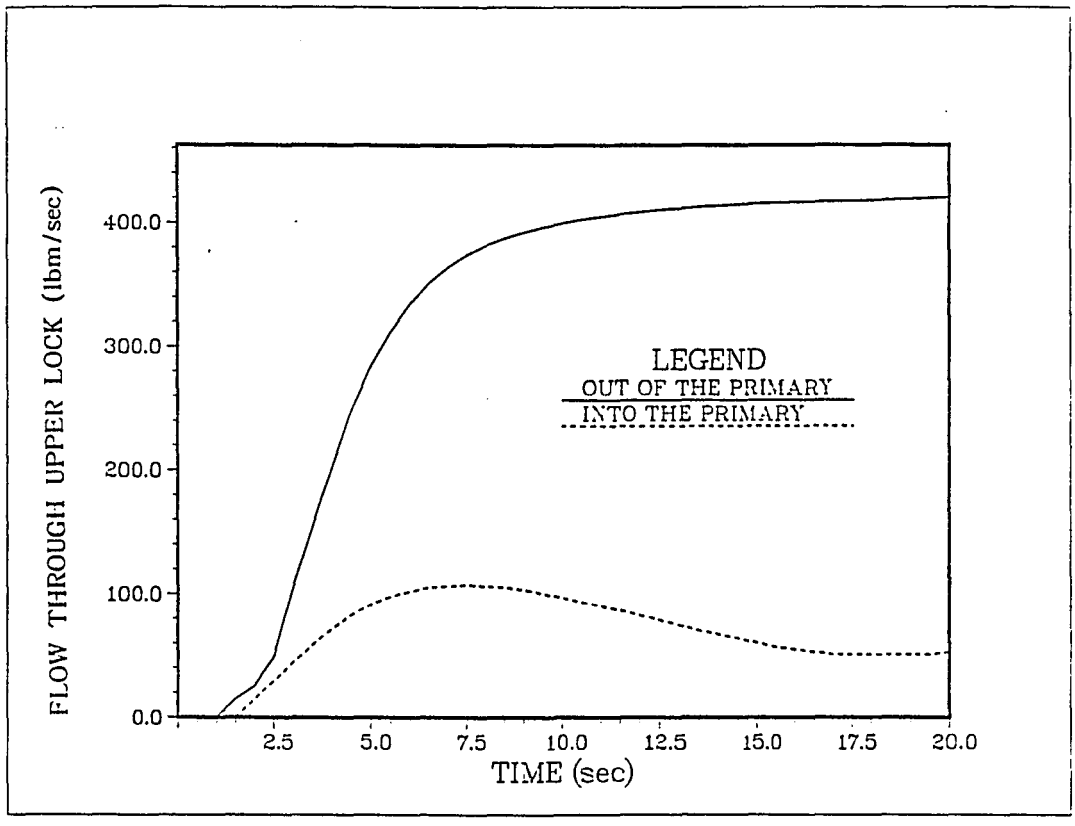

Figure 5.3--Continued

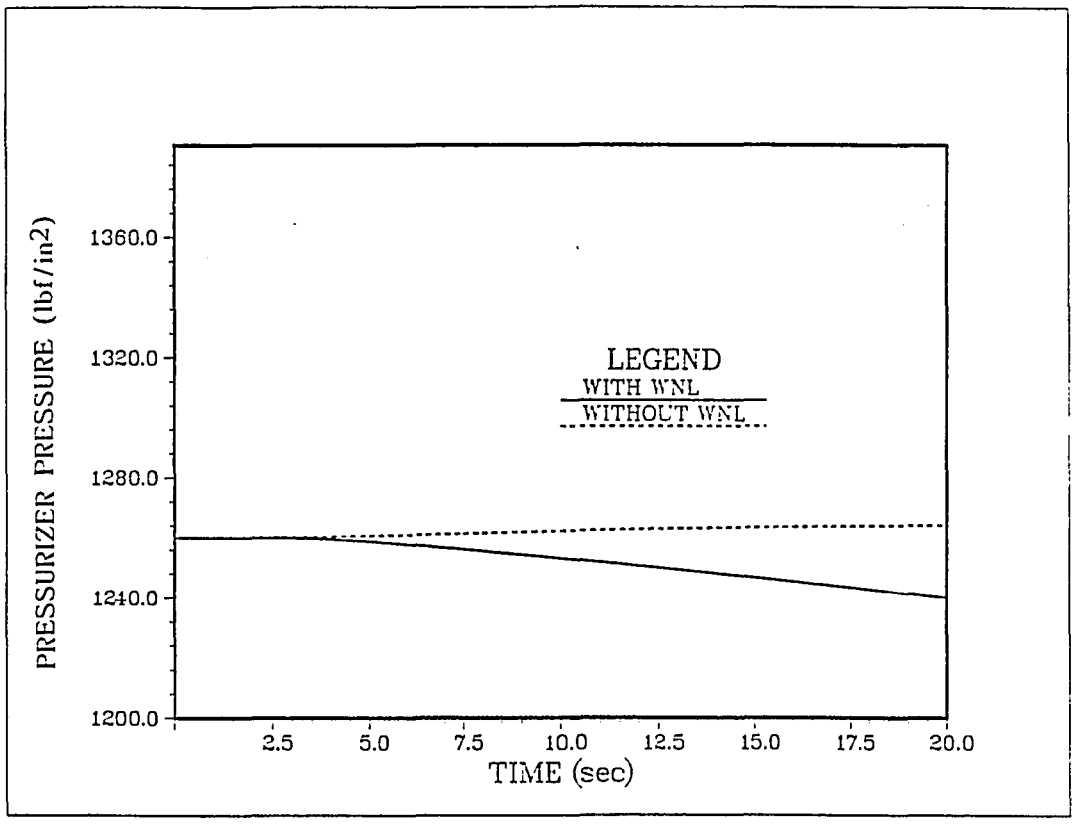

Figure 5.3--Continued

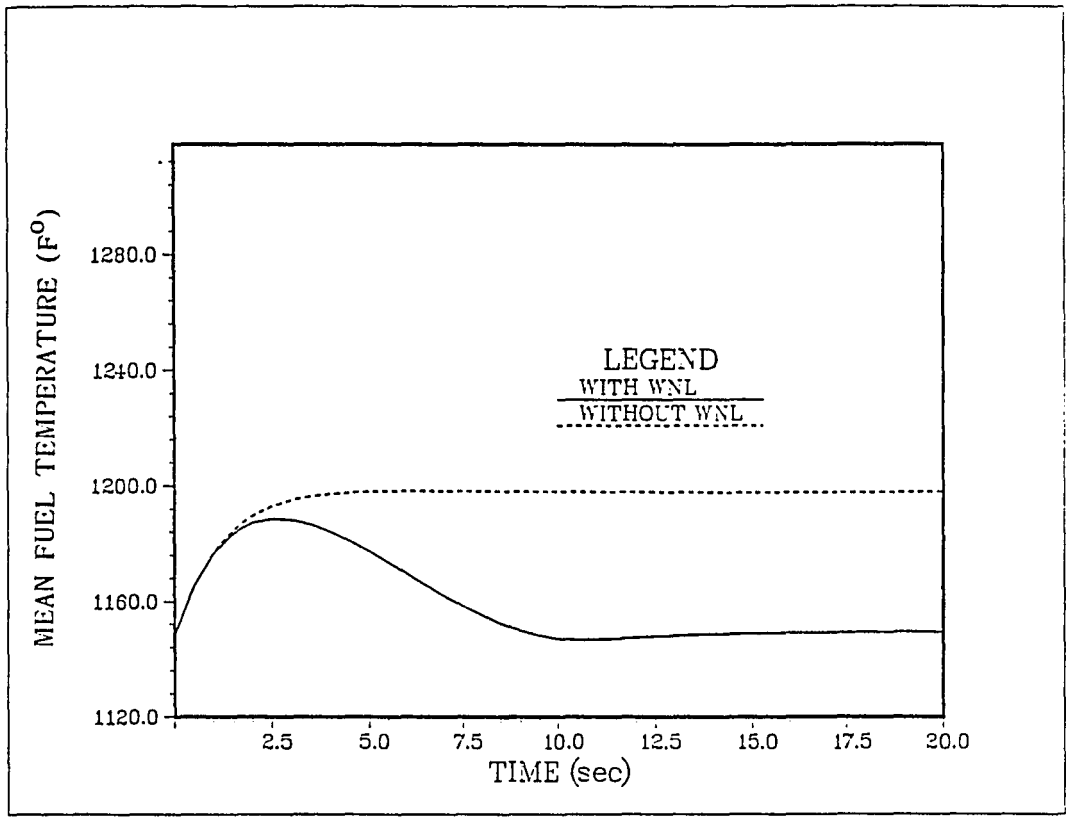

Figure 5.4 PIUS System Response to a Twenty-Five Cent Reactivity Insertion

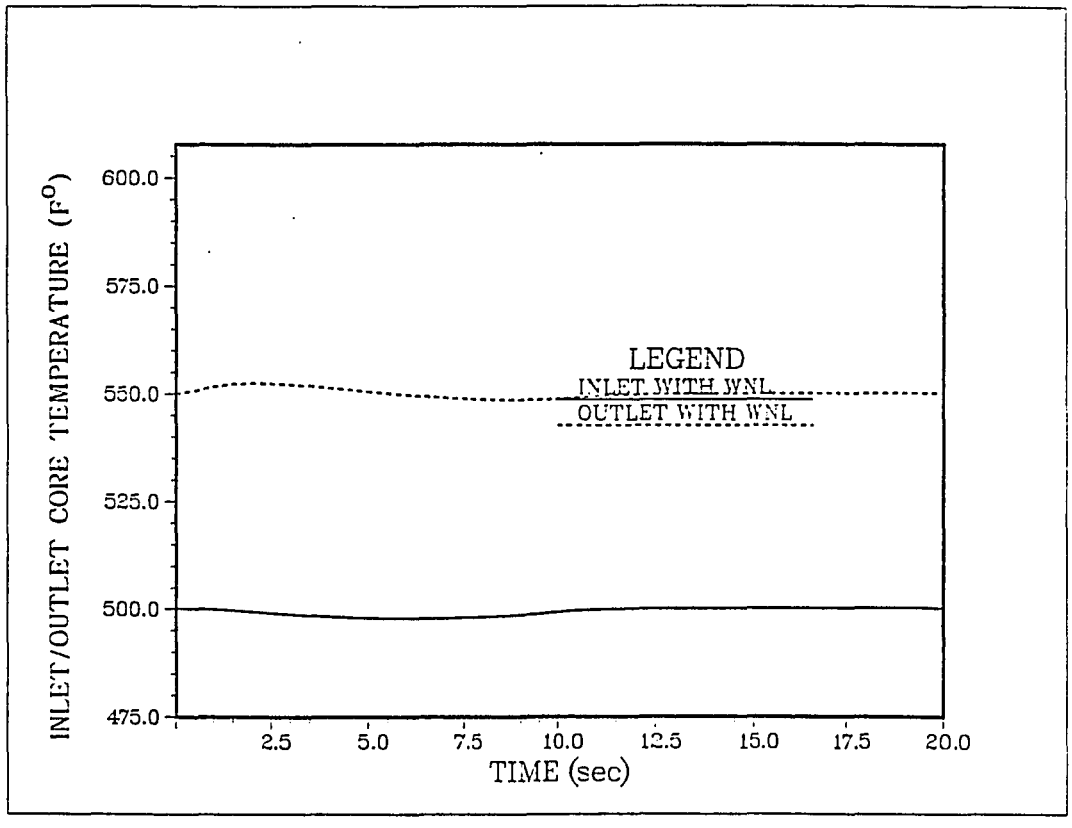

Figure 5.4--Continued

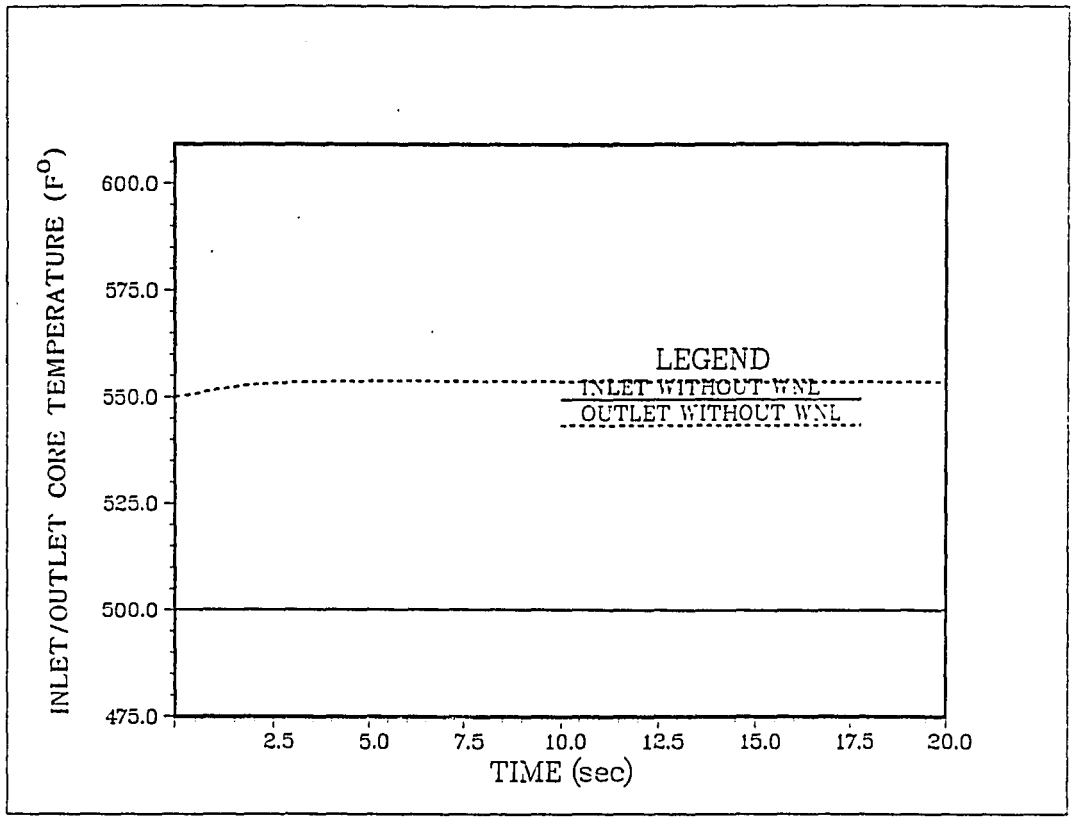

Figure 5.4--Continued

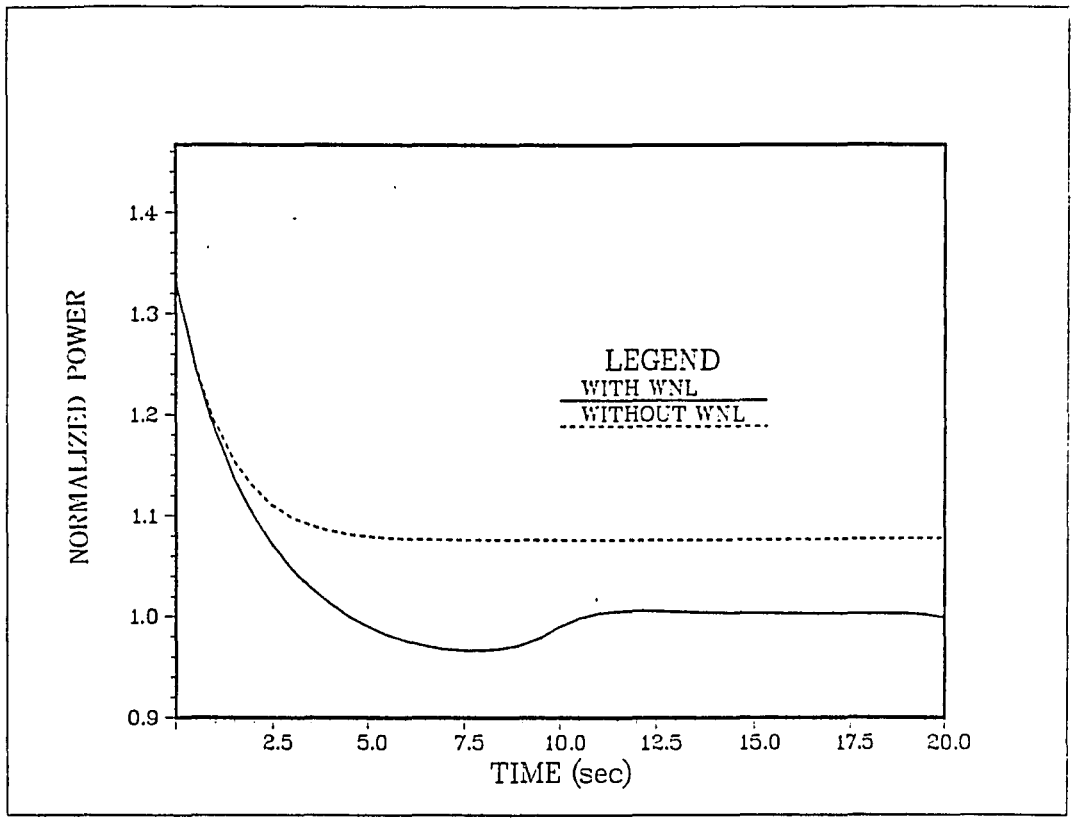

Figure 5.4 PIUS System Response to a Twenty-Five Cent Reactivity Insertion.--Continued

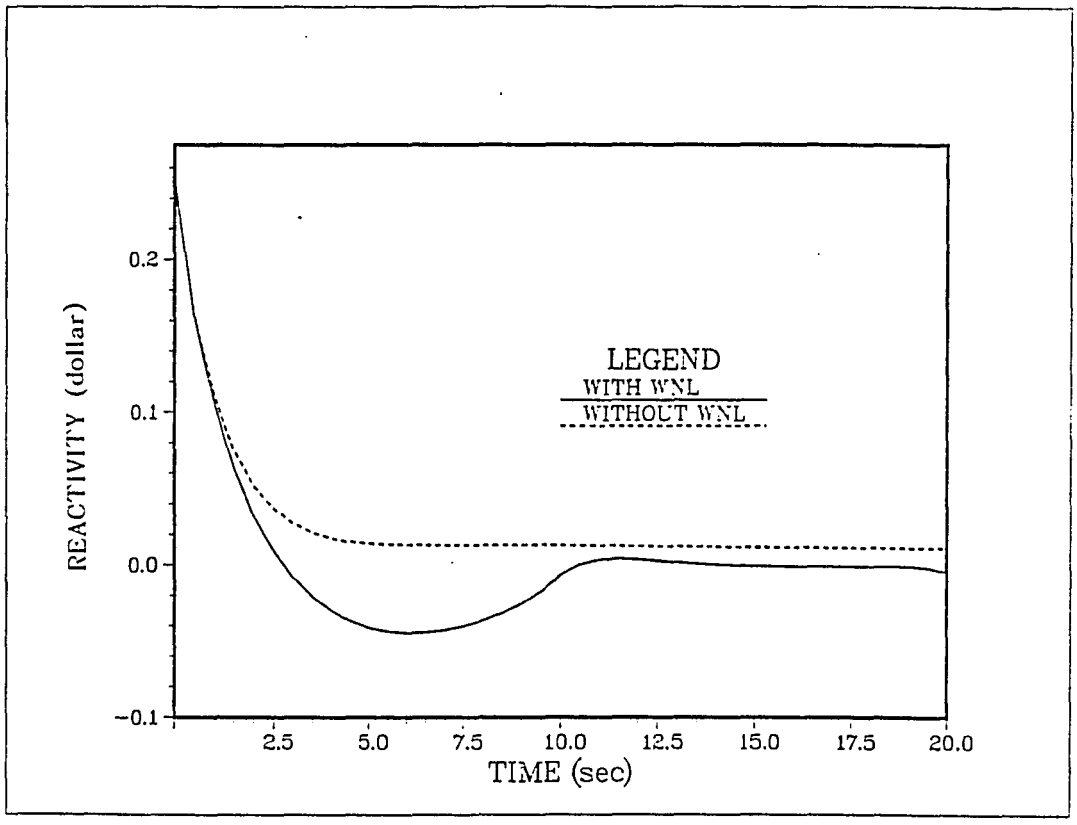

Figure 5.4--Continued

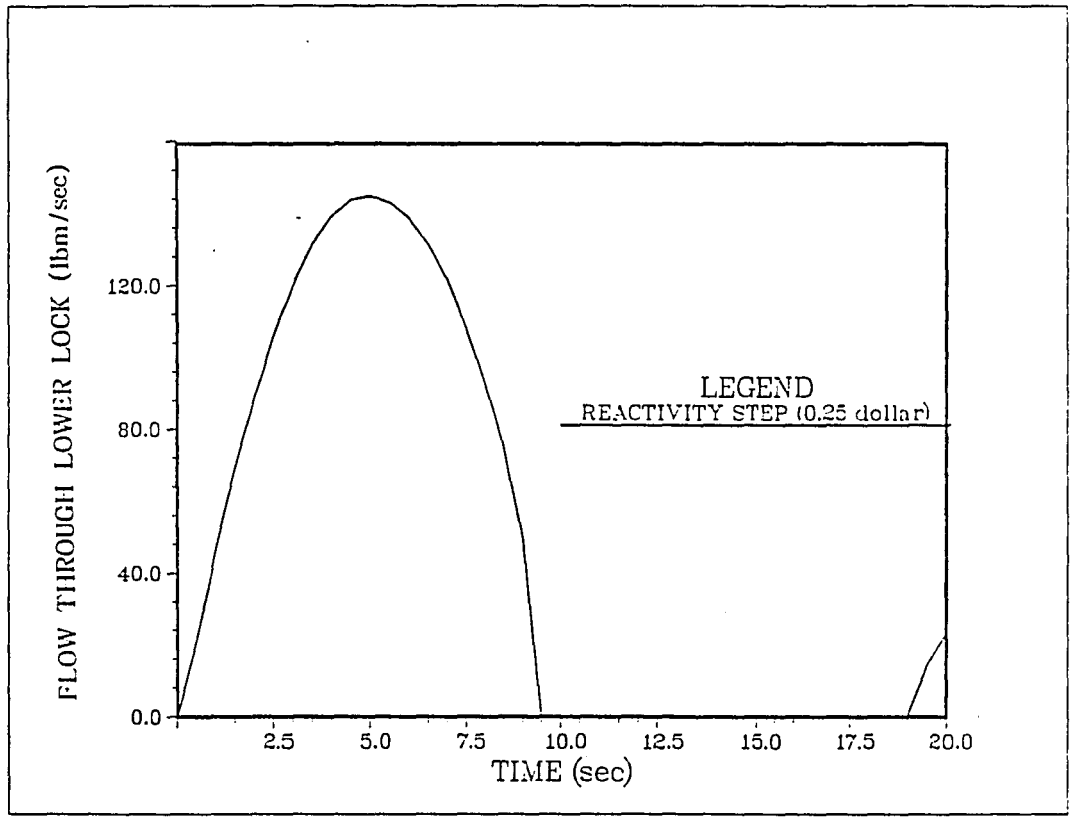

Figure 5.4--Continued

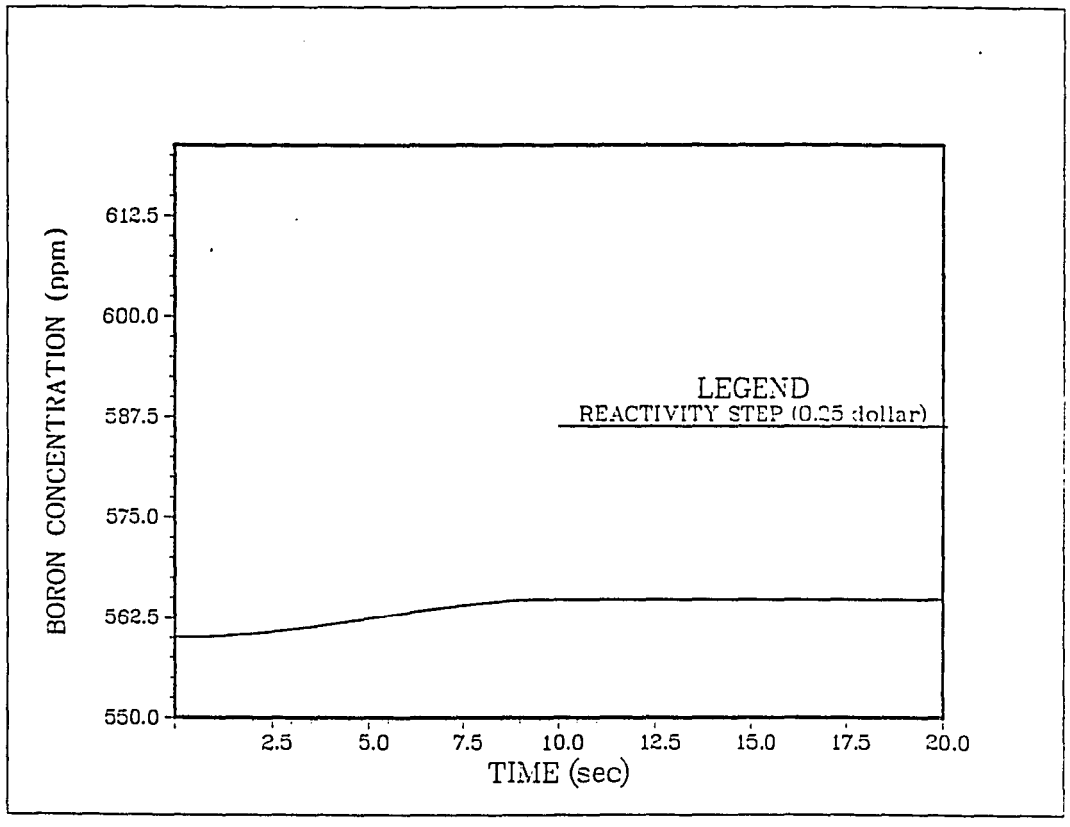

Figure 5.4 PIUS System Response to a Twenty-Five Cent Reactivity Insertion.--Continued

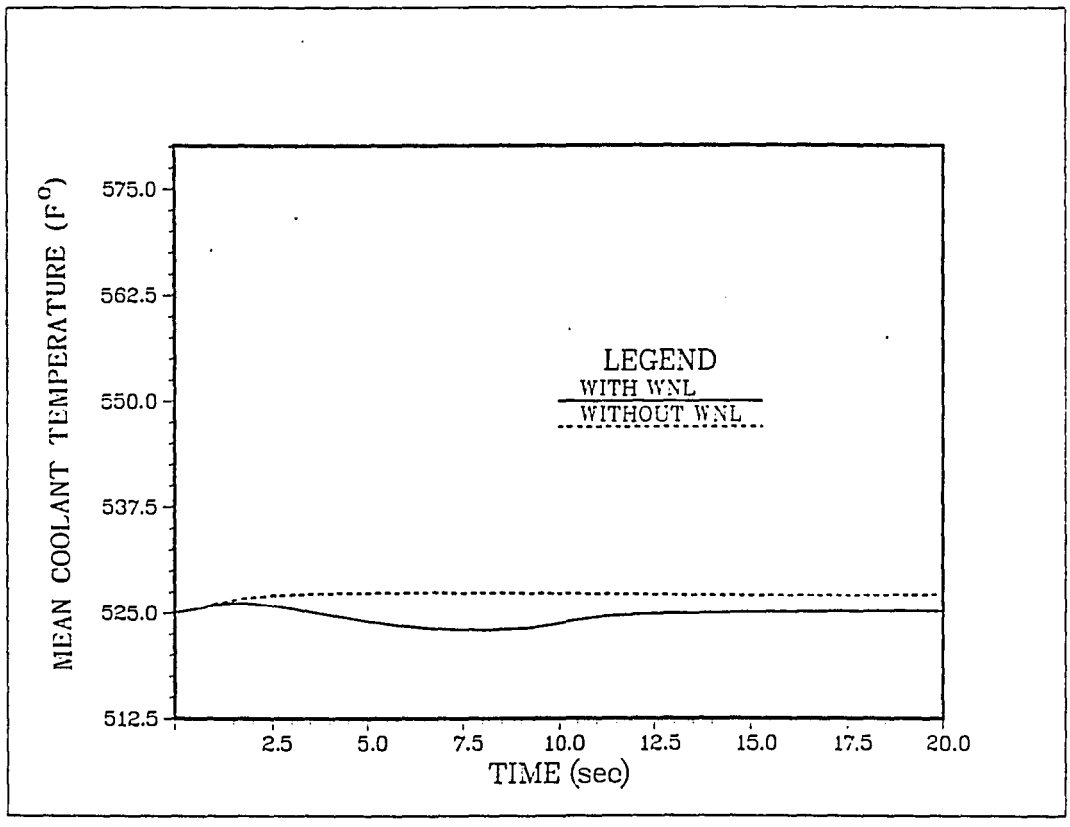

Figure 5.4--Continued

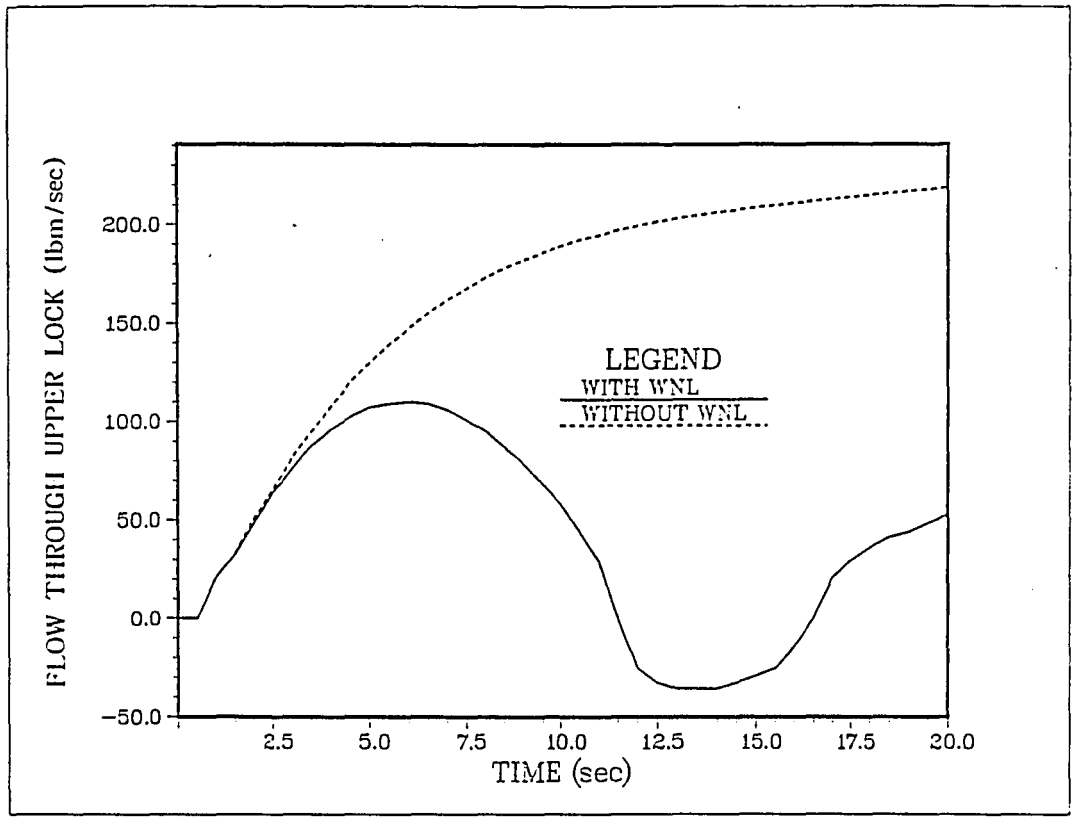

Figure 5.4--Continued

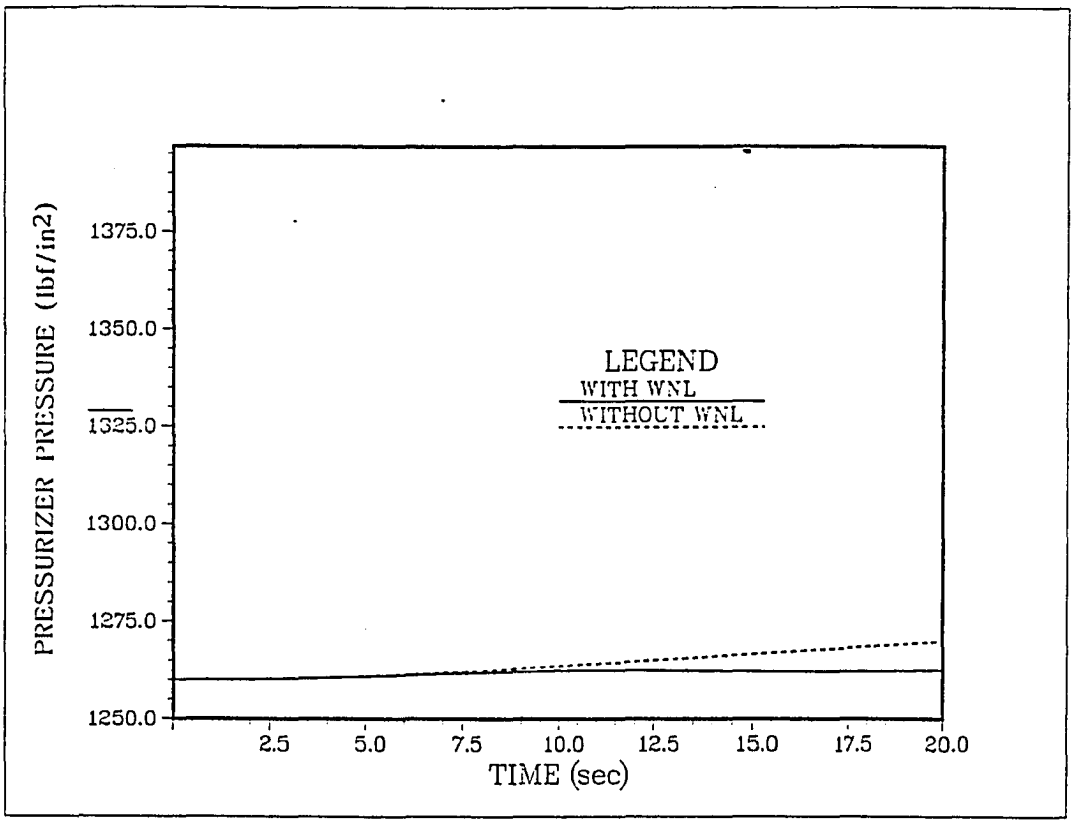

Figure 5.4 PIUS System Response to a Twenty-Five Cent Reactivity Insertion.--Continued

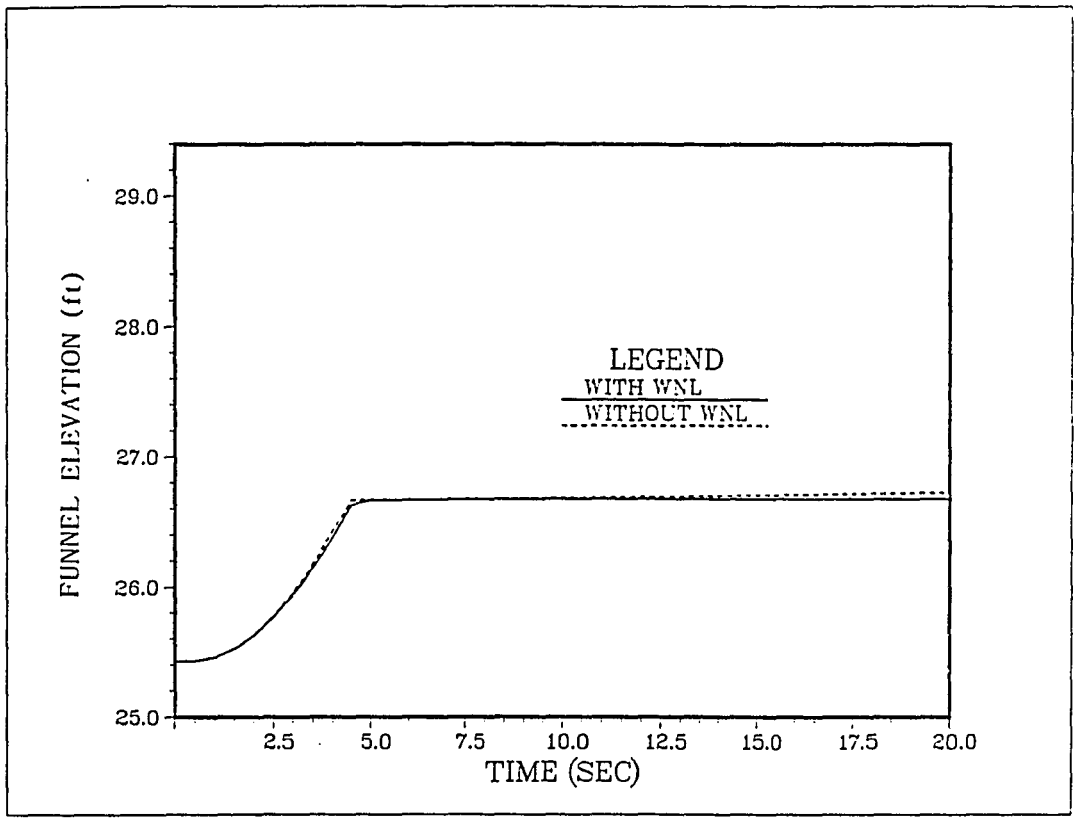

Figure 5.4--Continued

Following the reactivity step, a decrease in the total reactivity can be noticed for both cases. Such a decrease is attributed to the increase in magnitude of the negative feedback reactivity. However, in the first case (the complete opening of the lower density lock) the total reactivity drops much faster and becomes slightly subcritical due to the fact that additional negative reactivity is added to the system by the incoming pool water. In the second case, the total reactivity is dominated by the feedback effect of the fuel and coolant temperatures.

It can be seen from Fig. 5.4 that the normalized power drops rapidly and returns to its initial level for the first case. In the second case, it takes on new state which is approximately ten percent higher than the initial state. This new state appears to be a critical one.

The last two transients are initiated by changes in feedwater flow rate, first a twenty-five percent decrease, and then a twenty-five percent increase. Each is studied with and without flow through the lower density lock. The secondary system behavior for a flow increase is essentially opposite to that for a flow decrease, although the primary system does

not show the same symmetry. Only the cases of flow decrease are discussed.

Figure 5.5 illustrates the PIUS system response in the case of decreasing the feedwater flow rate, while Figure 5.6 illustrates the PIUS system response in the case of increasing the feedwater flow rate.

After the reduction of the feedwater flow, the heat extracted from the primary side decreases. As a result, the average primary coolant temperature increases slightly, causing the hydrostatic pressure on the primary side to decrease. The violation of the pressure balance across the lower density lock will result in an ingress of pool water into the primary loop. As can be seen from Fig. 5.5, the normalized power starts to drop, as does the fuel temperature. The incoming pool flow that enters the primary loop through the lower lock leaves the primary through the upper density lock.

However, in the case of a fictitious blockage, highly borated pool water enters the primary loop through the upper lock instead. This flow is expected to reduce the potential hazard in case of real situation that is similar to the above transient.

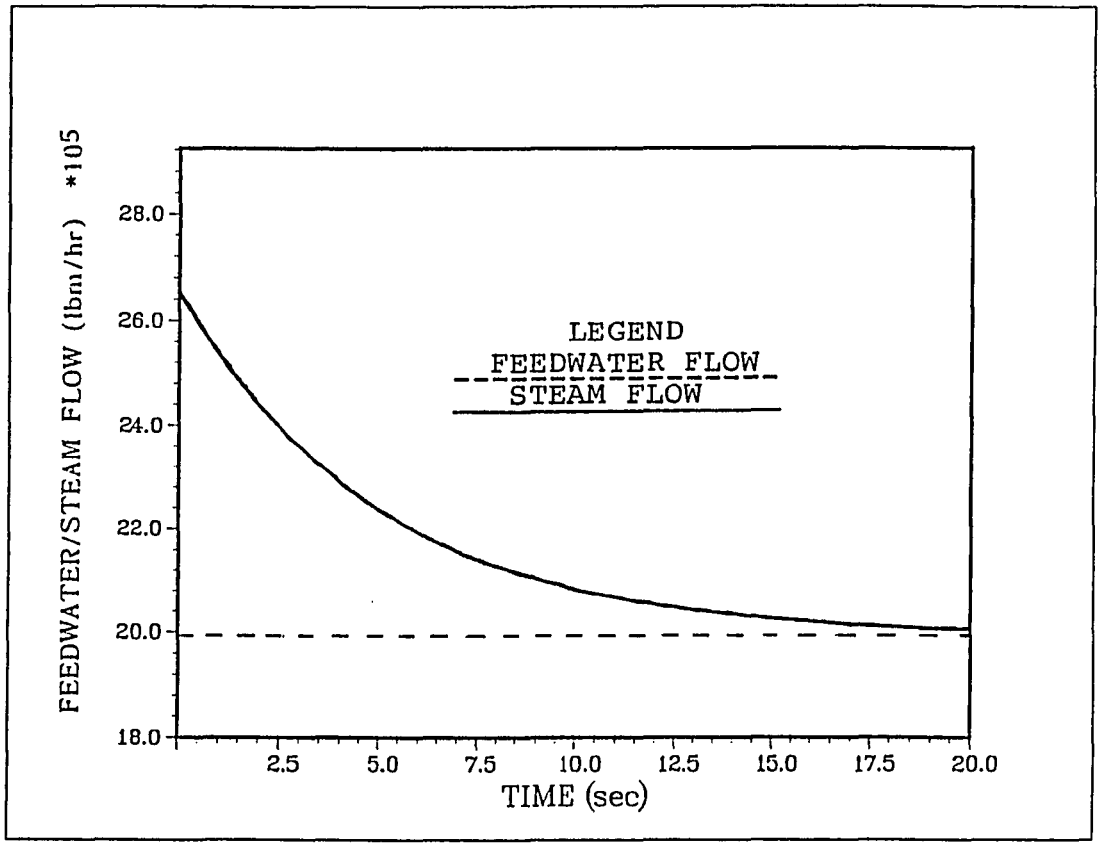

Figure 5.5 PIUS System Response to a Twenty-Five Percent Decrease in the Feedwater Flow Rate

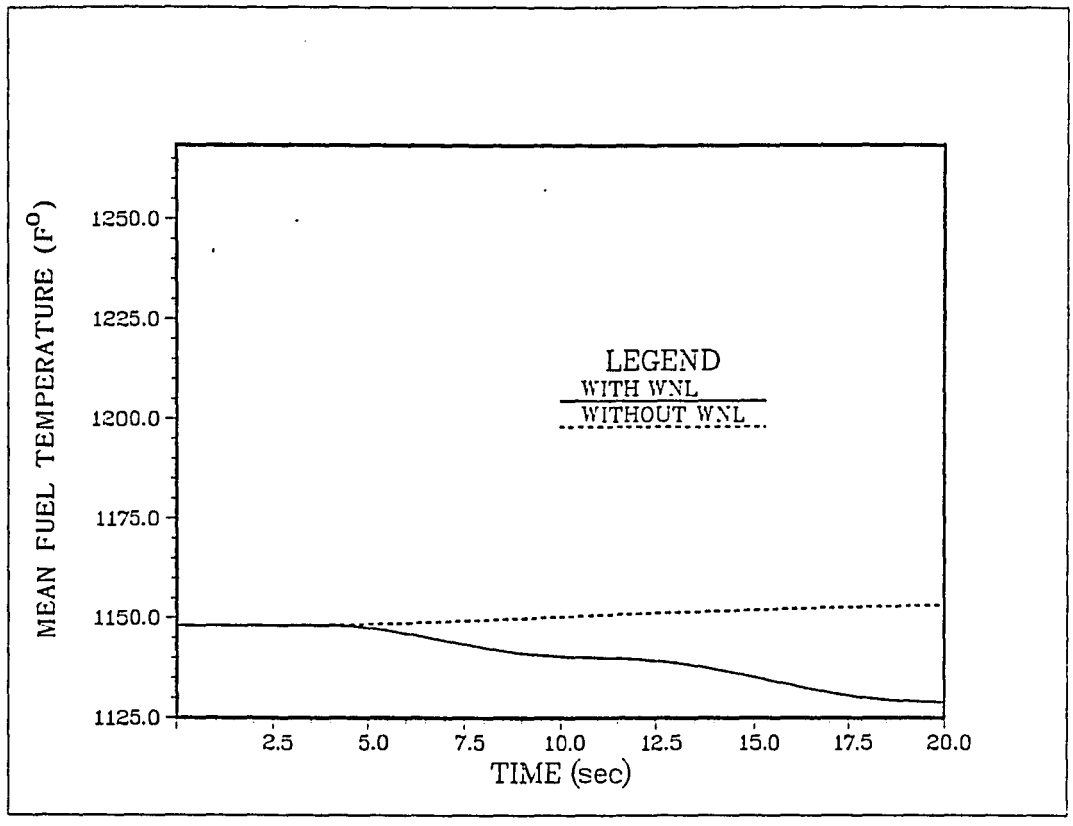

Figure 5.5--Continued

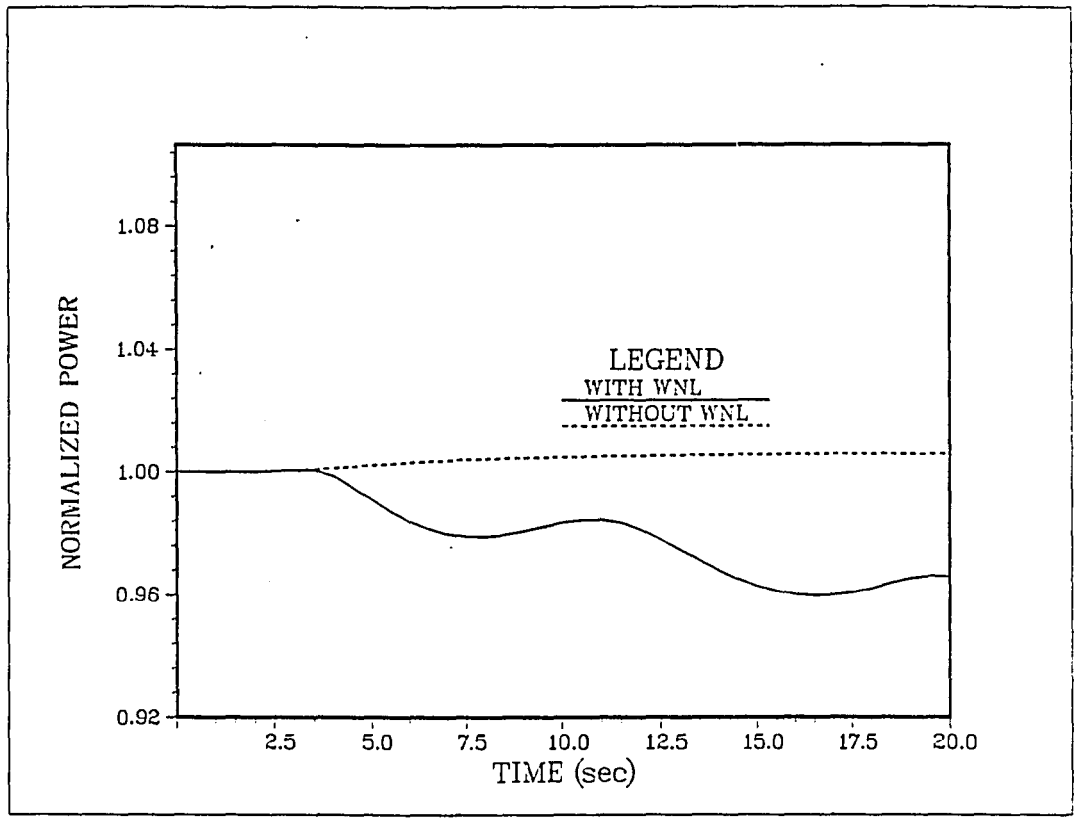

Figure 5.5--Continued

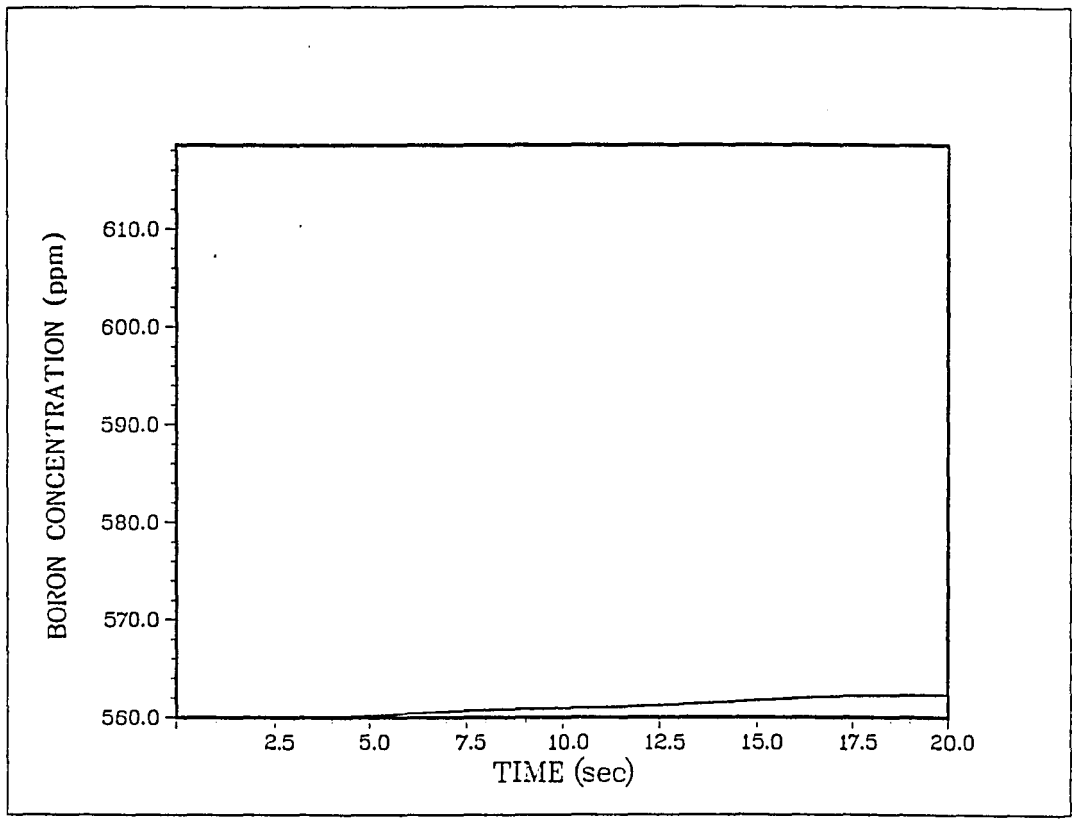

Figure 5.5 PIUS System Response to a Twenty-Five Percent Decrease in the Feedwater Flow Rate.--Continued

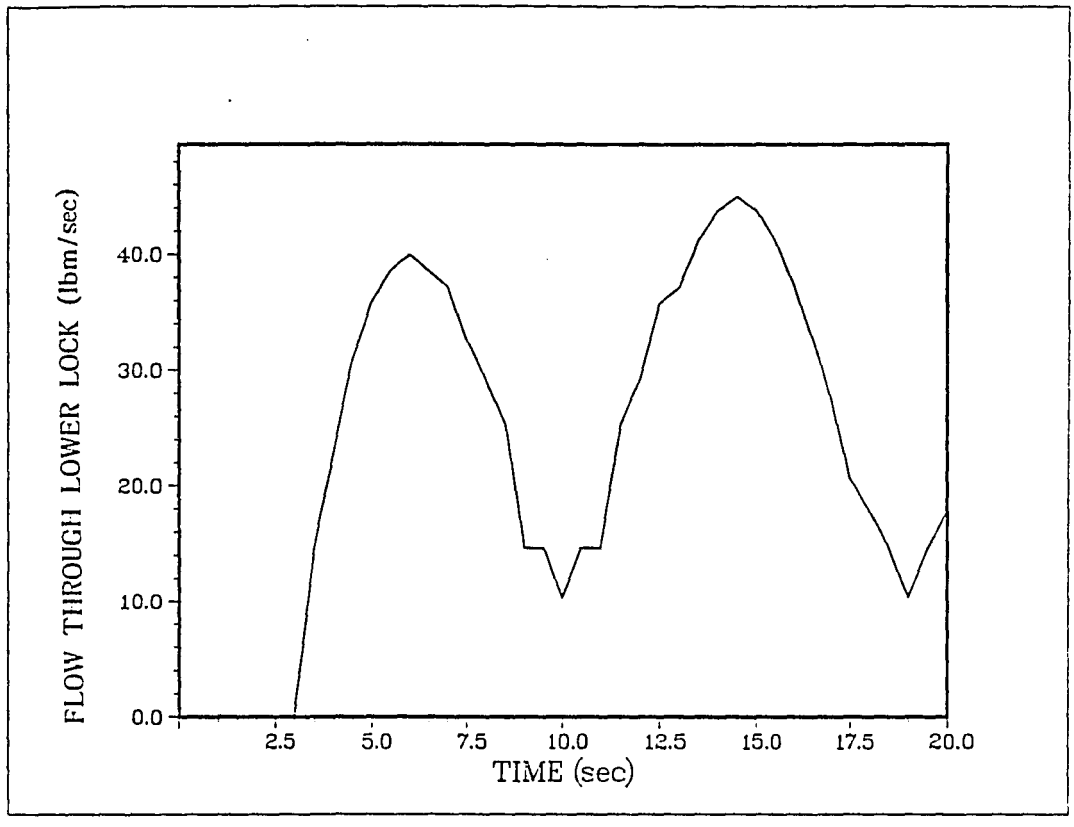

Figure 5.5--Continued

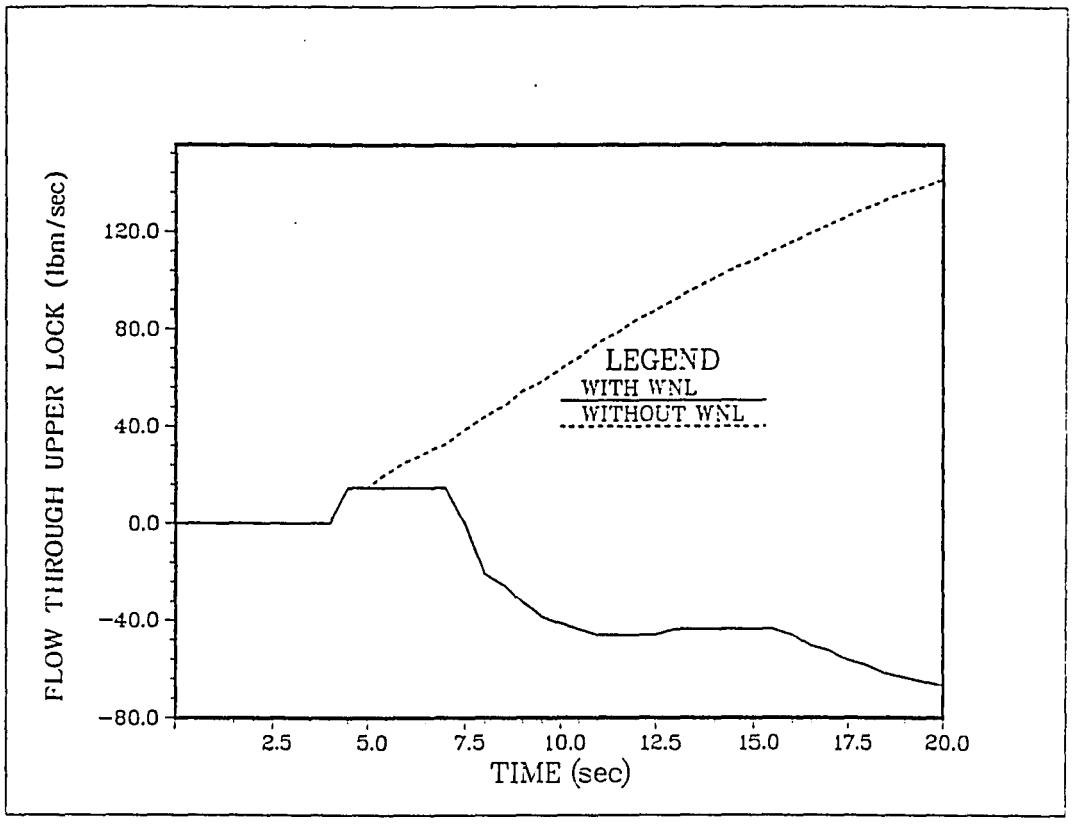

Figure 5.5--Continued

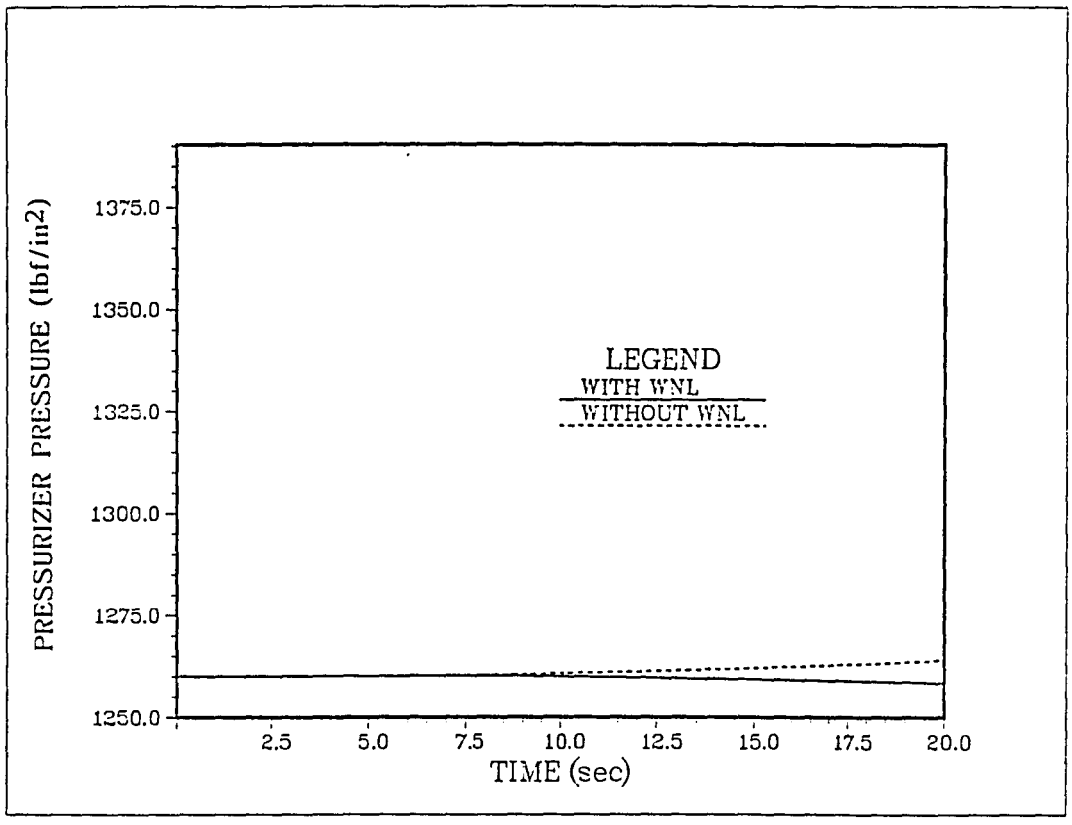

Figure 5.5 PIUS System Response to a Twenty-Five Percent Decrease in the Feedwater Flow Rate.--Continued

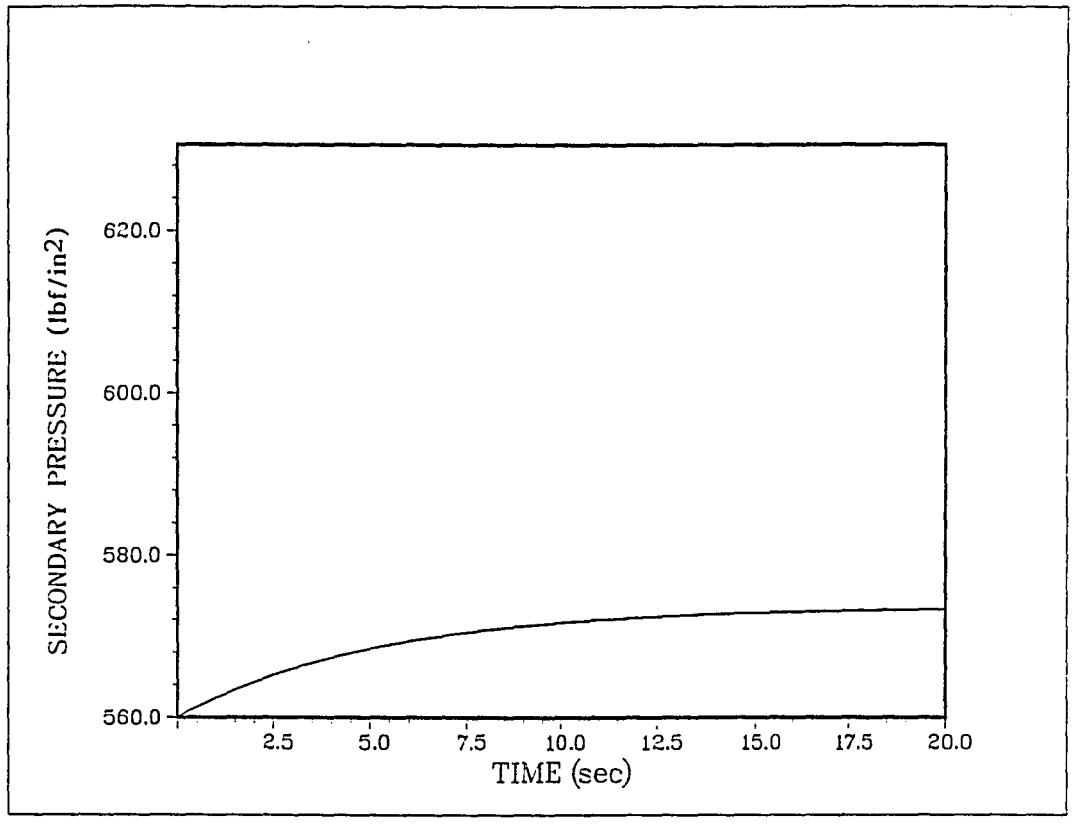

Figure 5.5--Continued

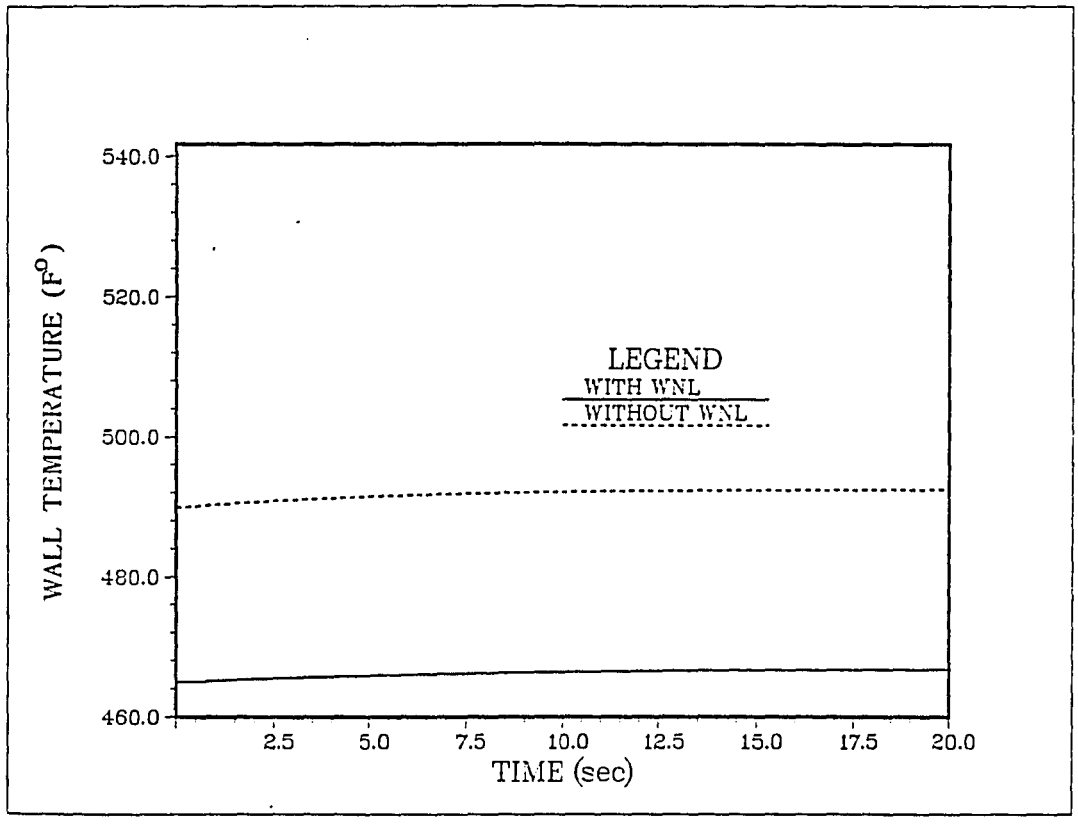

Figure 5.5--Continued

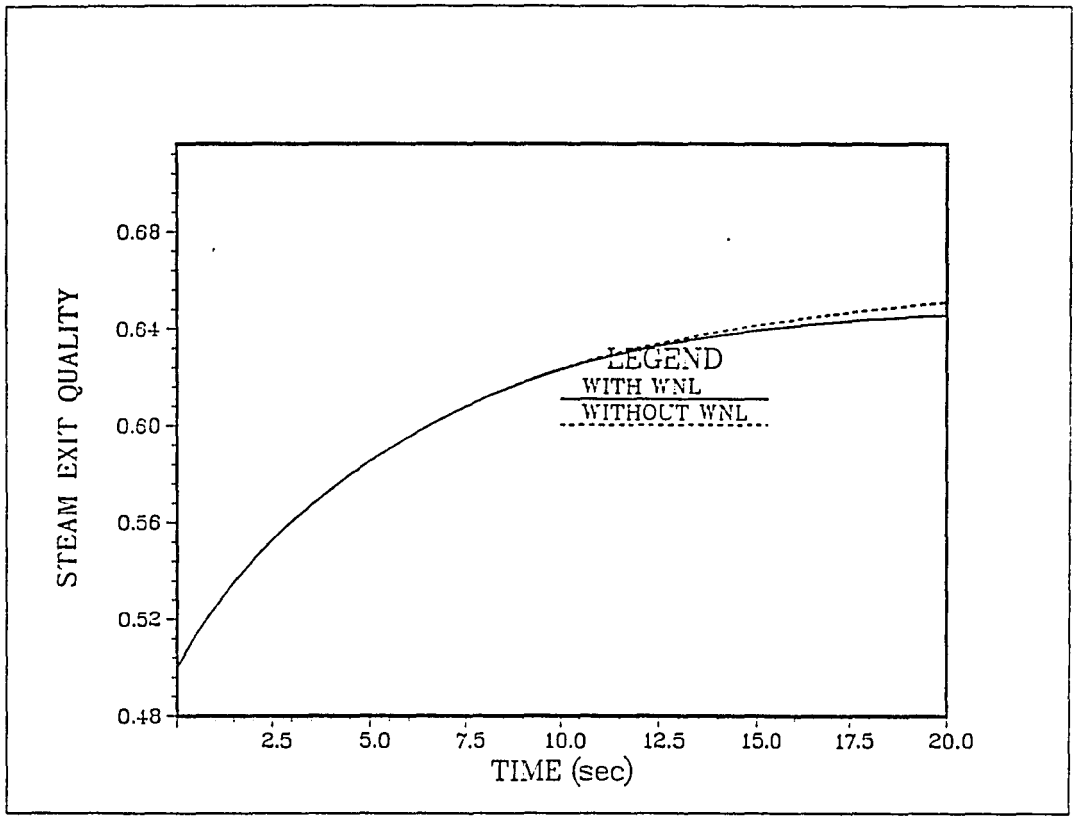

Figure 5.5 PIUS System Response to a Twenty-Five Percent Decrease in the Feedwater Flow Rate.--Continued

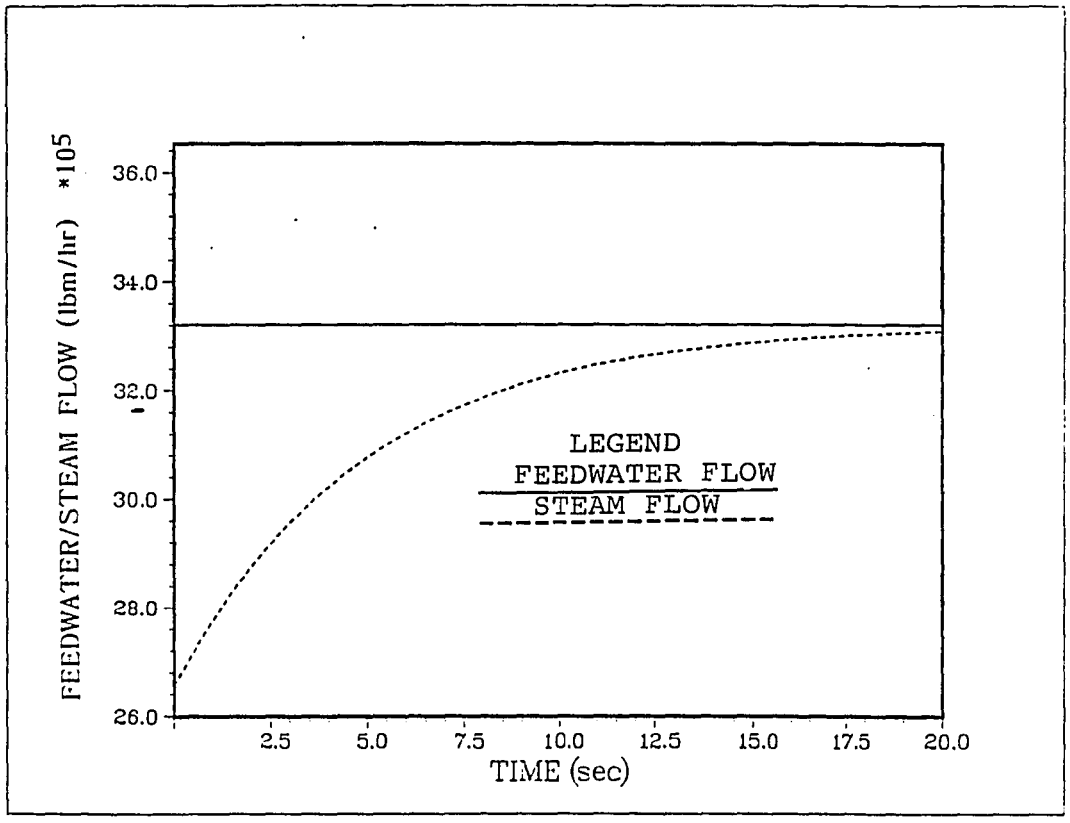

Figure 5.6 PIUS System Response to a Twenty-Five Percent Increase in the Feedwater Flow Rate

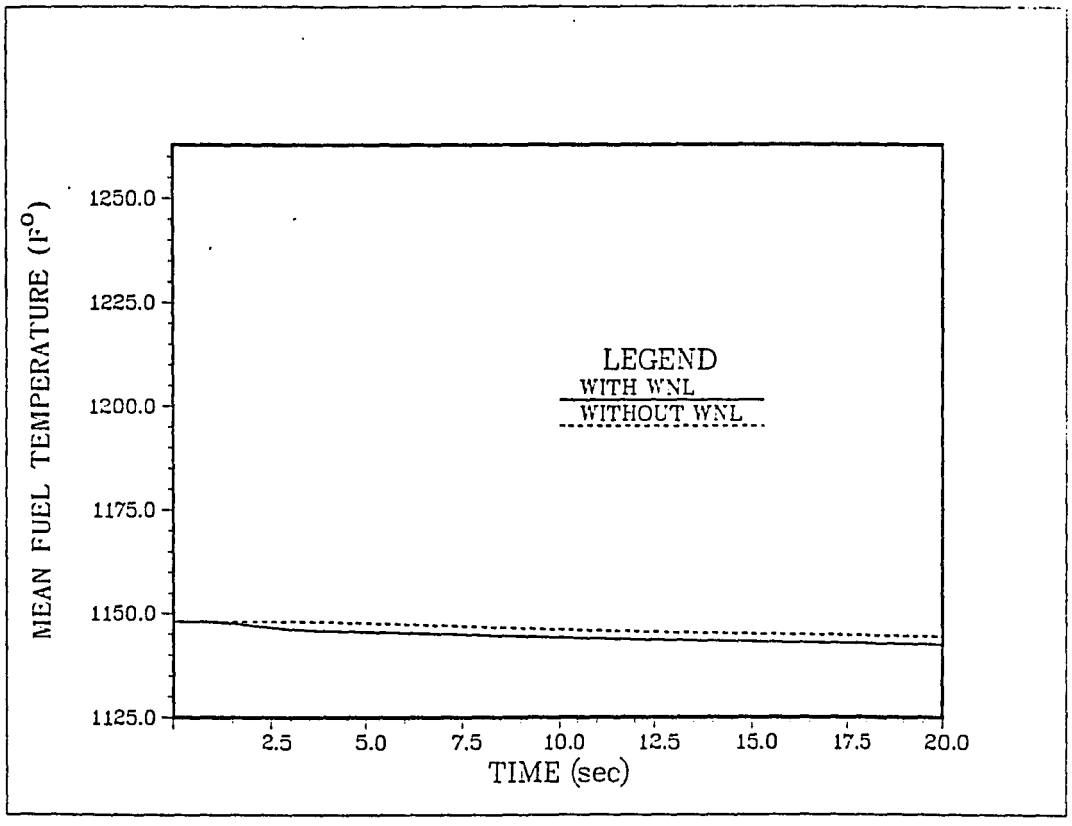

Figure 5.6--Continued

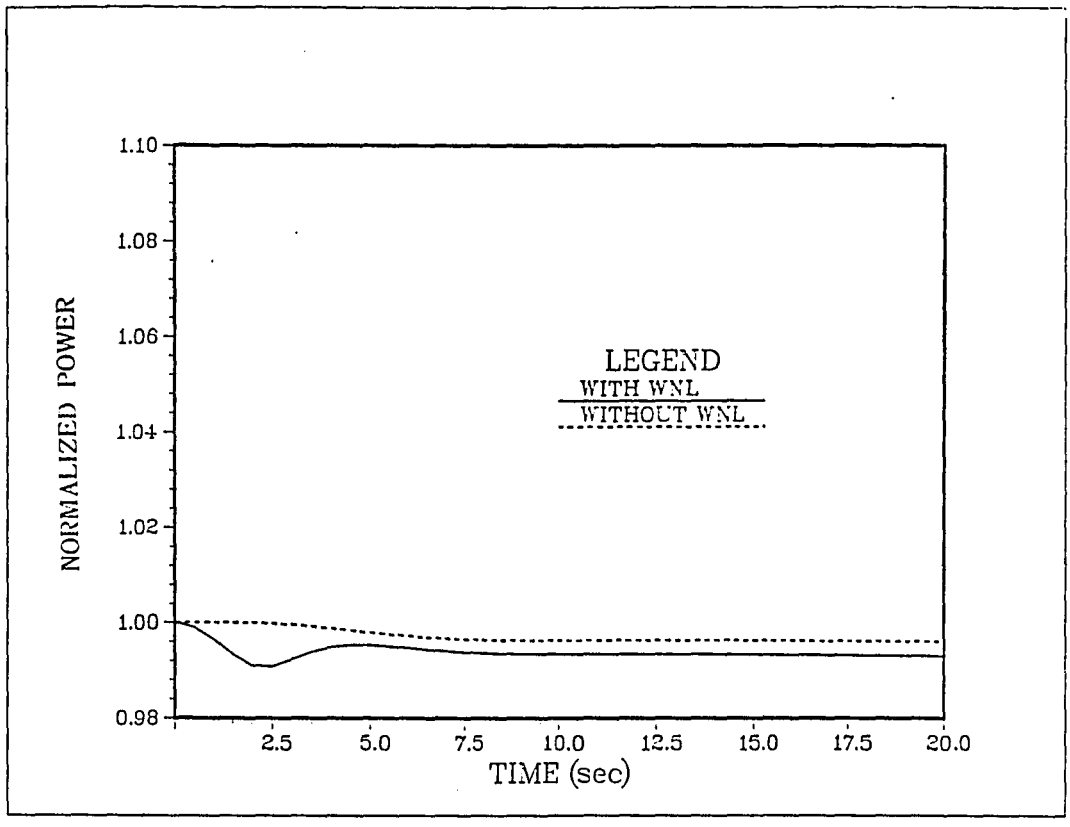

Figure 5.6--Continued

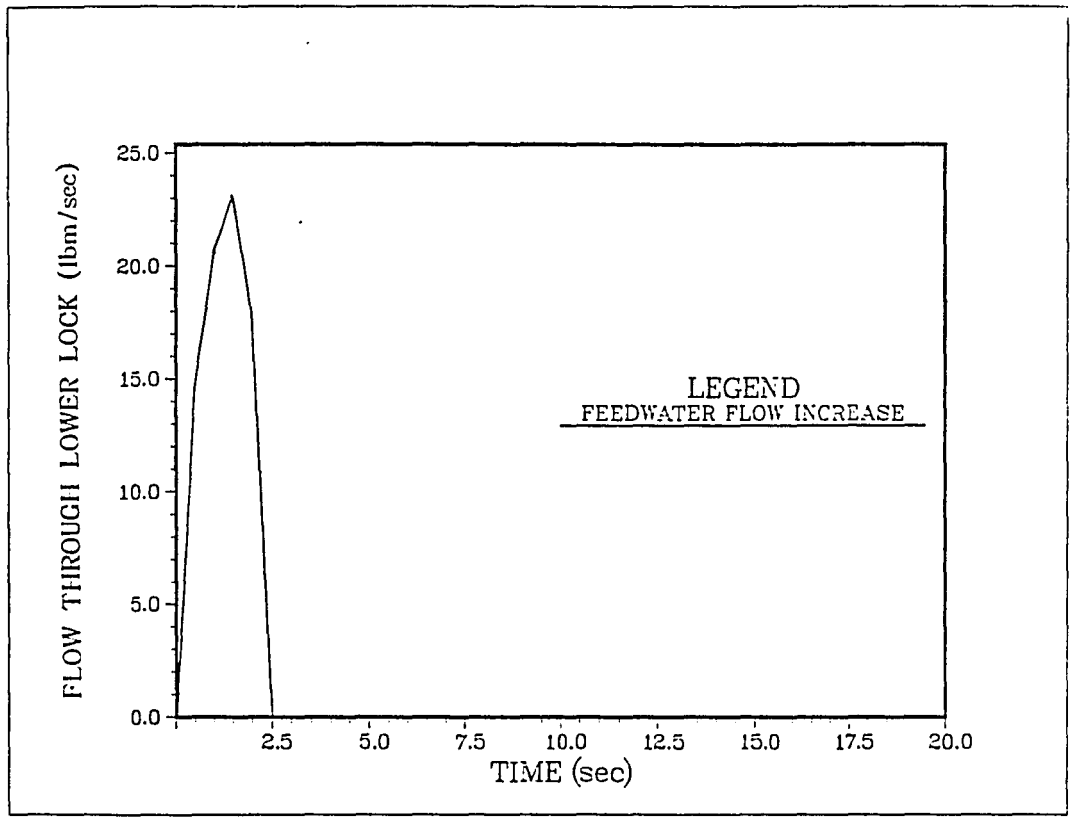

Figure 5.6 PIUS System Response to a Twenty-Five Percent Increase in the Feedwater Flow Rate.--Continued

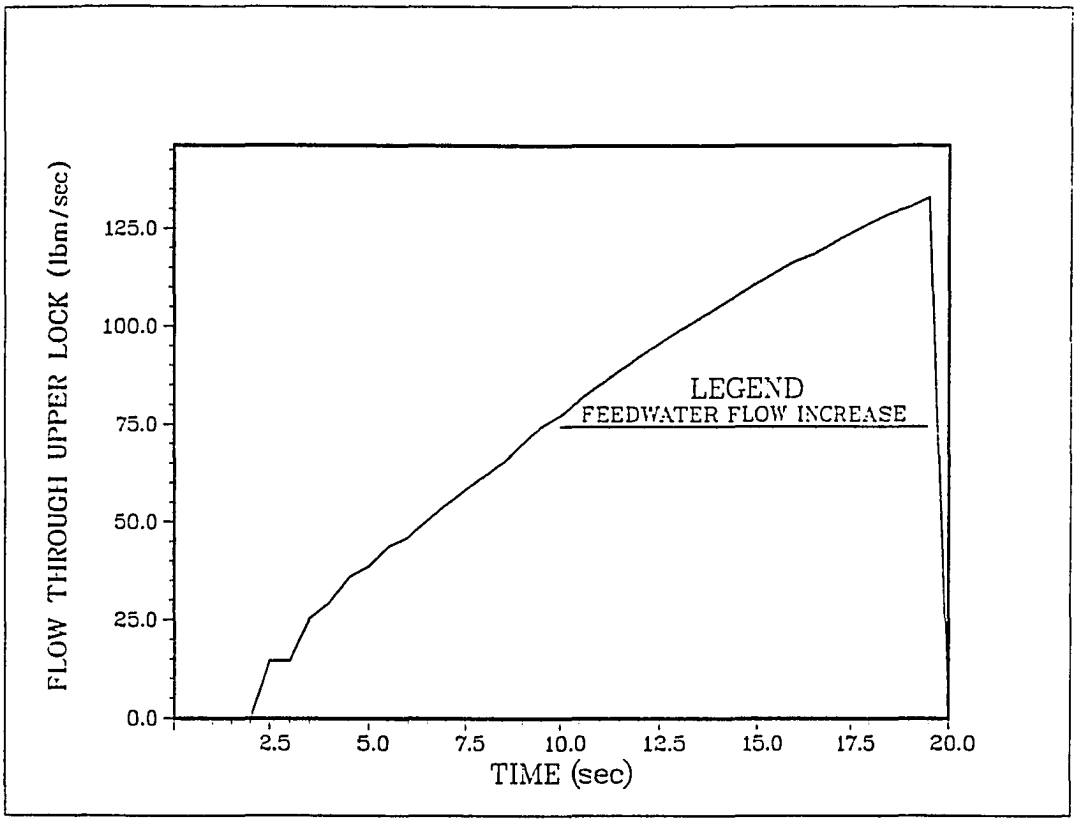

Figure 5.6--Continued

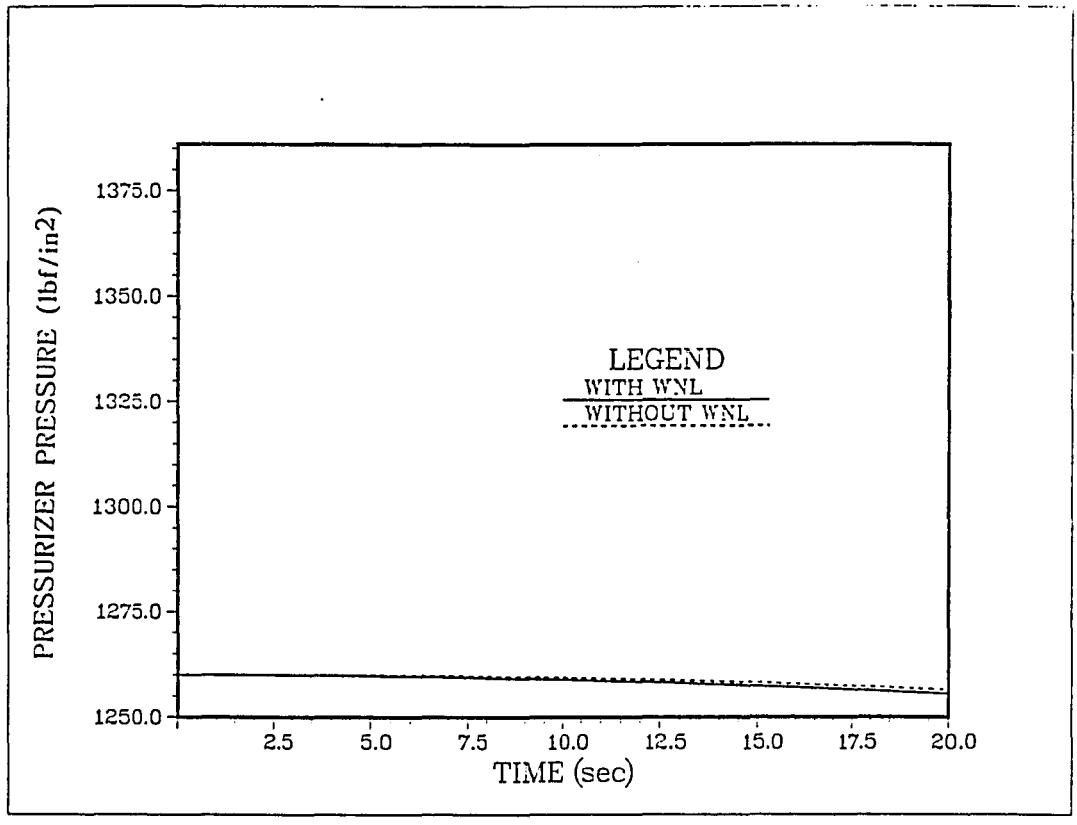

Figure 5.6--Continued

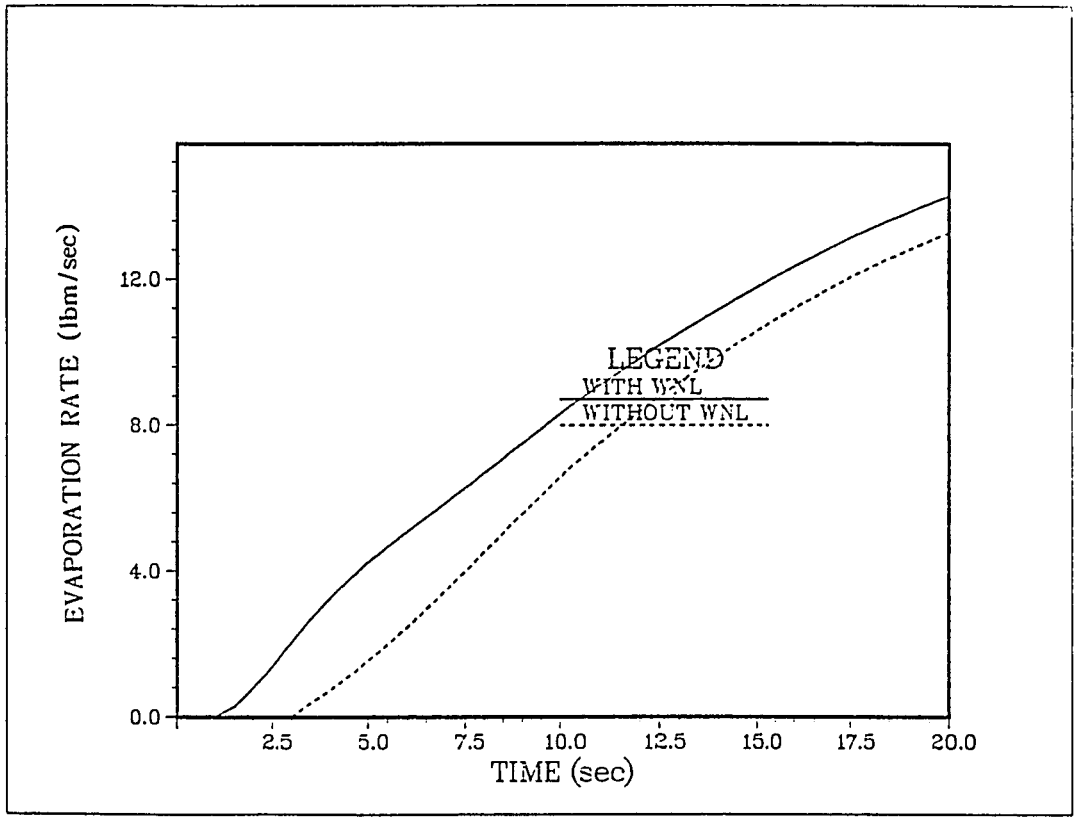

Figure 5.6 PIUS System Response to a Twenty-Five Percent Increase in the Feedwater Flow Rate.--Continued

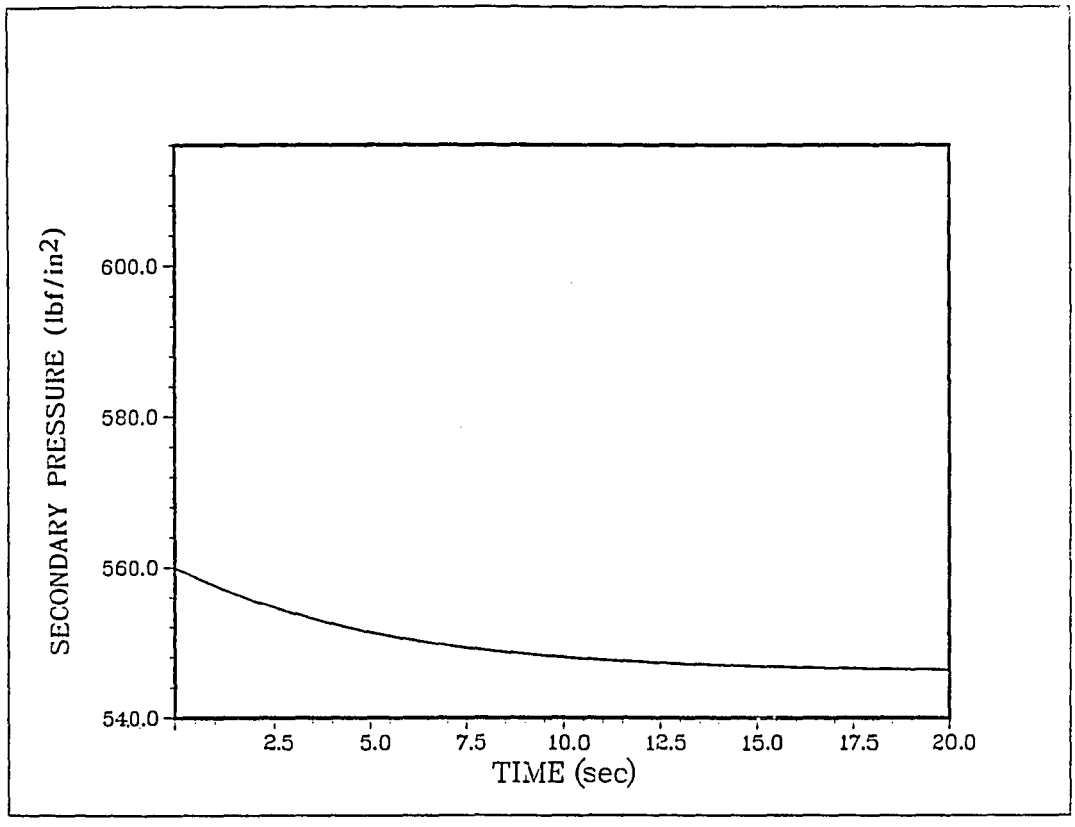

Figure 5.6--Continued

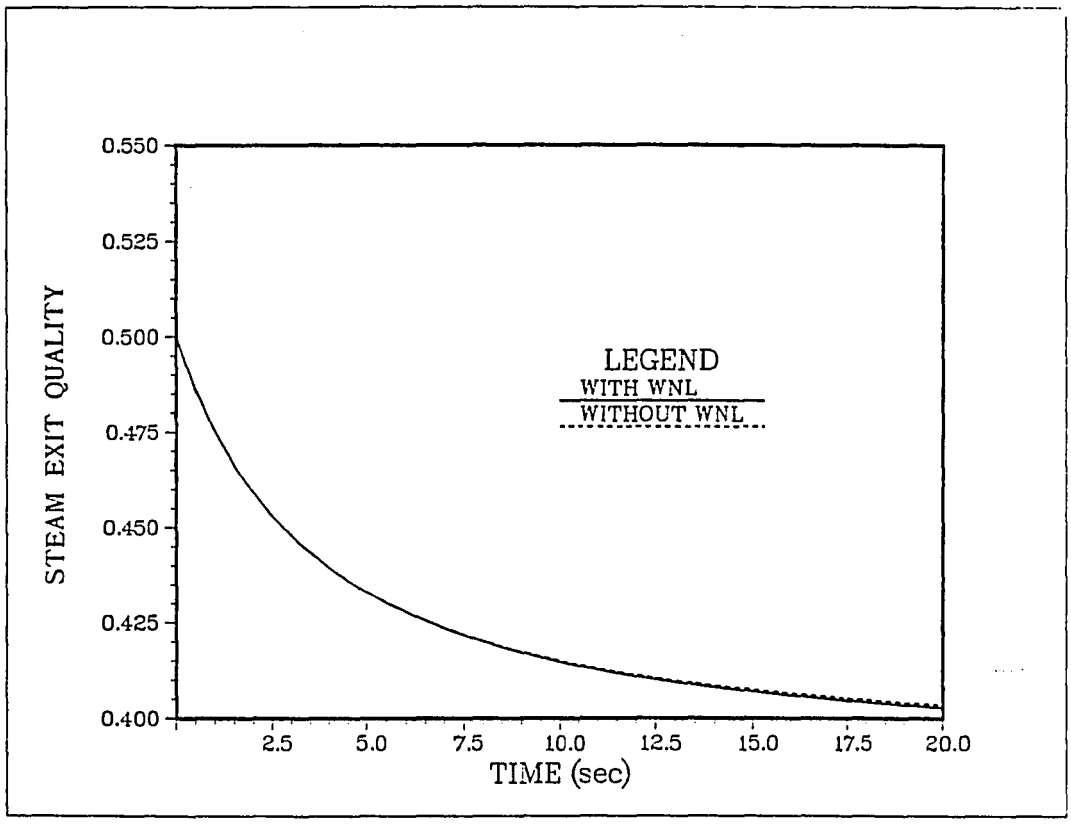

Figure 5.6--Continued

Other characteristics of this transient are the obvious increase in the steam exit quality, the exit steam pressure, and the steam generator tube wall temperature. It should be mentioned that better results for this transient would be obtained if steam voids in the primary loop were simulated and if heat transfer coefficients used in the modeling of the secondary system had not been held constant during transients.

CHAPTER 6

CONCLUSION AND RECOMMENDATIONS

6.1 Conclusion

As has been seen from the PIUS system behavior presented in this work, external disturbances, which have the potential of causing core damage in a PWR system, can be mitigated by the passive safety feature of the PIUS system, namely, the automatic entrance of pool water with a high boron content into the primary loop. Thus, the criterion of preventing core damage due to runaway heat generation may more easily be fulfilled by submerging the primary system in a large pool of highly borated water.

It was found that the neglecting of the change in the internal energy of the subcooled region during short transients is adequate for simulating the PIUS pressuruzer. This is an important simplification in this type of computation.

6.2 Recommendations

Although the inherent safety feature of the PIUS system has been demonstrated to some extent in this work, the results should be considered as only a

qualitative picture of the expected performance of the PIUS system. Attention should be called to the following topics as deserving of analysis in future research work:

- The switch from single phase flow, in the primary loop and the lower part of the pressurizer, i.e., the funnel, to a two-phase flow at the onset of nucleate boiling,
- Short term or transition decay heat removal by natural convection,
- The potential of thermal shock due to the incoming flow into the primary loop,
- The characteristics of primary circulation pump,
- Economics of operating such a very sensitive system,
- Limitations of the steam generator model, and
- Vaporization in the primary loop.

In the area of switching from single phase into two phase flow, the goal would be to develop a larger code that would handle both modes, the single phase mode and the two phase mode, with a control switch based on the comparison of the state enthalpy of the fluid with that of saturated liquid.

Stiffness of the dynamic model, as well as the limitation on the maximum number of the differential equations that the DARE language could handle, make it difficult to include such study as well as some of the recommendations mentioned elsewhere in this work. For example, the study of boron content in this work was limited to one differential equation that simulates the whole primary loop as one region. It is, therefore, recommended that additional attention be called to the distribution of boron concentration in different regions of the PIUS system.

In the area of decay heat removal, the future work should examine the behavior of the PIUS system due to the following interesting areas:

- The secondary loop and steam generator performance as an ultimate heat sink, and
- Behavior of the PIUS system during the natural convection mode as well as the stability of the system during this mode.

In the area of thermal shock analysis, it was found that a sudden drop in the inlet temperature of the core as a result of the incoming pool flow takes place. This should be investigated with respect to its effect on the following:

- Flow instability,
- Neutron power controllability, and
- Fatigue in the mechanical properties of the coolant channels.

In the area of the primary circulation pump, further study in the area of controlling the pump speed in connection with the inlet and outlet core temperature, as well as the motion of the lower hot/cold interface is needed. In addition, more accurate estimates of the pressure losses in the primary loop are recommended. Moreover, the effect of vibrations, the response of the pump to the entering pool flow from the pool, and the dynamic behavior of the pump under severe transients should also be considered. Furthermore, the relationship between the pump speed and the steam void during two phase flow should be established.

In the area of economics, it would be very interesting to study the cost of operating a plant that has the inherent passive safety measure and compare it to the operating cost for a conventional PWR system. For example, surveillance and maintenance of the boron system would be more complicated than that in a conventional PWR.

The steam generator was simulated as two axial regions. However, it is expected that, during transients, superheating may occur. It is, therefore, recommended that three axial regions (subcooled water, nucleate boiling, and superheat regions) be used on the steam/water side of the steam generator. In addition, the secondary system should be able to provide steam with a good quality under load-following operation modes. Moreover, the heat loss from the steam generator to the pool should also be investigated. Such heat loss is expected to be relatively high because the primary flow rate passes around the tubes in the steam generator and the steam is being generated inside the tubes. The steam generator shell is in contact with the cold primary water.

Finally, vapor formation in the primary system and its effect on heat transfer and reactivity should be investigated. This would be necessary for extending the range of severity and duration of transients that can be modelled successfully.

APPENDIX A

COMPARISON OF THE QUALITY MODEL WITH NAHAVANDI, BARON AND EPRI MODELS

It was mentioned in Chapter 1 that the quality model is just the fourth case of either Nahavandi's or Baron's model. To prove this, we find it necessary to repeat the mass, energy, and volume balances of each model and then make the comaprison. Let us start with the fourth case of Nahavandi's model:

A.1 Mass Balance

For the steam region (subscripted by G and g) and the liquid region (subscripted by F and f), we have:

$$\frac{dM_G}{dt} = m_{Gi} \qquad \text{A.1.1}$$

and

$$\frac{dM_F}{dt} = m_{Fi} \qquad \text{A.1.2}$$

where

$$m_{Gi} = \dot{m}_{re} - \dot{m}_{cs} - \dot{m}_r + \dot{m}_{bub} \qquad \text{A.1.3}$$

and

$$m_{Fi} = \dot{m}_{su} + \dot{m}_{cs} + \dot{m}_{sp} - \dot{m}_{bub} + \dot{m}_r \qquad \text{A.1.4}$$

A.2 Energy Balance

$$\frac{dU_G}{dt} = (m\ h)_{Gi} - 144/J\ P\ dV_G/dt \qquad A.2.1$$

and

$$\frac{dU_F}{dt} = (m\ h)_{Fi} - 144/J\ P\ dV_F/dt \qquad A.2.2$$

where

$$U_G = M_{Gf}\ h_f + M_{Gg}\ h_g - 144/J\ P\ V_G \qquad A.2.3$$

$$(m\ h)_{Gi} = -\dot{m}_{re}\ h_g - \dot{m}_{cs}\ h_f - \dot{m}_r\ h_f + \dot{m}_{bub}\ h_g \qquad A.2.4$$

and

$$U_F = M_{Ff}\ h_f + M_{Fg}\ h_g - 144/J\ P\ V_F \qquad A.2.5$$

$$(m\ h)_{Fi} = \dot{m}_{su}\ h_{su} + \dot{m}_{cs}\ h_f + \dot{m}_{sp}\ h_f - \dot{m}_r\ h_f - \dot{m}_{bub}\ h_f + Q_h \qquad A.2.6$$

A.3 Volume Balance

$$V_{tot} = V_F + V_G \qquad A.3.1$$

where

$$V_F = M_{Fg}\ v_g + M_{Ff}\ v_f \qquad A.3.2$$

and

$$V_G = M_{Gg}\ v_g + M_{Gf}\ v_f \qquad A.3.3$$

Finally, by definition, we have

$$M_G = M_{Gf} + M_{Gg} \qquad A.3.4$$

and

$$M_F = M_{Ff} + M_{Fg} \qquad A.3.5$$

In the quality model, we have the following: Mass balance equations are the same if we are willing to rename the bubble mass flow rate as m_{bub} instead of m_f. The energy balance equations are as follows:

$$\frac{d\ M_G\ (X_G\ h_{fg} + h_f)}{dt} = \dot{m}_f\ h_g - \dot{m}_c\ h_f + 144/J\ V_G\ dP/dt \qquad A.1$$

and

$$\frac{d\ M_F\ (X_F\ h_{fg} + h_f)}{dt} = -\ \dot{m}_{su}\ (X_F\ h_{fg} + h_f) - \dot{m}_f\ h_g + \dot{m}_c\ h_f + Q_h + 144/J\ V_F\ dP/dt \qquad A.2$$

Finally, the volume equations are:

$$V_{tot} = V_F + V_G \qquad A.3$$

where

$$V_F = M_F\ (X_F\ v_{fg} + v_f) \qquad A.4$$

and

$$V_G = M_G\ (X_G\ v_{fg} + v_f) \qquad A.5$$

Let us define the qualities of both steam and water regions as follows:

$$X_G = \frac{M_{Gg}}{M_G} \qquad A.6$$

and

$$X_F = \frac{M_{Fg}}{M_F} \qquad A.7$$

where M_F and M_G are the same as in the Nahavandi model.

Substituting the above definition in the volume equation of the quality model, we get

$$V_F = M_F \left[M_{Fg} (v_g - v_f) / M_F + v_f\right] \qquad A.8$$

Simplifying the above equation, we get the volume equation used by Nahavandi, i.e.:

$$V_F = M_{Ff} v_f + M_{Fg} v_g \qquad A.9$$

and

$$V_G = M_{Gg} v_g + M_{Gf} v_f \qquad A.10$$

For the energy equations, let us start with the quality model equations and use the definition of the quality and the volume equations as follows:

$$\frac{d\, M_G (M_{Gg} h_{fg} / M_G + h_f)}{dt} = \dot{m}_f h_g - \dot{m}_c h_f + 144/J \left(M_{Gg} v_{fg} / M_G + v_f\right) dP/dt \qquad A.11$$

Using equation (A.3.4), and rearranging equation (A.11), we get the following:

$$\frac{d\, (M_{Gg} h_g + M_{Gf} h_f)}{dt} = \dot{m}_f h_g - \dot{m}_c h_f + 144/J\, V_G\, dP/dt \qquad A.12$$

But, from equation (A.2.3) of Nahavandi, we have the following:

$$M_{Gf} h_f + M_{Gg} h_g = U_G + 144/J\, P\, V_G \qquad A.13$$

Then, substituting in equation (A.13), and rearranging:

$$\frac{d\ U_G}{d\ t} = \dot{m}_f\ h_g - \dot{m}_c\ h_f - 144/J\ P\ dV_G/dt \qquad A.14$$

which is the same equation as in Nahavandi; specifically, equation (A.2.1). The same procedure can be used in the case of the liquid region.

APPENDIX B

COMPARISON BETWEEN SUBCOOLING AND SATURATION

It was mentioned earlier in the introduction that Brown (1962) neglected the change in the internal energy in the subcooled region. This same assumption is used in the PIUS pressurizer model. The motive behind this assumption is that the temperature difference between saturation and subcooling of the liquid under consideration is small. In the PIUS pressurizer case, it is about 4 C degree. Therefore, the subcooled region can be replaced by a saturated region. Actually, the desire to reduce the number of differential equations is the main incentive for this.

Justification of the above assumption is made through the comparison between two simplified models. The first one consisted of a saturated steam region and a saturated liquid region. The other one consisted of a saturated steam region and a subcooled liquid region. Mass, energy, and volume balances were applied to each model as was the case in Chapter 4. It was found that the pressure change in the case of the saturated liquid region model is given as follows:

$$\frac{dP}{dt} = -[M_g\,\partial v_g/\partial P + M_f\,\partial v_f/\partial P - (M_g\,\partial h_g/\partial P + M_f\,\partial v_f/\partial P - V_{tot})(v_g - v_f)/(h_g - h_f)]/[v_f\,\dot{m}_s + (v_g - v_f)\,\dot{m}_s\,(h_{su} - h_f)/(h_g - h_f)] \qquad \text{B.1}$$

In the case of the subcooled region model, the pressure change is given as follows:

$$\frac{dP}{dt} = [v_s\,\dot{m}_s + (v_g - v_s)\,\dot{m}_s\,(h_{su} - h_s)/(h_g - h_s) + M_s\,dh_s/dt\,(\partial v_s/\partial h_s - (v_g - v_s)/(h_g - h_s))]/[M_g\,\partial v_g/\partial P + M_f\,\partial v_f/\partial P - (M_g\,\partial h_g/\partial P - V_{tot})(v_g - v_f)/(h_g - h_s)] \qquad \text{B.2}$$

If the above two equations were to be equal, the following conditions should be satisfied:

1) The specific volumes of both regions, the saturated and the subcooled, should be equal, and

2) $$M_s\,dh_s/dt\,(\partial v_s/\partial h_s - \frac{v_g - v_s}{h_g - h_s}) = -(\frac{v_g - v_f}{h_g - h_f})\,M_f\,\partial h_f/\partial P\,dP/dt$$

The first condition is achieved by the usual assumption of the incompressible liquid. To understand further what is meant by the second condition, we need to investigate the possibility of the equality that may exist between the left hand side (LHS) and the right hand side (RHS) of condition 2. Such equality may exist if the following is assumed:

1) The enthalpies of the saturated liquid and the subcooled liquid are the same, and

2) $M_S \, dh_S/dt \, \partial v_S/\partial h_S = 0$ B.3

The first requirement can be achieved because the subcooled liquid is only 4 C degree below saturation. The second requirement is satisfied only if the change in the internal energy with time is neglected. To elaborate further, let us apply the conservation of energy to the subcooled region:

$$\frac{d\,U_S}{d\,t} = \frac{d\,H_S}{d\,t} - P\,\frac{d\,V_S}{d\,t} - V_S\,\frac{d\,P}{d\,t} \qquad \text{B.4}$$

Using specific properties, as well as some of the conditions that have been assumed previously, we arrive at the following:

$$\frac{d\,u_S}{d\,t} = \left(\frac{\partial h_S}{\partial P} - v_S\right)\frac{d\,P}{d\,t} \qquad \text{B.5}$$

where

$$u_s = h_s - P\, v_s \qquad \text{B.6}$$

Equation (B.5) would be true only if the internal energy were assumed constant with time. This can be seen from the definition of the internal energy equation by taking the partial derivative with respect to time, which leads to the following:

$$\frac{\partial h_s}{\partial P} = v_s \qquad \text{B.7}$$

Therefore,

$$\frac{d\, u_s}{d\, t} \cong 0 \qquad \text{B.8}$$

Consequently, the pressure change for the saturated region model is approximately equal to that of the subcooled region model if we are willing to make the assumption that the change in the internal energy during transients is negligible.

APPENDIX C

LIST OF VARIABLES

SYMBOL	UNITS	PARAMETERS
A	ft^2	Area
C	ppm	Boron Concentration
c	$\Delta k/k/unit$	Coefficient of Reactivity kernel
T	F°	Temperature
M	lbm	Mass
t	sec	Time
Γ	$\Delta k/k/F°$	Temperature Reactivity Coefficient
$\dot{m}$	lbm/sec	Rate of Change of Mass
V	ft^3	Volume
v	ft^3/lbm	Specific Volume
H	Btu	Enthalpy
h	Btu/lbm	Specific Enthalpy
h_{fg}	Btu/lbm	Specific Enthalpy of Phase Change
U	Btu	Internal Energy
u	Btu/lbm	Specific Internal Energy
P	lbf/in^2	Pressure
Q	Btu/hr	Energy Transferred to the Fluid from the Heater Banks in the Pressurizer

X		Quality
k	Btu/ft^2-hr-F°	Thermal Conductivity
α	ft^2/hr	Thermal Diffusivity
c_p	Btu/lbm-F°	Specific heat
x	ft	Differential length
L	ft	Length
W	lbm/sec	Mass Flow Rate

SUBSCRIPTS		ATTACHED SYMBOL
f	Fuel	T
c	Coolant	T
fg	Phase change	h
re	Relief Valve	$\dot{m}$
FP1	Leaving region pool 1	$\dot{m}$
surge,su,s	Surge	$\dot{m}$
spill	Leaving the funnel to pool 1	$\dot{m}$
cs,c	Condensation in top of the pressurizer	$\dot{m}$
r	Condensation that falls down from the top to the bottom of the pressurizer	$\dot{m}$
bub,f	Bubbles in the bottom of the pressurizer	$\dot{m}$
sp	condensation on spray banks	$\dot{m}$
f	saturated fluid in a region	V,X,M,H,U
g	saturated steam in a region	V,X,M,H,U
s	subcooling	M,h,v,u

LIST OF REFERENCES

Abdallah, A.M., Mariy, A.M., Rabie, M.A., and Nagy, M.E.S., "Pressurizer Transients Dynamic Model," Nuclear Engineering Design, 73, 447, 1982.

Asahi, Y. and Wakabayashi, H., "Some Transient Characteristics of PIUS," Nuclear Technology, 72, 24-33, 1986.

Babala, D., "A Fast Semi-Implicit Integration Method for Thermohydraulic Networks," Trans. Am. Nucl. Soc., 47, 295, 1984a.

Babala, D., "Computer Simulation of the Thermohydraulic Self-Protecting Properties of the SECURE-P(PIUS) Primary System during Severe Transients," Trans. Am. Nucl. Soc., 47, 296, 1984b.

Babala, D., Private Communications, 1985.

Babala, D., and Hannerz, K., "PWR Inherent Core Protection by Primary System Thermohydraulics," Nucl. Sci. Eng., 90, 400, 1985.

The Babcock & Wilcox Company, "Modular Modeling System (MMS): A Code for the Dynamic Simulation of Fossil and Nuclear Power Plants," ERPI CS/NP - 2989, Palo Alto, California, 1983.

Baek, S.M. and No, H.C., "A Nonequilibrium Three Region Model for Transient Analysis of Pressurizer Water Reactor Pressurizer," Nuclear Technology, 74, 260-266, 1986.

Baron, R.C., "Digital Model Simulation of a Nuclear Pressurizer," Nuclear Science and Engineering, 52, 283-291, 1973.

Brown, D.H., "Transient Thermodynamic Analysis of Thermal Systems," General Electric, Report 62GL36, 1962.

El-wakil, M.M., Nuclear Heat Transport, International Textbook Company, Scranton, Pennsylvania, 1971.

Hannerz, K., "Towards Intrinsically Safe Light Water Reactors," Oak Ridge, Tennessee, July 1983a.

Hannerz, K., "Applying PIUS to Power Generation: The SECURE P LWR," Nuclear. Eng. Int., 41, December 1983b.

Hannerz, K., Isperg, P., "Nuclear Power Plant Design Simplification through Inherent Safety: The PIUS Approach," Trans. Am. Nucl. Soc., 47, 286 (1984).

Henry, A.F., Nuclear Reactor Analysis, MIT Press, Cambridge, Massachusetts, 1975.

Hetrick, D.L., Dynamics of Nuclear Reactors, University of Chicago Press, Chicago, 1971.

Hetrick, D.L., Girijashanker, O.A., Palusinski, O.A., Keepin, W.N., and Roten, C.D., "Solution Methods for Simulation of Nuclear Power Systems," ERPI Research Project Report NP-1928, RP-1381, 1981.

Khamis, I.A., "Dynamic Simulation of a Process Inherent Ultimate Safety Power Plant (PIUS)," M.S. Thesis, University of Arizona, 1986.

Kim, S.N., "An Experimental and Analytical Model of a PWR Pressurizer during Transients," Ph.D. Thesis, Massachusetts Institute of Technology, 1984.

Lewis, E.E., Nuclear Power Reactor Safety, John Wiley and Sons, Inc., New York, 1977.

Mathieu, P. and Distexhe, E., "Modeling of Boron Control During Power Transients in a Pressurized Water Reactor," Nuclear Technology, 72, 135-146, 1986.

Nahavandi, A.N. and Makkenchery, S., "An Improved Pressurizer Model with Bubble Rise and Condensation Drop Dynamics," Nuclear Engineering and Design, 12, 135-147, 1970.

Rust, J.H., Nuclear Power Plant Engineering, Haralson Publishing Co., Buchanan, Georgia, 1979.

Sami, S.M., "A Dynamic Model for Predicting CANDU Pressurizer Performance," Nuclear Technology, 72, 7-23, 1986.

Shinaishin, M.A., "Dynamic Simulation of a Sodium Cooled Fast Reactor Power Plant," Ph.D. Dissertation, University of Arizona, 1976.